Prediction of California Bearing Ratio of Fine Grain Soil from Index Properties of Soil Using Artificial Neural Network

Liya Melaku Dessalegn

A Thesis Submitted to department of Civil Engineering,
School of Civil Engineering and Architecture

Presented in Partial Fulfilment of the Requirements of Master of Science in Civil Engineering (Specialization in Geotechnical Engineering)

Office of Graduate Studies

Adama Science and Technology University

September 2023
Adama, Ethiopia

Prediction of California Bearing Ratio of Fine Grain Soil from Index Properties of Soil Using Artificial Neural Network

By

Liya Melaku Dessalegn

Advisor: Dr. Argaw Asha (PhD)

A Thesis Submitted to the department of Civil Engineering,
School of Civil Engineering and Architecture

Presented in Partial Fulfilment of the Requirements of Master of Science in Civil Engineering (Specialization in Geotechnical Engineering)

Office of Graduate Studies
Adama Science and Technology University

September 2023
Adama, Ethiopia

DECLARATION

I hereby declare that this Master Thesis entitled "**Prediction of California Bearing Ratio of Fine Grain Soil from Index Properties of Soil Using Artificial Neural Network**" is my original work. That is, it has not been submitted for the award of any academic degree, diploma or certificate in any other university. All sources of materials that are used for this thesis have been duly acknowledged through citation.

__________________________ _______________________ _____________________

Name of the student Signature Date

RECOMMENDATION

I, the advisor of this thesis, hereby certify that I have read the revised version of the thesis entitled '**Prediction of California Bearing Ratio of Fine Grain Soil from Index Properties of Soil Using Artificial Neural Network'** prepared under my guidance by Liya Melaku Dessalegn submitted in partial fulfillment of the requirements for the degree of Masters of Science in Civil Engineering (Geotechnical Engineering).

Therefore, I recommend the submission of revised version of the thesis to the department following the applicable procedures.

Major Advisor	Signature	Date

APPROVAL OF ADVISOR

I, the advisor of the thesis entitled "**Prediction of California Bearing Ratio of Fine Grain Soil from Index Properties of Soil Using Artificial Neural Network**" and developed by Liya Melaku Dessalegn; hereby certify that the recommendation and suggestions made by the board of examiners are appropriately incorporated into the final version of the thesis.

____________________	____________________	____________________
Major Advisor	Signature	Date

APPROVAL OF THE BOARD OF EXAMINERS

We, the undersigned, members of the Board of Examiners of the thesis by Liya Melaku Dessalegn have read and evaluated the thesis entitled '**Prediction of California Bearing Ratio of Fine Grain Soil from Index Properties of Soil Using Artificial Neural Network'** and examined the candidate during open defense. This is, therefore, to certify that the thesis is accepted for partial fulfillment of the requirement of the degree of Master of Science in Civil Engineering (Geotechnical Engineering).

Chairperson	Signature	Date
Internal Examiner	Signature	Date
External Examiner	Signature	Date

Finally, approval and acceptance of the thesis is contingent upon submission of its final copy to the Office of Postgraduate Studies (OPGS) through the Department Graduate Council (DGC) and School Graduate Committee (SGC).

Department Head	Signature	Date
School Dean	Signature	Date
Office of Postgraduate Studies, Dean	Signature	Date

ACKNOWLEDGEMENT

Foremost, I want to extend my deepest appreciation to God for guiding me throughout the process of completing this thesis.

I would like to convey my genuine thanks and acknowledge the immense contribution of my advisor, Dr. Argaw Asha.

Furthermore, I'd like to recognize the vital role of Adama Science and Technology University, Addis Ababa City Road Authority (AACRA), particularly Behaylu.G, and Addis Ababa Science and Technology University (AASTU). Their substantial contributions in gathering essential data and conducting laboratory work for this study are deeply appreciated.

Lastly, I am indebted to my family, friends and colleagues who have been a steadfast pillar of support during this thesis undertaking. Their unwavering encouragement and belief in my capabilities have consistently motivated me

ABSTRACT

This study focuses on expediting the determination of the soaked California bearing ratio (CBR) in laboratory assessments, which traditionally demand substantial time and effort. This research endeavors to create predictive models for CBR in Addis Ababa city using artificial neural network modeling techniques. These models are developed based on input parameters encompassing Gravel percentage (G), Sand percentage (S), Fines percentage (F), Liquid limit (LL), Plastic limit (PL), Plasticity Index (PI), maximum dry density (MDD), and optimum moisture content (OMC).The study begins with a sensitivity analysis to identify influential parameters, as there exist varying perspectives among researchers regarding which parameters carry the most significance for predicting the soaked CBR of fine-grained soils. Initial simple regression analyses conducted in this study reveal that Fine percentage and PI exhibit stronger correlations with soaked CBR of fine-grained soils, with correlation coefficients of 0.66 and 0.47, respectively, compared to maximum dry density and optimum moisture content. Based on these correlations, neural network and multiple regression prediction models are developed, incorporating varying numbers of input parameters. The results demonstrate that neural network models excel in utilizing less influential parameters, in contrast to multiple regression models. Neural network analysis proves particularly advantageous in situations where uncertainty exists regarding the most influential input parameters, as it enables the simultaneous consideration of all such influential parameters, thereby enhancing model performance. The research employs a multi-layer perceptron network with feed-forward back propagation, utilizing a dataset comprising 318 primary and secondary soil test results for index properties and CBR, conducted in accordance with ASTM Standards. During testing, the developed models exhibit noteworthy success in predicting CBR, achieving correlation values of approximately 0.9002. The models undergo cross-validation using primary soil test data. Ultimately, the study's findings underscore the superiority of the artificial neural network approach in predicting CBR, outperforming multiple regressions, which yielded a correlation coefficient of 0.75 for the combination of Gravel, Fine, Sand, and PI.

Keywords**:** ANN, Shear Strength, CBR, MDD, OMC, Prediction, Index Properties, Sensitivity analysis.

Table of Contents

LIST OF FIGURES

LIST OF TABLES

ABBREVIATIONS AND SYMBOLS

AACRA	Addis Ababa City Road Authority
AASHTO	American Association of States Highway and Transportation Officials
AASTU	Addis Ababa Science and Technology University
AI	Artificial Intelligence
ANN	Artificial Neural Network
ASTM	American Society of Testing and Materials
ASTU	Adama Science and Technology University
BP	Back Propagation
CBR	California Bearing Ratio
Cc	Coefficient of Curvature
CH	High plasticity inorganic clay
CL	Low plasticity inorganic clay
Cu	Coefficient of Uniformity
Fine %	Fine grained soil content percentage
Gs	Specific gravity
LGP	Linear Genetic Programming
LL/Wl	Liquid limit
MAE	Mean Absolute Error
MaxAE	Maximum absolute error
MDD	Maximum Dry Density
MH	High plasticity inorganic silt
MinAE	Minimal absolute error
ML	Low plasticity inorganic silt
MLP	Multilayer Perceptron Network
MSE	Mean Squared Error
NN	Neural Network
OH	High plasticity organic clay
OL	Low plasticity organic clay
OMC	Optimum Moisture Content
PI	Plastic index

PL/Wp	Plastic limit
R	Correlation coefficient
R^2	Coefficient of determination
RMSE	Root Mean Squared Error
Sand %	Sand sized soil content percentage
USCS	Unified Soil Classification System

CHAPTER ONE

INTRODUCTION

1.1 Background of the study

The California bearing ratio (CBR) is a fundamental parameter in geotechnical engineering fields. It's used to characterize the strength of pavement subgrade materials as compared to the crushing strength of standard rocks (Black 1962; Yildirim and Gunaydin 2011). The value is expressed as a percentage of the load required to cause penetrations of 2.5 mm or 5.0 mm by standard loads. The concept of CBR value was first introduced in the 1920s by the State Highway Department of California and was later adopted by the US Corp of Engineers in the 1940s for military airfield purposes (Bienen et al. 2012). Today, the CBR test is the most commonly used method worldwide to assess the quality of road materials and to determine pavement thickness (Taskiran 2010). It's invaluable when it comes to assessing civil engineering risks associated with subsoil conditions. Moreover, fast determination of CBR is essential for speedier construction times (Stephens 1992; Taskiran 2010). All these elements make this an indispensable part of many infrastructure projects today (Cheng et al. 2020; Diallo et al. 2019; Huang et al. 2013; Tai et al. 2020).

The CBR value of soil specimens can be estimated in either soaked or unsoaked conditions. However, it should be noted that the CBR value obtained for soaked samples is lower than that of unsoaked samples, and thus considered a conservative estimate of subgrade materials. Unfortunately, determining the CBR value for samples prepared at Optimum moisture content (OMC) involves a time-consuming process of submerging the samples for four days (Sadrossadat et al. 2018; Taskiran 2010; Tenpe and Patel 2020a). This affects construction time greatly, which can be costly in terms of time, cost, necessary equipment, and labor, especially when analyzing CBR for many samples. To overcome these limitations, predictions of CBR can be made using different statistical approaches, including simple linear regression analysis and multiple linear regression analysis (Stoltzfus 2011).

The development of predictive models can be an alternative cheap and fast solution for estimating the CBR of soil based on few input parameters, such as particle size distributions, Atterberg's limits (AL), OMC, maximum dry density (MDD), etc. These tests are easy to determination, and usually carried out on any soil samples whenever it is first brought to the laboratory. While these methods are commonly used, they may not always provide accurate correlations (Bardhan et al. 2021) Therefore, more sophisticated approaches are needed. One approach is to use artificial intelligence (AI) to predict CBR.

AI models are designed to identify patterns in data and make predictions based on those patterns, making them more accurate than traditional methods (Shahin et al. 2001). Among the available AI techniques, Taskiran (2010) used two AI-based models, ANN and GEP, to correlate the CBR of fine-grained soils and achieved an accuracy of over 90%. Yildirim and Gunaydin (2011), Kumar et al. (2013), Varghese et al. (2013), Bhatt et al. (2014), Sabat (2015), Erzin and Turkoz (2016), Sadrossadat et al. (2018), Suthar and Aggarwal (2018), González Farias et al. (2018), Fikret Kurnaz and Kaya (2019), Alam et al. (2020), and Islam and Roy (2020) used the ANN-based predictive models were established using different soil types and achieved significant accuracy. Also, the SVM model's performance developed by Sabat (2015), using stabilized soils was satisfactory. Tenpe and Patel (2020) used 389 soil test data and developed two AI-based models, namely SVM and GEP to predict the CBR. artificial neural networks (ANNs), genetic programming (GP), evolutionary polynomial regression (EPR), support vector machines, M5 model trees, and K-nearest neighbors are widely used in different studies. Artificial neural networks (ANNs) have shown promising results in predicting California Bearing Ratio (CBR) values and have been widely used in geotechnical engineering. ANNs can predict CBR values from other soil-characterizing parameters, such as particle size distributions, Atterberg's limits, OMC, and MDD, even when there is a nonlinear relationship between the variables.This study aims to find a correlation between CBR values and index properties, such as liquid limit, plastic limit, plasticity index, OMC, and MDD of soil samples taken from various locations in Addis Ababa city.

1.2 Problem Statement

The California bearing ratio (CBR) value is a widely used measure of the strength of pavement, which is determined by the subgrade or sub-base materials (Haupt and Netterberg 2021). The California bearing ratio (CBR) test can be carried out either in the field or in the laboratory. In the laboratory, the CBR test is conducted on compacted samples, while in the field, it is performed on the ground or on a leveled surface created by excavation in a test pit, trench or bulldozer cut (Yildirim and Gunaydin 2011). However, the CBR test requires a relatively large amount of sample, making it a complex, expensive, and time-consuming process that also requires skilled technicians (Chandrakar and Yadav

2016; Janjua and Chand 2016; Katte et al. 2019; Patel and Desai 2010; Strajhar et al. 2016). This can result in significant delays in project completion, especially as materials for pavement construction often come from highly variable sources. Any delay in construction can lead to a rise in project costs (Chandrakar and Yadav 2016). In contrast, laboratory tests to determine other index properties of soil are much simpler and less time-consuming than the CBR test, although the impact of soil type, Atterberg's limits, and compaction characteristics on the CBR value cannot be ignored (Puri and Jain 2015). Therefore, correlations have been developed between CBR and other soil properties. Other tests are more economical and rapid than the CBR test (Korde and Yadav 2015; Roksana and Muqtadir 2018). In order to predict CBR values for subgrade soil using easily determinable parameters, statistical analysis can be utilized (Katte et al. 2019).

Several studies have utilized simple and multiple linear regression analysis, however, in the field of geotechnical engineering, correlations between different soil properties often exhibit a nonlinear relationship (Shahin 2013). In such cases, the use of artificial neural networks (ANNs) to predict CBR values from index properties is more suitable as the variables are nonlinear and highly variable. Regression analysis can only be applied if prior knowledge about the non-linearity between variables is available. However, in the case of ANN models, such prior knowledge is not required and the nonlinearity between variables can be easily modified by changing the transformation function and the number of hidden layers (Shahin et al. 2001). Due to this reason ANN has been introduced.

ANNs can be used as a powerful data mining tool to model complex phenomena and make predictions based on input data, and thus can be used to predict CBR values to a reasonable degree of accuracy (Tenpe and Patel 2020a). However, most studies in this area have certain limitations. For instance, the amount of data can be limited in some studies, so an artificial neural network may not be able to generate an accurate correlation if the amount of data is not sufficient. It has been found that a number of researchers have been unable to identify the strongest correlation, resulting in inaccurate R and MAE values (Bardhan et al. 2021). For a model to be useful for prediction, there needs to be a thorough understanding of how input parameters interact with output parameters, and a variety of data sets need to be used to train the model in order to ensure that there is an adequate correlation between input parameters and output parameters. Finally, the method needs to be validated properly before it can be used in the real world. Therefore, this study will be able to fill the research gap by developing ANN models using a total of 318 primary and secondary data that will be collected from different parts of Addis Ababa city.

1.3 Research questions

The current study intends to answer the following questions through the research objectives.

1. What is the accuracy and reliability of the developed ANN model in predicting the CBR value of fine-grained soil?
2. Which input parameters in the Artificial Neural Network (ANN) model have the greatest impact on accurately predicting the California Bearing Ratio (CBR) value of fine-grained soil based on its index properties?
3. What are the differences in the performance of a developed Artificial Neural Network (ANN) model and a multiple regression model, and how do they compare in accurately predicting the target variable?
4. How can the accuracy and reliability of the prediction models for the California Bearing Ratio (CBR) value of soil, developed using Artificial Neural Network (ANN), be validated using laboratory soil tests?

1.4 Objective of the study

1.4.1 General objective of the study

The main objective of this study is to develop prediction model for California Bearing Ratio (CBR) of soil based on its index properties using Artificial Neural Network (ANN).

1.4.2 Specific objectives of the study

1. To develop a reliable Artificial Neural Network (ANN) model that can estimate/ predict the California Bearing Ratio (CBR) value for fine-grained soil based on their index properties.
2. To conduct sensitivity analysis to see the most efficient input parameter for output CBR value of fine-grained soil in ANN model.
3. To compare the developed ANN model with a multiple regression model.
4. To validate the ANN prediction model using primary data.

1.5 Significance of the Study

The significance of this research's findings is that the developed ANN model will be used to immediately acquire soil CBR rather than conducting tests on the soil in the study area, saving time and money in the study area. Additionally, this will benefit designers and contractors as they will be able to identify which important properties need to be determined to know the precise strength of the soil. As a result, instead of performing all tests, they will only perform those tests that will determine those important properties. Researchers, practitioners, and others interested in the prediction model of CBR value will find the study's conclusions useful.

1.6 Scope of the study

The research will be conducted using soil test results from different road projects done in Addis Ababa city. Neural network models will be developed to predict the soaked CBR value of fine-grained soil from the index properties. The input and output parameters will be index properties and CBR, respectively. The index properties will include grain size distribution, compaction characteristics and Atterberg limits (i.e., plastic limit, liquid limit, and plasticity index), comprising a total of eight input parameters, and the output parameters will be the soaked CBR value for fine-grained soil.

1.7 limitation of the study

A limitation of this research was the difficulty in obtaining a sufficient amount of data from projects located in Addis Ababa, which made it challenging and time-consuming to develop the prediction models, thus affecting the accuracy of the model. Additionally, due to the wide range of the sample area, it was challenging to conduct all the necessary laboratory tests, further limiting the accuracy of the research findings.

1.8 structure of the study

The research is organized into five chapters as described below.

Chapter one: Introduction is an introductory part containing discussions on background, research problems, the objective of the research, significance of the research, scope, and limitation of the research, and organization or layout of the research.

Chapter Two: Literature review presents relevant related literature on the concept and overview of California bearing ratio (CBR) test, index properties of soil, soil compaction, regression analysis, correlation using regression analysis, Artificial Neural Network, ANN application in geotechnical engineering and research gap.

Chapter Three: Methodology this chapter covers how the research is carried out and covers the research method, material used, procedures, and the data analysis method.

Chapter Four: Results and discussion this chapter presents the analysis of the data that was conducted (primary and secondary) and its result.

Chapter Five: Conclusions and recommendations based on what has been discussed in the previouschapters.

CHAPTER TWO

LITERATURE REVIEW

2.1 Introduction

This chapter focuses on using artificial neural networks to predict California bearing ratio test results. This section mainly categorized in two parts, theoretical and empirical literature review and lastly the literature gap found during reviewing different research papers. It reviews various literature studies that have developed California bearing ratio test prediction models using artificial neural networks. The theoretical part introduces the California bearing ratio test, soil classification, soil index properties, statistical analysis correlations, and artificial neural networks. The empirical part focuses on the applications of artificial neural networks in geotechnical engineering, explicitly presenting studies that have used neural networks to develop prediction models for the California bearing ratio test.

2.2 California Bearing Ratio (CBR)

The development of both rural and urban areas requires a well-connected network of roads, ports, runways, and railways (Fikret Kurnaz and Kaya 2019). However, to establish these infrastructure projects, it is essential to have a firm subgrade or sub-base material (Alam et al. 2020). The strength of the material is measured by the California Bearing Ratio (CBR) value (Erzin and Turkoz 2016; Patel and Patel 2012; Yildirim and Gunaydin 2011), which is a percentage of the actual load required to cause penetration of 2.5mm or 5.0mm compared to standard loads (Arora 2004). California's State Highway Department initially developed the CBR test in the 1920s and later adopted by the US Corp of Engineers in the 1940s for military airfields US (Ibrahim 2017). The CBR value measures the supporting strength of soil and is crucial for geotechnical engineering. Factors such as soil density, moisture content, water content, and prevention of plunger penetration affect the result of a CBR test (Venkatramaiah 1995). Nowadays, CBR testing is widely used globally to assess road materials, pavement subgrade, pavement thickness (Taskiran 2010), highway embankments, retaining walls, earthen dams, and bridge abutments to ensure the quality of the material (Sharma et al. 2020).

2.3 CBR Test Method

The CBR test measures the shearing resistance of soil under specific moisture and density conditions to produce a bearing ratio number. However, the CBR value only applies to the tested soil condition and should be performed at a specific moisture content (Mohammad et al. 1999). The CBR value is often used in the design of road foundations and to determine the suitability of soil for use in roadway construction. The CBR value is determined by comparing the unit load (in kN/m^2) required to penetrate a specific depth of a compacted soil sample at a certain water content and density to the unit load needed to achieve the same penetration depth on a standard specimen of stone. It is the ratio of the pressure per unit area required to penetrate a soil mass with a standardized cylindrical piston at a speed of 1.25 mm/min to that needed for the corresponding penetration of a standard material (Trong et al. 2021) that is expressed in the equation:

$$\text{CBR}(\%) = \frac{\textit{Test unit}\ \text{load}}{\text{Standard load}} * 100 \qquad 2.1$$

The CBR test can be conducted in both laboratory and field settings (Ibrahim 2017), using three different methods. The specimen can be prepared by (i) remolding in the laboratory, (ii) extracting an undisturbed specimen from the field and fitting it tightly into a standard mold in the laboratory, or (iii) testing a fully in-situ specimen on the field (Mishra and Tegar 2019).

2.3.1 Laboratory Testing

The Laboratory CBR (California Bearing Ratio) test, conducted according to AASHTO T 193-63 or ASTM D 1883-73 standards (Molla 2019), assesses soil samples at their ideal moisture content. This content is determined by a standard or adjusted compaction test. The CBR is calculated at the ideal water content or within a specified range of water content from a predetermined compaction test and a specified dry unit weight (AASHTO 2001). Soil specimens are prepared by remolding them at the ideal moisture content and density, compacting three soil molds using standard proctor test (ASTM D 698) or modified proctor test (ASTM D 698) (ASTM 2000). The test method involves a standard plunger advancing into a remolded soil specimen at a predetermined amount of penetration. A modified method with varying numbers of blows and saturating them for 96 hours with an extra charge equivalent to the weight of asphalt in the field. Soaking the sample provides data on the estimated soil spreading under the asphalt, and swell analyses are conducted intermittently.

After soaking, the penetration test is performed at a speed of 1.27 mm/min, and the load needed for penetration is recorded every 0.5 mm. Load resistance is then plotted against penetration distance, and adjustments are made to the load-penetration plot. The bearing ratio is calculated using revised values from the load-penetration plot at 2.54 mm and 5.08 mm penetration, dividing the revised load by the standard load and multiplying by 100. Bearing ratios range from 0 (worst) to 100 (best), and the reported value depends on the penetration depth. In laboratory tests, the design CBR value is based on the bearing ratio rules fulfilled by a specimen remolded at one density and moisture content. If a range of densities is used, the bearing ratio is obtained for each sample and plotted on a Density-CBR graph to estimate the design CBR corresponding to the ideal dry thickness (NCHRP 1-37A 2004). The results of a typical CBR test are depicted in Figure 2.1.

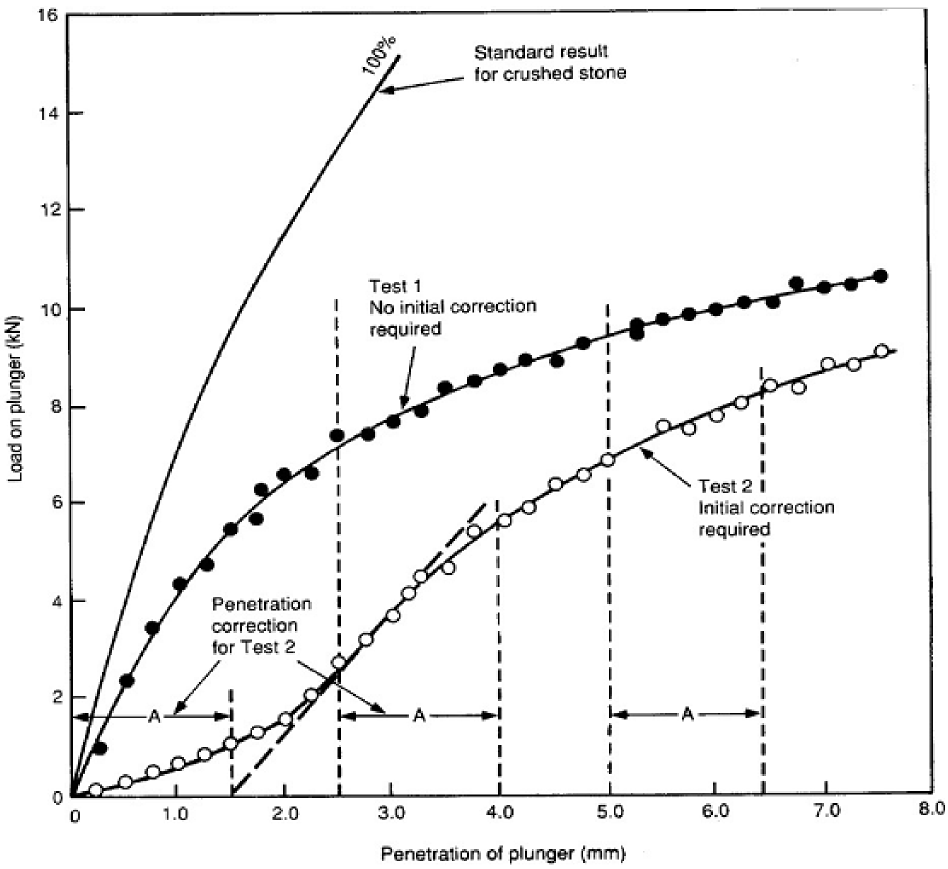

Figure 2. 1 Typical CBR Test Result

2.3.2 In-Situ Testing

Suppose the Field CBR test is to be used directly for design or evaluation without considering changes in water content. In that case, it should be conducted under specific conditions outlined in ASTM D 4429-93 or AASHTO T-193 for soils in the field. The Field CBR test involves preparing the equipment for the penetration test and allowing a plunger to penetrate the soil at a given rate. The force required for penetration at different depths is measured using a modified modeling ring. The results obtained from the in-situ soil are then compared with the relationship between pressure and penetration for a standard material like a stone base (AASHTO 2001). Experimental setup,schematic diagram and test apparatus shows in figure 2.2 (Raja et al. 2022).

Figure 2. 2 Experimental setup for the CBR tests: (a) schematic diagram of the specimen, (b) layout/placement of reinforcement layer at a predetermined depth in CBR mold, (c) test apprunts

In-situ testing can be affected by larger particles that may negatively impact the test outcome, especially in coarser types of in-situ material. Laboratory CBR tests, on the other hand, are limited to particles passing a 3/4-inch (19 mm) sieve size. to ensure consistent results, preventive measures are needed in construction testing activities like evaluation or compression.

To calculate the CBR value, the load required to cause a penetration of 2.54 mm and 5.08 mm is determined from a graph. These values are divided by the standard load of 13.44 kN and 20.15 kN, respectively, required to produce the same penetration in standard crushed stone. The CBR value at 2.54 mm is generally higher than that at 5.08 mm, and the former is used for design purposes. The test should be repeated if the CBR value for 5.08 mm is higher than that for 2.54 mm. If identical results are obtained, the CBR value corresponding to 5.08 mm penetration should be used for the design (AASHTO 2001).

2.4 Interpretation of CBR Value

Asphalt design charts are helpful tools for determining the appropriate thicknesses of subbase, base course, and asphalt-based on estimated wheel loads and design traffic class. These charts allow users to input the CBR or structural number and then read off the required thicknesses (Yoder and Witczak 1991). The CBR is sometimes converted to a subgrade modulus using appropriate graphs or equations before entering the charts. These charts are also used to evaluate the condition of existing asphalt layers. By providing information on suitable asphalt configurations, these charts are essential for designing cost-effective and optimal asphalt thicknesses (Leonardo et al. 2015).

The California Bearing Ratio (CBR) is a crucial parameter used to assess the subgrade's stiffness modulus and shear strength. As the subgrade soil is typically unable to withstand construction and commercial traffic, an asphalt layer is necessary to support the traffic load. The thickness of the asphalt layer depends on the strength of the subgrade, making information on the shear strength of the subgrade necessary before designing any asphalt configuration. A high CBR value indicates that the subgrade is firm, and the thickness of the asphalt can be reduced accordingly. In contrast, a low CBR value means that the thickness of the asphalt must be increased to spread the traffic load over a larger area of the weak subgrade. Alternatively, the subgrade soil may need to be treated or stabilized (Desalegn 2012). The CBR value for a particular soil depends on its density, molding moisture content, and water content, and the penetration resistance of the plunger also affects the CBR test results. The table 2.1 provides relative ratings of supporting strengths as a function of CBR values (Venkatramaiah 1995). Clay soils must have a CBR value of at least 6, while silty and sandy soils should have a CBR value of 6 to 8. Sands and gravels are preferred for highway construction since their CBR values typically exceed 10.

Table 2. 1Relative CBR values for sub-base and sub-grade soil

CBR	Material	Rating
>80	Subbase	**Excellent**

50-80	Subbase	**Very good**
30-50	Subbase	**Good**
20-30	Subgrade	**Very good**
10-20	Subgrade	**Fair-good**
5-10	Subgrade	**Poor-Fair**
<5	Subgrade	**Very poor**

2.5 Index properties of soil

Soil index properties are integral to the classification of soils, and they can be determined via basic laboratory tests. They also act as indicators for specific soil-based engineering applications. Usually, soils with comparable index properties share similar engineering properties (Arora 2004). Soil index properties can be divided into two main classes: grain properties and aggregate properties. Grain properties are related to individual particle features such as size, shape, and mineral makeup, while aggregate properties describe the soil mass overall. As a reminder, the group comprises solid matter and voids containing either water or air (Teferra and Leikun 1999). The critical grain property for fine-grained soils is the mineral composition of the smallest particle, while the primary aggregate property is soil consistency. In contrast, coarse-grained soils' most significant grain property is their grain size distribution, and their most crucial aggregate property is relative density (Mathur et al. 2017).

2.5.1 Classification of soil

There are various classification systems for soils: These systems categorize soils based on their particle size, mineral composition, organic matter content, and other properties that are important for engineers and scientists to consider when studying or using soils in various applications (Arora 2004; Das 2011; V. Murthy 2002).

USCS stands for the Unified Soil Classification System, which was developed by the American Society for Testing and Materials (ASTM) and the United States Bureau of Reclamation. The system categorizes soils into two primary groups: coarse-grained soils, which have particle sizes greater than 0.075 millimeters, and fine-grained soils, which have particle sizes less than 0.075 millimeters. Each group further classifies soils based on their mineral composition and plasticity (Muni Budhu 2011).

ASTM and BS classification systems are similar to USCS, with some variations in terminology and categorization. For example, ASTM classifies soils into seven groups based on their hydraulic conductivity, compressibility, and shear strength. BS categorizes soils into eleven groups based on their plasticity, shear strength, and permeability (Smith and Smith 1988).

AASHTO, or the American Association of State Highway and Transportation Officials, developed its classification system specifically for soils used to construct highways and other transportation infrastructure. The AASHTO system categorizes soils into seven groups based on particle size distribution, plasticity, and estimated strength characteristics (Das 2015).

Overall, soil classification systems provide a helpful framework for understanding and working with various soils in different regions and environments. Some classification systems below offer a range of sizes for each category, as detailed in Figure 2.3 (Muni Budhu 2011).

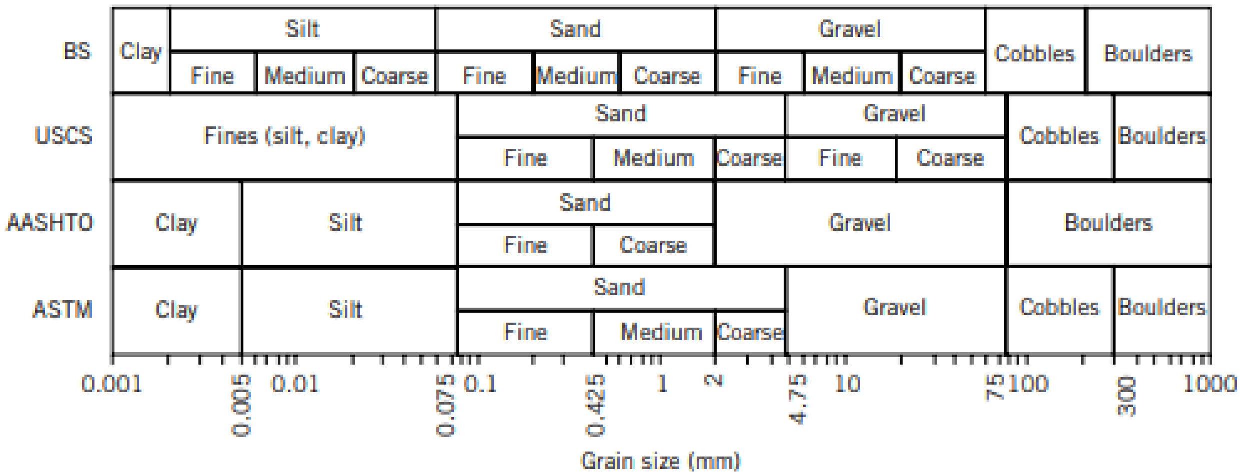

Figure 2. 3 compares four systems for describing soils based on particle size.

2.5.2 Grain size distribution

Grain size distribution is the distribution of soil particles in a soil mass expressed in terms of their size. The distribution of soil particles and their size affects soil properties and strength. Particle size analysis defines the percentage proportion of different sizes of particles in the soil mass. Sieve analysis and hydrometer are the two ways to determine grain size distribution for coarse-grained and fine-grained soils, respectively (Teferra and Leikun 1999). Soil grain size distribution is typically represented by grain size distribution curves, which visually display the range of particle sizes in a soil mass. These curves show that soil masses can be classified as well-graded, uniformly-graded (poorly graded), or gap-graded. Well-graded soil has various particle sizes, from coarse gravel to fine particles. In well-graded soil, nearly all particle sizes are represented to some degree within the soil mass. Conversely, uniformly-graded or poorly-graded soil contains particles mainly of the same size. Gap-graded soil is characterized by missing particle sizes, with little or no representation of soil particles within a specific range. Figure 2.4 displays the gradation curves for each soil type (Muni Budhu 2011).

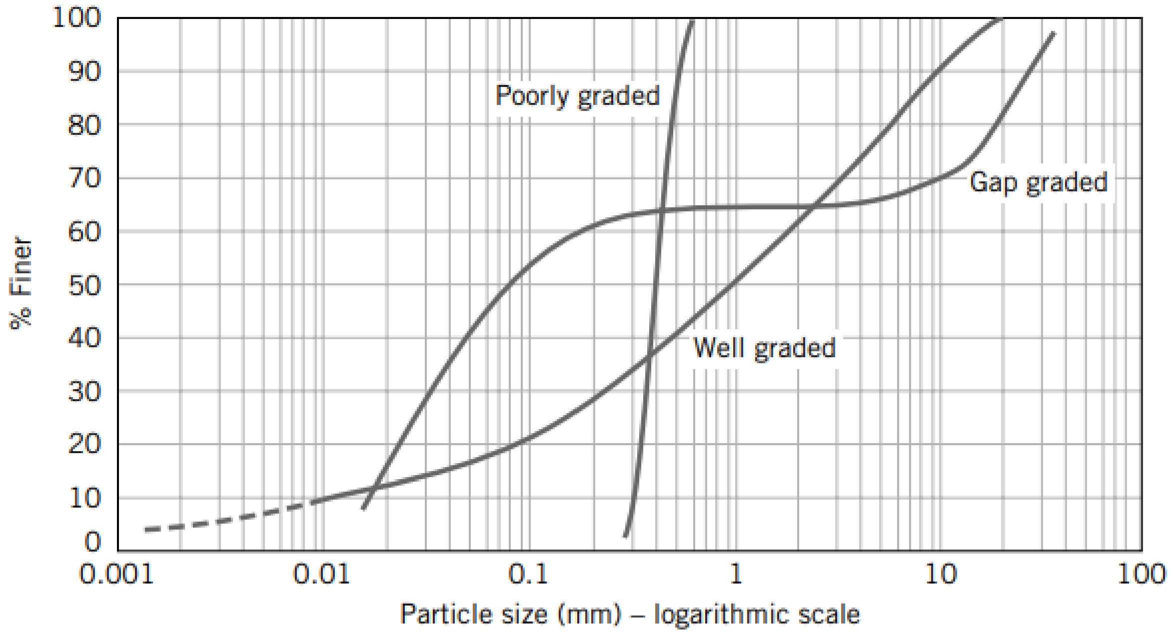

Figure 2. 4 Gradation Curve

There are two parameters commonly used to define soil gradation as poorly graded or well-graded mathematically. These are the coefficient of uniformity and the coefficient of curvature. Since gap-graded soil cannot be detected using the coefficient of uniformity, another parameter called the coefficient of curvature is defined (Arora 2004).

$$CU = \frac{D60}{D10} \tag{2.2}$$

$$CC = \frac{(D60)^2}{D60 * D10} \tag{2.3}$$

The D60 refers to the particle size diameter in the soil beneath which 60% of the particles are smaller, while D10 is the diameter for which 10% of the soil has particles smaller than this size (also known as the effective size). D30, on the other hand, represents the particle diameter beneath which 30% of the particles are smaller.

A soil with a Cu value greater than or equal to 6 is considered well-graded gravel soil, while a Cu value greater than 4 indicates well-graded sand. If the Cu value falls below 2, it shows uniformly-graded soil. Additionally, for soil to be classified as well-graded, it should have a coefficient of curvature (Cc) value between 1 and 3 (Arora 2004; Muni Budhu 2011).

2.5.3 Soil Consistency

The term consistency is a measure of how firm soil is. It is essential for fine-grained soils, which are highly sensitive to changes in moisture content. The consistency of these soils is commonly described using terms such as soft, firm, stiff, or hard, depending on how easily they deform (Arora 2004). To quantify this property, engineers use Atterberg limits, which define the boundaries between different physical states of soil. These states include liquid, plastic, semi-solid, and solid; the soil's water content determines them. Swedish agriculture engineer Albert Atterberg proposed a series of tests to measure these limits, known as consistency or Atterberg limits (Teferra and Leikun 1999). figure 2.5 shows Atterberg limits graph (Das 2011).

I. Liquid Limit

A liquid state of soil means it has a very high moisture content, causing it to flow like water. The soil in this state has no shear strength and cannot resist deformation, no matter how slight. As the moisture content decreases, the soil becomes less fluid and gains some stiffness. At this point, it starts to act plastically and gains some strength (Bowles 1992). The water content level where the soil transitions from a liquid to a plastic state is called the liquid limit, designated as LL or WL.

II. Plastic Limit

When fine-grained soils have a lower moisture content than the liquid limit, they are in a plastic state and can be molded and deformed without breaking. However, if the moisture content is reduced, the soil will become stiffer and crumble when rolled into a thread. As the moisture content is further decreased, the soil transitions from plastic to semi-solid. The moisture content level at the boundary between the plastic and semi-solid states is called the plastic limit, denoted by PL or WP (Arora 2004).

III. Shrinkage Limit

When the moisture content of the soil is below the plastic limit, it is in a semi-solid state. This state is called the solid state. The soil crumbles when molded in this state, and any moisture content reduction results in a volume change. However, if the moisture content is further decreased, the soil will reach a point where no further reduction in moisture content will cause any other volume change. The moisture content at which the soil changes from a semi-solid to a solid state is called the shrinkage limit, denoted by SL or WS. The soil has a constant volume at the shrinkage limit, and no further shrinkage will occur (Arora 2004).

IV. Plasticity Index

The plasticity index is a property of fine-grained soil that indicates the moisture content range in which the soil remains in a plastic state. It is calculated by subtracting the plastic limit from the liquid limit and is denoted by PI or IP (Teferra and Leikun 1999). This index is important because it helps us understand the soil's plasticity. If the plastic or liquid limits cannot be determined, the soil is classified as non-plastic (NP). If the plastic limit exceeds the liquid limit, the plasticity index is considered zero, not negative (Mathur et al. 2017). The value of the PI tells us how plastic the soil is (Bowles 1992). table 2.2 shows plasticity index with its range (V. Murthy 2002).

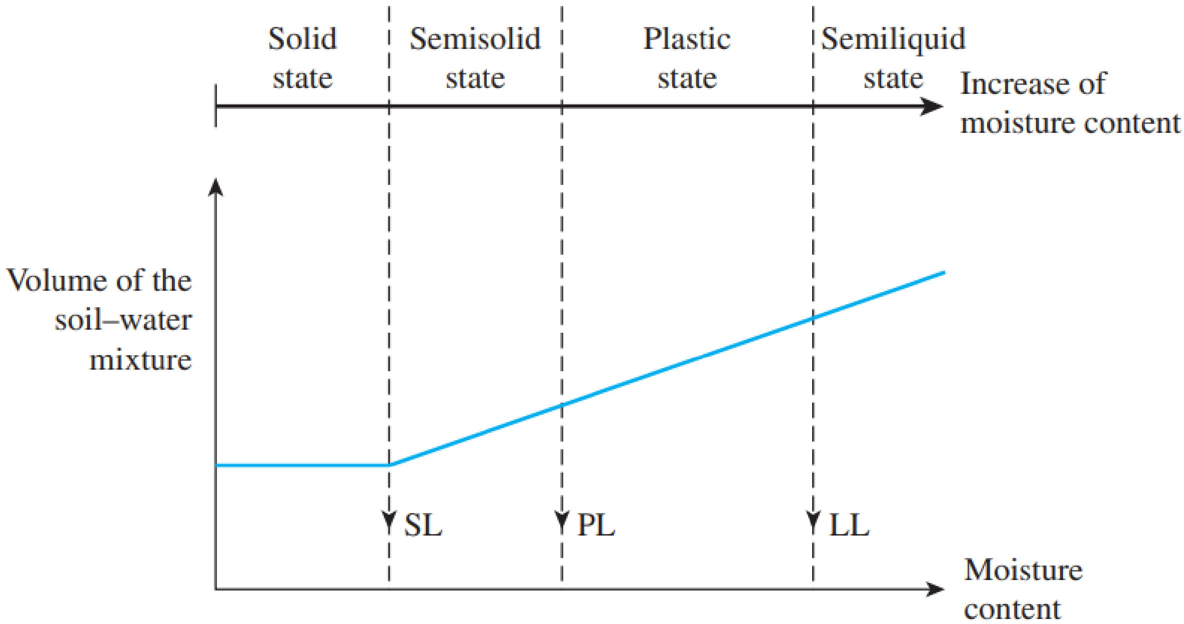

Figure 2. 5 Atterberg Limits

Table 2. 2 Plasticity Index of Soil

Plasticity index	Plasticity
0	Non-Plastic
<7	Low Plasticity
7-17	Medium Plasticity
>17	High Plasticity

The plasticity characteristics of fine-grained soils are used to classify them into different categories. The USCS soil classification system uses a plasticity chart, shown in Figure 2.6 (Das 2011), to classify these soils. The A-line on the chart is used as a dividing line between clay and silt soils. Soils above the A-line are classified as clay soils, while those below it is silt soils. These soil types are further categorized as highly plastic and low plastic soils based on their liquid limit values. A liquid limit value of 50 is used to separate highly plastic and low plastic soils. Soils with a liquid limit greater than 50 are considered highly plastic, while those with a value below 50 are regarded as low plastic. Fine-grained soils are generally classified based on their location relative to the A-line and liquid limit values. The classifications include CH (high plasticity inorganic clay), OH (high plasticity organic clay), CL (low plasticity inorganic clay), OL (low plasticity organic clay), MH (high plasticity inorganic silt), OH (high plasticity organic silt), ML (low plasticity inorganic silt), and OL (low plasticity organic silt) (Arora 2004).

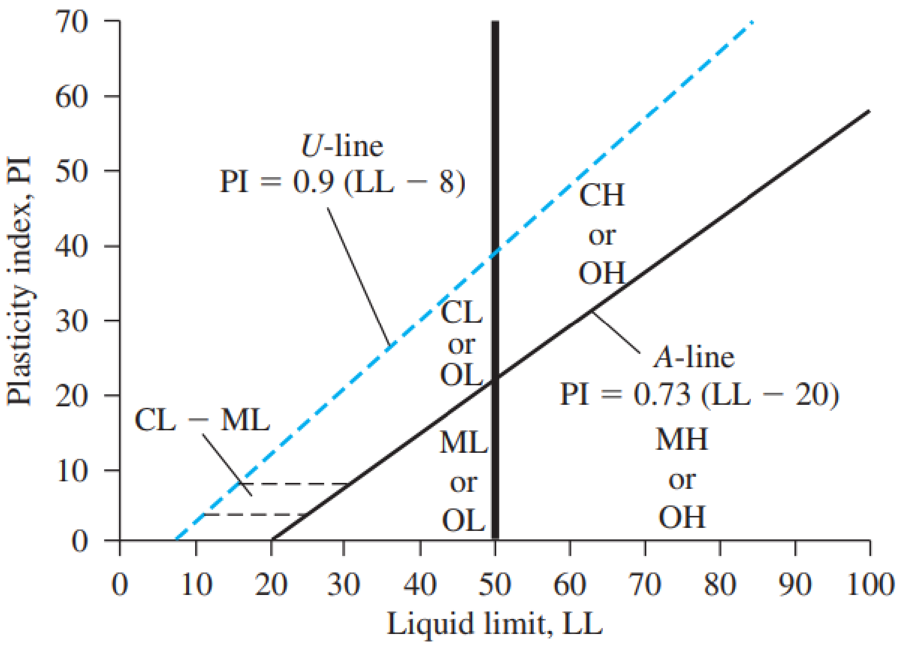

Figure 2. 6 Plasticity Chart

2.5 Soil Compaction

Compaction is a soil improvement technique that rearranges soil particles to achieve a maximum density with a minimal void ratio (Bowles 1992). The natural soil found at construction sites may not always have the strength to support structural loads. In such cases, compaction increases dry soil density and enhances soil strength. When the existing soil condition is unsuitable for construction, replacing the natural soil with suitable fill material may be necessary. Compaction is also essential to place the fill material in layers (Das 2011).

2.5.1 Compaction Laboratory Test

Before conducting compaction in the field, it is necessary to perform a laboratory compaction test to determine the appropriate compaction energy and moisture content required. There are two common types of laboratory compaction tests: the standard Proctor test and the modified Proctor test (also known as the modified AASHTO test). The maximum dry density and optimum moisture content values obtained from the laboratory test serve as the standard for the field compaction.

The standard Proctor test was developed by Ralph Roscoe Proctor in 1933, while the modified Proctor test was standardized by the American Association of State Highway and Transportation Officials (AASHTO). The modified Proctor test uses more compaction energy than the standard Proctor test, resulting in higher dry density at a lower optimum moisture content (Arora 2004).this shown in figure 2.7.

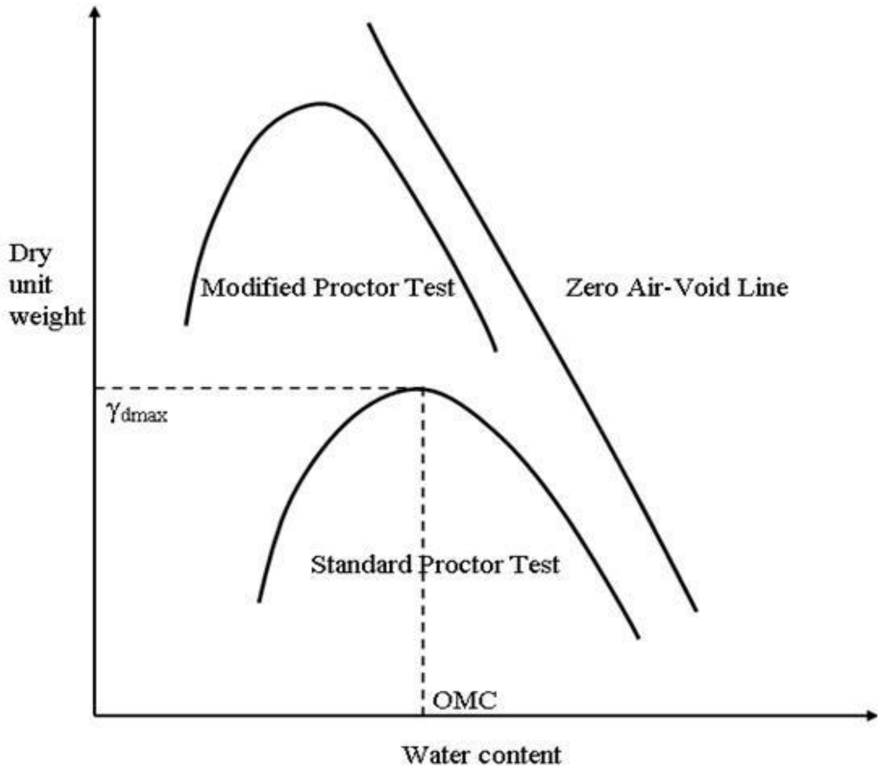

Figure 2. 7 Standard and Modified Compaction Curves

To achieve maximum dry density during field compaction, the results from laboratory tests must be applied as closely as possible. The natural moisture content of the soil in the field should be adjusted to the optimum value previously determined in the laboratory as shown in table 2.3 (Hn and Naagesh 2014). If the field soil has an excess moisture content, it should be allowed to dry out, and if it has less than the optimum value, water can be added either through sprinkling or directly into the borrow pit. Typically, the desired moisture content can be achieved within a range of error between 2% to 3% (Terzaghi Karl 1996).

2.6 Regression Analysis

Regression analysis is a statistical technique used to examine and quantify the relationship between one or more independent variables and a dependent variable. In regression analysis, the goal is to find the best-fitting line through observations. This line is determined by minimizing the squared difference between the observed and predicted values based on the line. The resulting line is the regression line or the line of best fit. The dependent variable is the outcome variable influenced by changes in one or more independent variables.

Table 2. 3 Compaction Laboratory Test Methods

	Standard Proctor ASTM 698			Modified Proctor ASTM 1557		
	Method A	Method B	Method C	Method A	Method B	Method C
Material	≤20% Retained on No. 4 Sieve	> 20% Retained on No. 4 ≤20% Retained on 3/8" Sieve	>20% Retained on No. 3/8" <30% Retained on 3/4" Sieve	≤20% Retained on No. 4 Sieve	> 20% Retained on No. 4 ≤20% Retained on 3/8" Sieve	>20% Retained on No. 3/8" <30% Retained on 3/4" Sieve
For test sample, use Soil Passing	Sieve No.4	3/8" Sieve	3/4" sieve	Sieve No.4	3/8" Sieve	3/4" sieve
Mold	4" DIA	4" DIA	4" DIA	6" DIA	4" DIA	6" DIA
No. of Layers	3	3	3	5	5	5
No. of blows/layer	25	25	56	25	25	56

The independent variables are the predictors or factors that are used to explain the variation in the dependent variable. The relationship between the dependent and independent variables can be expressed mathematically using a regression equation (Sarstedt and Mooi 2014).

$$Y = f\left(x\right) \qquad 2.4$$

Where Y denotes the dependent variable, and X represents the independent variable in statistical analysis, relationships between variables are imperfect and may not follow a strict function. Therefore, regression analysis aims to identify the best-fitting line that provides the most accurate representation of the relationship between the dependent and independent variables. This best-fit line is determined by minimizing the difference between the observed data and the line. Regression analysis is used to determine how much an independent variable affects the value of a dependent variable. It also helps to determine which independent variable strongly influences the dependent variable.

Furthermore, regression analysis can be used to predict future outcomes based on the observed data.

Regression analysis is categorized into two types based on the relationship between dependent and independent variables: linear and non-linear regression analysis. Linear regression assumes a linear relationship between the variables, while non-linear regression is used when the connection is non-linear. Non-linear regression models are more appropriate when the linear regression model fails to describe the relationship accurately.

Regression models are also classified based on the number of independent variables used: simple and multiple regressions. The choice of model depends on the nature of the relationship between the variables and the number of independent variables used in the analysis. A simple regression model contains only one independent variable, while a multiple regression model has more than one independent variable. The use of multiple regression models can provide more accurate predictions and help identify the individual contributions of each independent variable to the dependent variable. In summary, regression analysis offers various options to analyze the relationship between variables, including linear and non-linear regression models and simple and multiple regression models.

2.7 Correlations using Regression Analysis

Research on CBR conducted in the past wasn't always able to be done due to certain limitations, leading researchers to develop various predictive models based on test data. One early model was Black's (1962) correlation for estimating the CBR of cohesive soils using parameters like plasticity and liquidity indices. Johnson and Bhatia (1969) proposed another correlation between CBR and suitability index considering properties such as plasticity, grading characteristics etc. Agarwal and Ghanekar (1970) identified a correlation between CBR, LL, PI and OMC where they found an improved correlation when using OMC with LL resulting in a high measure of accuracy that can allow preliminary identification of soils to be undertaken with confidence.

Stephens (1992) examined the viability of existing models by collecting archival data from Natal Roads department in Pietermaritzburg. He observed that most of the existing models were insufficient and focused on clay fraction's impact on CBR. He drew upon soil gradation and shrinkage properties to calculate the minimum CBR for non-shrinking and shrinking soils. Further, he remarked about lack of a suitable correlation for universal implementation. To build upon his research, Al-Refeai and Al-Suhaibani (1997) conducted an extensive investigation into prediction of CBR using dynamic cone penetrometer test data. Later, National Cooperative Highway Research Program NCHRP 1-37A (2004) proposed two empirical equations connecting CBR to index properties of soil – one each for clean (fine content ≥12%) and coarse grain soils (non-plastic).

A study by Kin (2006) revealed the limitations of NCHRP's equation when it came to calculating CBR values. For coarse-grained soils, there was a significant difference between predicted and measured CBR values. Meanwhile, in fine-grained soils, the correlation between predicted and actual CBR yielded moderate accuracy as Kin (2006) obtained. In addition, various regression equations have been proposed over the years, with authors utilizing simple and multiple regression techniques on basic soil properties (grain sizes, compaction characteristics, Atterberg Limits, OMC, MDD, etc.); to ascertain its CBR. These studies provide insight into effective ways of predicting soil strength based on its characteristics (Alawi and Rajab 2013; Bhatt et al. 2014; Erzin and Turkoz 2016; Fikret Kurnaz and Kaya 2019; González Farias et al. 2018; Katte et al. 2019; Patel and Desai 2010; Suthar and Aggarwal 2018; Talukdar 2014; Varghese et al. 2013; Yildirim and Gunaydin 2011).

After reviewing the many studies conducted (Agarwal and Ghanekar 1970; Al-Refeai and Al-Suhaibani 1997; Black 1962; De Graft-Johnson et al. 1969; Kin 2006; NCHRP 2004; Stephens 1992), it became apparent that most of these empirical equations had limited applicability, due to an insufficient degree of accuracy (Taskiran 2010). Furthermore, subsequent analyses (Alawi and Rajab 2013; Bhatt et al. 2014; Erzin and Turkoz 2016; Fikret Kurnaz and Kaya 2019; González Farias et al. 2018; Katte et al. 2019; Patel and Desai 2010; Suthar and Aggarwal 2018; Talukdar 2014; Varghese et al. 2013; Yildirim and Gunaydin 2011) were lacking in reliability due to the small sample sizes used in their regression analysis (Wang and Yin 2020).These results indicate that a more sophisticated, yet reliable, method is needed for predicting CBR based on existing experimental data.

2.8 Artificial Neural Networks

Artificial intelligence (AI) is a scientific field focused on constructing and optimizing algorithms used to create behavior based on empirical data. AI can be used in engineering problems when physical meanings are complex and hard to explain (El-Shahat 2018). AI techniques have the advantage over most physically-based empirical and statistical methods because they can learn examples from data presented to them, allowing for the capture of subtle functional relationships between the data (Shahin 2016). Almeida (2002) state AI algorithms as one of the most applicable for the prediction of non-linear engineering issues is artificial neural networks (ANN).

McCulloch and Pitts published the first paper on Artificial Neural Networks (ANNs) in 1943 (McCulloch and Pitts 1943). As Bendana et al. (2008) explain, ANNs are a parallel distributed processor that can take input data and store it in memory within its network. Fundamentally, ANNs are computational models based on the workings of the human brain and nervous system (Cebrián 2021) as seen in Table 2.4 (Dongare et al. 2012) and Figure 2.8 (El-Shahat 2018). These networks are composed of numerous elements that are interconnected and process information in response to external inputs – they 'learn' from presented data examples instead of relying on prior knowledge about the nature of the relationships. This gives them an advantage over traditional approaches when dealing with complex behaviors or unknown situations between inputs and outputs, rendering them a practical method for many application (Fatehnia and Amirinia 2018).

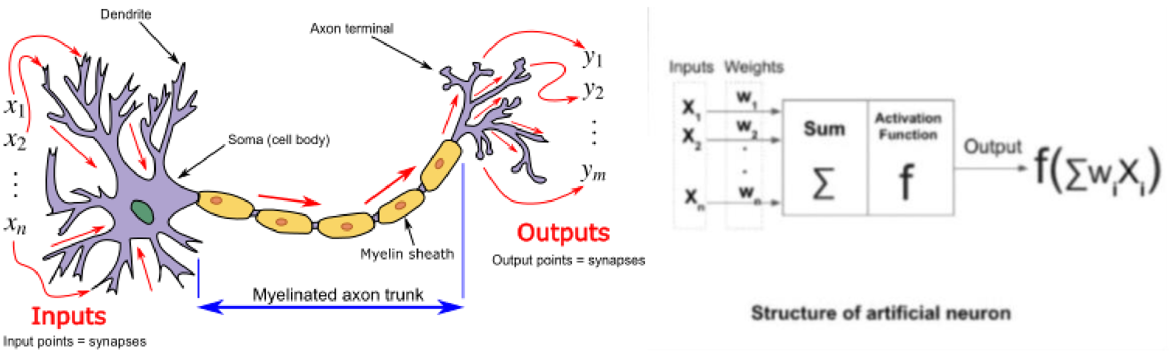

Figure 2. 8 Neural network (biological and artificial

Table 2. 4 Terminology of Neuron

Biological Terminology	ANN Terminology
Neuron	Node/Unit/Cell/Neurons
Synapse	Connection/Edge/Link
Synaptic Efficiency	Connection Strength/Weight
Firing Frequency	Node Output

ANNs have been successfully applied to a wide range of engineering problems since the early 1990s. The typical structure of an ANN consists of interconnected processing elements, or neurons, arranged in logical layers. These layers include the input, hidden, and output layers, as illustrated in Figure 2.9 (El-Shahat 2018). Neurons in each layer are connected to all the neurons in the next layer via weighted connections (Fatehnia and Amirinia 2018).

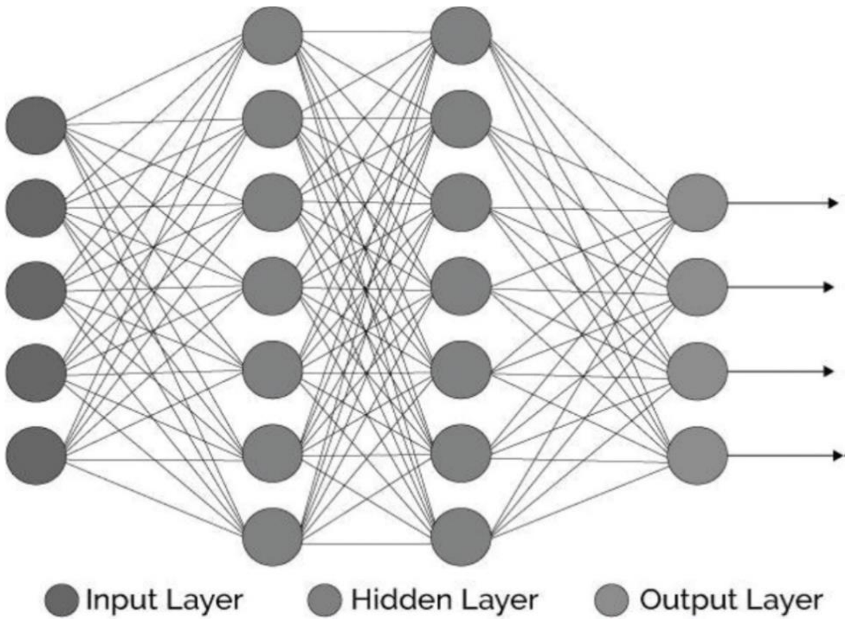

Figure 2. 9 Multilayer neural network

Thoroughly explain the above by mentioning Fatehnia et al. (2016) as: Inputs are presented to the network through the input layer, which communicates to one or more hidden layers where complex computations are performed through a system of weighted connections. The hidden layers enable ANNs to represent and compute intricate associations between inputs and outputs. The output layer then connects to the hidden layer and provides the network's response to the input. Additionally, there is a bias with modifiable weighted connections that are only connected to neurons in the hidden and output layers. ANNs can be autonomous and learn from external "teachers" or even self-teach from written rules. The performance of an ANN model can be evaluated based on several criteria, including the coefficient of determination (R^2), mean squared error (MSE), mean absolute error (MAE), minimal absolute error (MinAE), and maximum absolute error (MaxAE). A well-trained model should result in an R^2 value close to 1 and small values for error terms (Banimahd et al. 2005).

2.8.1 Types of ANN

A neural network can be broadly classified into the following types based on its architecture, i.e., how neurons are connected;

- Feedforward Neural Network and
- Recurrent Neural Network

The feedforward neural network can be used to model relationships between input variables and output variables (Barza et al. 2005). In feedforward neural networks, signals travel only in one direction from input to output. In any layer, the output does not travel to other nodes within that layer or previous layers. The result of such an architecture is usually a straightforward neural network.

Feedforward neural networks can be classified as either single-layer or multilayer, depending on the number of layers they contain as shown in table 2.5 (Kim 2017). A single-layer neural network has only one input and one output layer, making it the simplest form of neural network. Single-layer networks are only capable of computing linearly separable problems. In contrast, multilayer neural networks have one or more hidden layers in addition to the input and output layers (Tesfaye and Potdar 2020). A neural network with a single hidden layer is known as a shallow neural network or vanilla neural network. A multilayer neural network with two or more hidden layers is referred to as a deep neural network Deep neural networks are the most commonly used models in practice and figure 2.10 shows types of neural network (Kim 2017).

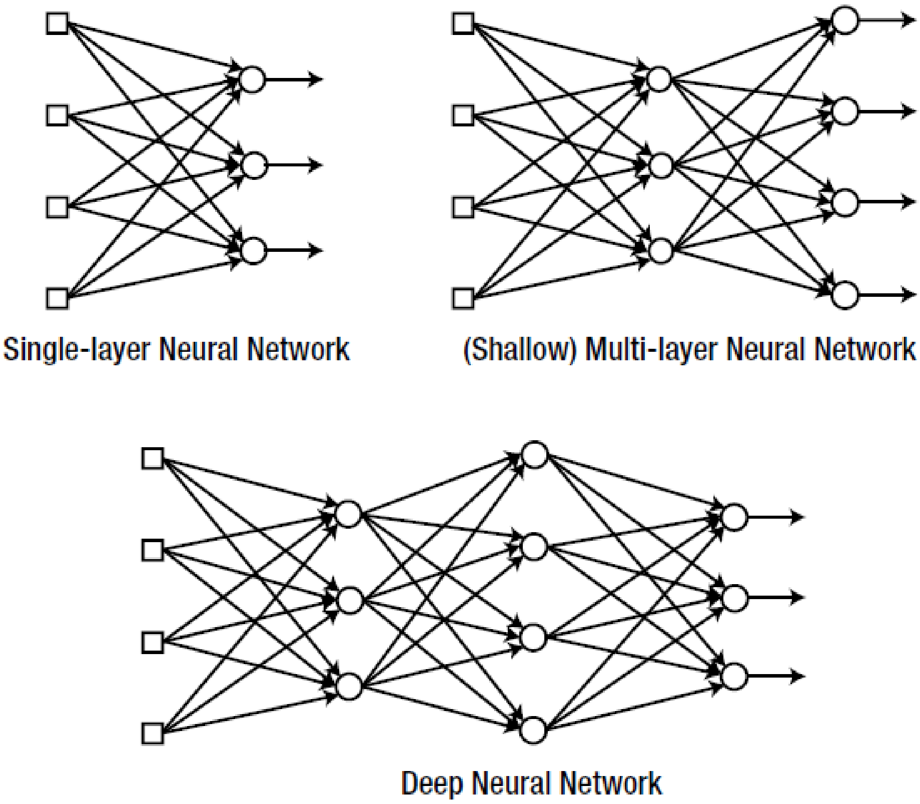

Figure 2. 10 The type of the neural network depends on the layered architecture.

Table 2. 5 Illustration of type of neural network

Single-Layer Neural Network		Input Layer-Output Layer
Multi-Layer Neural Network	Shallow Neural Network	Input Layer- Hidden Layer-Output Layer
	Deep Neural Network	Input Layer-Hidden Layer-Output Layer

Recurrent Neural Networks (RNNs) use a feedback architecture that allows signals to travel in both forward and backward directions, creating a loop. This architecture is highly powerful and suitable for various applications. Unlike multilayer feedforward neural networks that are limited to static problems, RNNs can be applied to dynamic systems and can process time-series information. At least one feedback connection is required in recurrent networks, which can lead to complex network structures. In networks with a feedback architecture, the complexity can increase significantly as shown in figure 2.11 (Alavi et al. 2010).

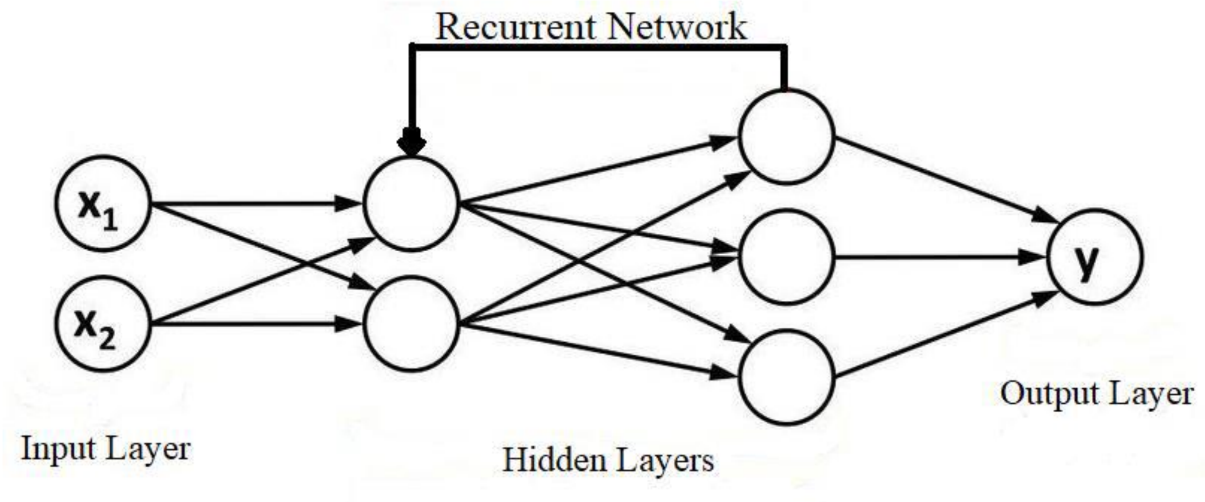

Figure 2. 11 Recurrent Neural Network

2.8.2 Learning Methods of ANN

A wide range of Machine Learning techniques have been developed to address problems in various fields. These techniques can be broadly classified into three types based on the training method used as:

- Supervised Learning
- Unsupervised Learning
- Reinforcement learning

1. Supervised Learning, also known as Associative Learning, involves providing both inputs and outputs to the network during training as shown in figure 2.12 (Dongare et al. 2012). The network processes the input and compares its resulting output to the desired output. Any errors are then propagated back through the system, causing the weights that control the network to be adjusted. This process is repeated multiple times, with the weights being continually refined. The set of data used for training is referred to as the "training set," and during training, the same data is processed many times as the connection weights are adjusted to improve performance (Maind and Wankar 2014).
2. Unsupervised Learning or Self-organization in which an (output) unit is trained to respond to clusters of patterns within the input. Unlike the supervised learning paradigm, there is no a priori set of categories into which the patterns are to be classified; rather the system must develop its own representation of the input stimuli (Dongare et al. 2012). In this paradigm, the system is supposed to discover statistically salient features of the input population.

3. Reinforced Learning is a type of Learning that may be considered as an intermediate form of the above two kinds of Learning. Reinforcement learning employs sets of input, some output, and grade as training data. It is generally used when optimal interaction is required, such as control and game plays (Kim 2017).

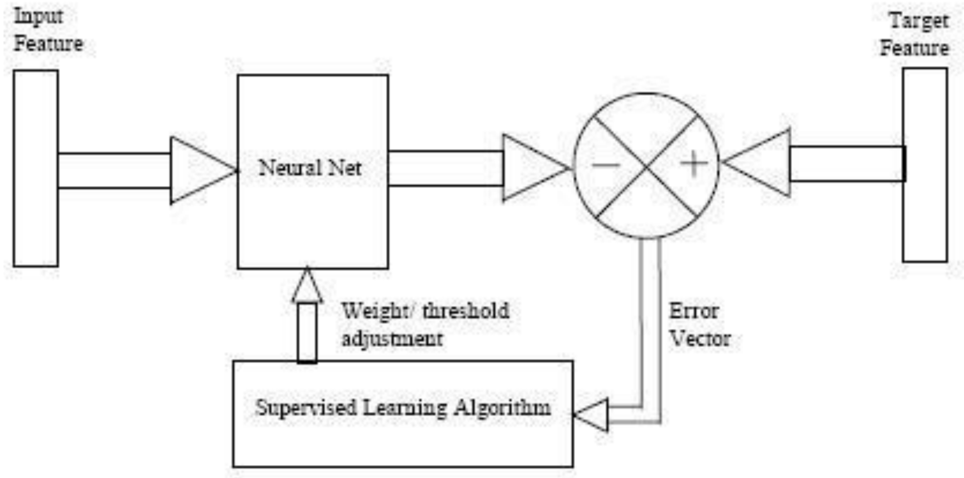

Figure 2. 12 Supervised Learning

2.8.3 ANN Computation

The fundamental processing unit of an ANN is the artificial neuron, as illustrated in Figure 2.13, The neuron performs mathematical operations on the inputs xi to compute the output y using the following equations:

$$y = \varphi\left(\sum_i \left(\omega_i x_i\right) + b\right) \tag{2.5}$$

ANN's basic processing unit is the artificial neuron, shown in Figure 13. The neuron applies the following mathematical operations in the inputs x_i to calculate the output y:ω_i is the synaptic weights, b is the bias, which increases or decreases the activation function input, and φ is the activation function, which limits the neuron output to a predetermined range as shown in figure 2.13 (De Oliveira et al. 2017).

In the equation, x_1,$x_{2,}x_3$…….x_m,ω_1, ω_2, ω_3 ... ω_m and y represent the input, weight, and output values, respectively. As inputs propagate from the input layer neurons to the neurons in the subsequent layer, they are multiplied by their corresponding weights. When they reach the next neuron, their sum is computed, and the bias b is added to the weighted sum of inputs (Kim 2017).

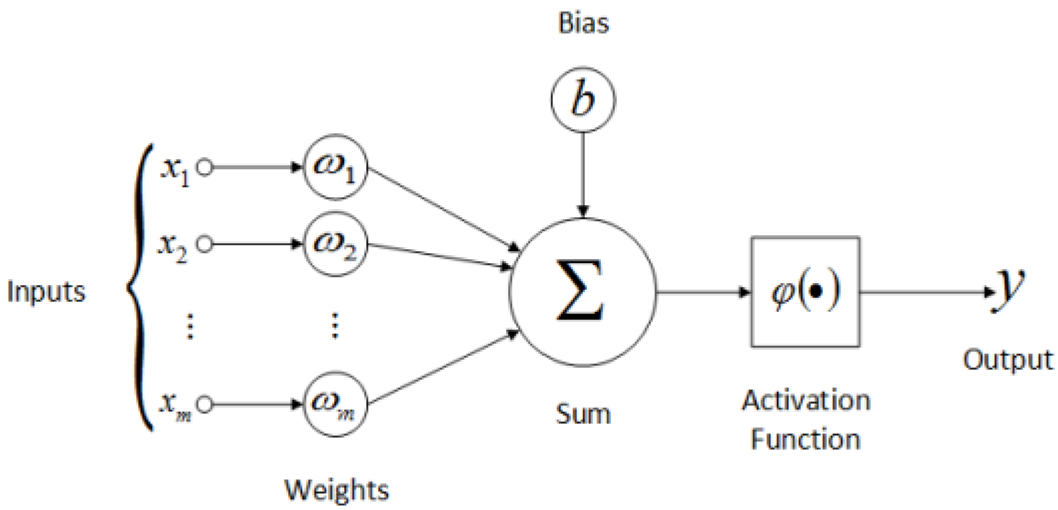

Figure 2. 13 Mathematical model of artificial neuron

$$\sum = \left((x_1\omega_1) + (x_2\omega_2) + \ldots (x_m\omega_m) \right) + b \tag{2.6}$$

In order to infer more complex relations between inputs and outputs, multiple neurons are connected in several architectures (De Oliveira et al. 2017), shown in Figure 2.14. The weighted sum then will be entered into the activation function to give the output value.

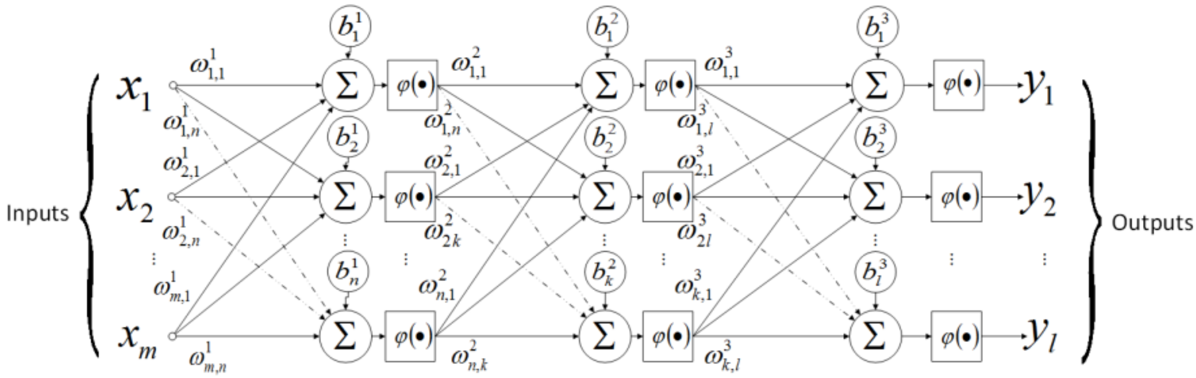

Figure 2. 14 Generic multilayer feedforward neural network

2.8.3.1 Inputs

Getting input data right is critical as it forms the basis for learning and evolving networks. Inputs are the building blocks of neural network training. They refer to data from outside a neuron with origin points within or outside the given neuron (Karsoliya 2012).

2.8.3.2 Weights

Weights, represented by w coefficients, indicate how much influence input data has on neuronal cells. Every input has a weight that must be considered during the connection between inputs and output values. The higher the weight, the greater its effectiveness; conversely, low weights imply that input is insignificant (Elmas 2007).

2.8.3.3 Summing function

The purpose of a linear combiner is to estimate the net input received by a neuron. This is done by summing up all the entries and weights, then selecting the most suitable function to do this depending on the circumstances. The effectiveness of the summing function can be determined through trial and error (Park et al. 2015).

2.8.3.4 Activation function

The neuron's output value is kept within a defined range through an activation function. This function establishes a connection between the cell's input and how it should create the output. Through careful evaluation of the total amount of input, the appropriate result for each stage can be effectively produced (Haykin and Network 2004). Neurons are activated according to purpose, commonly by sigmoid or hyperbolic tangent functions. This activation enables the neuron to fulfill its intended role in the neural network and contribute to the desired output (Cebrián 2021).

Table 2. 6 Activation Functions Performance Analysis of Various Activation Functions in Artificial Neural Networks

Activation function name	Function	Range
Binary Activation Function	$f(x) = 1\ if\ x > 0,\ f(x) = 0\ if\ x < 0$	(0,1)
Sigmoid function	$f(x) = \frac{1}{(1+e^{-x})}$	(0,1)
Hyperbolic tangent function (Tanh)	$f(x) = \frac{e^{x}-e^{-x}}{e^{x}+e^{-x}}$	(-1, 1)
Sinusoidal function	$f(x) = \sin(x)$	[-1, 1]
Linear Activation Function	$f(x) = x$	(-∞,∞)
Logistic symmetric function	$f(x) = \frac{(1+e^{-x})}{2}$	(0, 1]

Gaussian function	$f(x) = e^{-x^2}$	(0, 1)

2.8.4 Steps for Training an Artificial Neural Network

The following are significant steps for training a multilayer feedforward neural network with supervised Learning.

I. Data Preprocessing

Ensuring your data is ready for machine learning is critical to successful algorithms. Data preprocessing helps improve raw datasets with noise, outliers, and inconsistencies to prepare them for processing better. Various techniques, such as cleaning, reduction, and transformation of the data, helps normalize different measurements into an equal range and provide a suitable form for the model. The most popular transformation methods are Min-max and Z scores normalization. With these critical steps completed, you can ensure that any ML algorithm runs efficiently and gives the desired results (Han et al. 2011).

II. Data Division

After the data has been preprocessed, it is split into three categories, namely training, validation, and test sets. The proportions of data in these sets can vary, and there are no strict rules for dividing the data in this way. In supervised learning, the training set comprises data that is used to train the neural network, and it contains labeled inputs and outputs. When the model processes the inputs, its outputs are compared to the actual outputs, and the difference between them is used to compute the error (El-Shahat 2018). The weights of the network are then updated to minimize this error using the gradient descent method, which is a commonly used optimization algorithm in supervised neural networks (Kim 2017).

A validation set is a set of data that is distinct from the training set and is not used in the training process. Its purpose is to determine when to terminate the training process and prevent overfitting. Overfitting occurs when a model performs well on the training set but poorly on the validation set, indicating that it has become too specialized to the training data and lacks generalization ability on other datasets. This is a common challenge in training neural network models (Kim 2017).

A test set is comprised of data that is distinct from both the training and validation sets. In this set, the neural network is presented with input values only, without the corresponding output values. The network's task is to generate output values for the new test data. The purpose of a test set is to evaluate the performance of the network and its ability to generalize to new data (Gallo 2015).

III. Define the Architecture of the Neural Network

To define the architecture of an artificial neural network, the number of inputs, output, and hidden neurons in each layer must be determined. The number of input neurons in the input layer is equal to the number of input variables used in training, and the number of output neurons in the output layer is equal to the desired number of output variables. However, determining the number of hidden layers and hidden neurons is more complex. There are various methods suggested by researchers to determine the appropriate number of hidden layers (Vujičić et al. 2016), which depends on the amount of training data and the complexity of the problem. Typically, two hidden layers are sufficient to solve most non-linear complex problems (Varghese et al. 2013). However, for applications where accuracy is crucial and training time is not limited, multiple hidden layers can be used to increase model accuracy. It is important to note that increasing the number of hidden layers beyond the optimal value can lead to overfitting, which reduces the generalization ability of the model. To address this issue, researchers have developed different approaches to estimate the number of hidden layers, with a structured trial and error method being the most commonly used (Karsoliya 2012).

IV. Back Propagation

The most commonly used type of training algorithm in supervised learning is the backpropagation algorithm. In this algorithm, after computing the error (i.e., the difference between the model's output and the actual output), the error is propagated back through the hidden layers to the primary input layers. The aim of backpropagation is to modify the weights during this process. An epoch refers to one cycle from the input layer to the output layer and back from the output layer to the input layer through the hidden layers (Hecht-Nielsen 1992). During training, the neural network undergoes several epochs to minimize the error within a specified range. The network is considered trained when the error between the model output and the actual output is minimized or falls within a given range. The final adjusted weights of the trained network can then be used to compute the outputs of new data sets (Cebrián 2021).

2.8.5 Learning Data Sets

Artificial Neural Networks have three learning data sets:

I. A training data set is a collection of samples that is utilized to teach the neural network how to adjust its parameters (Anupama. U 2016), i.e., weights. During the training process, the network is presented with the training set, and one complete training cycle is executed. The network's parameters are adjusted based on the error it produces during this training cycle (Varghese et al. 2013).

II. A validation data set is a collection of examples that is utilized to fine-tune the parameters, i.e., architecture, of the neural network. For instance, it can be used to determine the optimal number of hidden units in a neural network. After the weights have been corrected, the network is then validated using a separate set of known samples that have not been used in training. This validation process aims to assess the generalization capacity of the neural network using data that has not been seen during the training process (Othman and Abdelwahab 2022).

III. A test data set is a collection of examples that is solely used to evaluate the performance and generalization ability of a fully specified neural network or to make predictions for a given input. These examples do not affect the training process and thus provide an unbiased measure of network performance during and after training (Othman and Abdelwahab 2022).

Once the architecture is defined, the model must undergo training and validation. During the training phase, the weight vector is modified by comparing the results obtained from a previous configuration with the desired output for known sample data. This comparison produces an error for each neuron, and the weights are then adjusted accordingly. The training process continues until the error for all neurons is minimized, as determined by a predefined threshold or stopping criterion (Bardhan et al. 2021).

2.9 Applications of ANNs in Geotechnical Engineering

Geotechnical engineering is a field of engineering that deals with materials such as soil and rock, and it forms the basis for various construction projects. Traditional methods used in geotechnical engineering are limited in their ability to accurately predict the non-linear and plastic properties of soil and rock. Machine learning techniques, on the other hand, are capable of effectively addressing these non-linear and plastic issues and avoiding the limitations of older methods. Among the machine learning algorithms, the artificial neural network (ANN) algorithm is a particularly popular choice in geotechnical engineering. The two most prevalent applications of ANN in supervised learning are classification and prediction. Classification involves determining which group a set of data belongs to, while prediction aims to estimate a specific value based on given inputs (Shahin 2013). There are numerous applications of ANN in geotechnical engineering, such as soil classification, prediction of California bearing ratio, soil permeability, slope stability, settlement of structures, and more (Shahin et al. 2001).

In recent years, researchers have sought out machine learning and artificial intelligence techniques to address complex geotechnical problems (Alam et al. 2020; Fikret Kurnaz and Kaya 2019; Hassan et al. 2021; Islam and Roy 2020; Nagaraju et al. 2021; Onyelowe et al. 2021; Othman and Abdelwahab 2022; Raja et al. 2022; Salahudeen et al. 2019; de Souza et al. 2022; Suthar and Aggarwal 2018; Taha et al. 2019; Tenpe and Patel 2020a; Tesfaye and Potdar 2020; Trong et al. 2021). These advanced ML models are particularly suited for non-linear modeling, making them a feasible approach for simulations. Studies have shown that several AI-based models can effectively predict the California Bearing Ratio (CBR) of soils (Tien Bui et al. 2018). Among these methods include Artificial Neural Network (ANN), support vector machine (SVM), gene expression programming (GEP), generalized regression neural network (GRNN), multilayer perceptron neural network (MLPN), and group method of data handling (GMDH) modeling techniques. The results demonstrate the power of ML/AI methodologies in predicting the CBR values of soils.

Alam et al. (2020), Suthar and Aggarwal (2018), Salahudeen et al. (2019), Othman and Abdelwahab (2022), (Raja et al. 2022), (Khasawneh et al. 2022), (Onyelowe et al. 2021) and (Fikret Kurnaz and Kaya 2019) used experimental data (the number of data was in the range of 40 to 158 only) of different soils to establish the ANN-based predictive models and achieved significant accuracies (values of R^2 ranging from 0.94 to 1.0). (Salahudeen et al. 2019) developed the ANN model, and the available data (a total of 72 data sets) were divided into their subsets. In this work, the data were randomly divided into three sets: a training set for model calibration, a testing set, and an independent validation set for model verification. In total, 70% of the total data set was used for model training, 15% was used for model testing and the remaining 15% was used for model validation. Once available data are divided into their subsets, the input and output variables were pre-processed, in this step, the variables were normalized between -1.0 and 1.0. For the normalized data used in training, testing, and validating the neural network, the performance of the simulated network was very good having R values of 0.9986 and 0.991 for the soaked and unsoaked CBR respectively. These values met the minimum criteria of 0.8 conventionally recommended for strong correlation conditions. All the obtained simulation results are satisfactory and a strong correlation was observed between the experimental soaked and unsoaked CBR values as obtained by laboratory tests and the predicted values using ANN.

Using 207 experimental datasets of different soils, (Taha et al. 2019) established an ANN-based prediction model of CBR and found satisfactory prediction accuracy of about 97% (R2 = 0.97). (Tenpe and Patel 2020a) used 389 soil test data and developed two AI-based models, namely ANN and GEP to predict the CBR. The developed model for ANN resulted in maximum accuracies of about 89% (based on R^2 value), respectively. (Nagaraju et al. 2021) developed the ANN model using 480 tests data and found decent accuracy (about 91% based on R^2 value) as well. (de Souza et al. 2022) with large number of data set (1790) developed a model that result about 94% accuracy based on R^2 value.

From the literature presented above, it is observed that the ANN model was mostly used to predict the CBR of soils, and a high degree of accuracy (values of R^2 ranging from 0.89 to 1.0) was usually achieved in many cases. However, detailed scrutiny of the studies given above reveals that the works performed with small datasets (number of datasets was smaller than 200) showed higher predictive accuracies (values of R^2 were scattered between 0.94 and 1.00) compared to the studies conducted with large datasets ranging from 389 to 1790 soil test results (Nagaraju et al. 2021; de Souza et al. 2022; Tenpe and Patel 2020). When small datasets are used for AI-based models, the extremely high performance of the model is obtained but these are generally overlearned and have not generalization ability. On the other hand, the results also indicated that the prediction accuracy of the ANN model decreases with an increase in number of samples (accuracy attained in the range of 0.89 to 0.95 in terms of R^2), which is quite disagreeable (Wang and Yin 2020). It is pertinent to mention that the works based on large dataset are more reliable compared to the works performed with limited number of samples. This means, a predictive model with a greater accuracy level derived from studying a large number of samples should be accepted with more conviction.

The performance of the developed models was assessed based on six widely used performance parameters (Bardhan et al. 2021; Verma and Kumar 2022),namely, coefficient of determination (R^2), variance account factor (VAF), root mean square error

(RMSE), mean absolute error (MAE), and mean square error (MSE).It is pertinent to mention that, many researchers used two to three parameters, such as R^2, RMSE, MAE, etc. for assessing the performance of the prediction models (Fikret Kurnaz and Kaya 2019; Hassan et al. 2021; Islam and Roy 2020; Othman and Abdelwahab 2022; Raja et al. 2022; Salahudeen et al. 2019; de Souza et al. 2022; Suthar and Aggarwal 2018; Taha et al. 2019; Tenpe and Patel 2020) Theoretically, the value of the correlation coefficient (R) ranges between - 1 and + 1. Strong negative correlation between the actual and predicted variable is indicated by R = - 1, whereas a value of R = +1 indicates strong positive correlation. In case of R = - 1, the value of predicted variable decreases with the increase of actual values, while it is vice versa when R = +1. To neutralize the –ve term of the correlation coefficient, R^2 is normally used.

Therefore, it is not easily possible to judge the prediction capability of any model based on the values of R^2 only. Typically, we assume that a model with $R^2 = 1$ is a perfect model, which may not be correct in every time. We cannot assure that a model with $R^2 = 1$ will have zero RMSE or MAE values; instead, a model with RMSE or MAE equal to zero, should have $R^2 = 1$. On the other hand, the concept of perfect model (i.e., $R^2 = 1$ and RMSE = MAE = 0) is a utopian idea. Thus, it is always recommended to determine at least 3 to 4 error parameters (such as RMSE, MAE, MSE, VAF etc.) along with 3 to 4 trend measuring parameters (such as R^2, VAF etc.) for assessing the performance of any predictive model from different aspect.

Table 2. 7 Summary of the recent papers that used ANNs for the prediction of the CBR value for the soil subgrade samples.

ANN Models	**Data sets**	**Input Parameters**	**R^2**
(Suthar and Aggarwal 2018)	51	MDD, OMC, lime percentage, lime sludge percentage and curing period days for predicting the CBR of Stabilized Pond Ash with Lime and Lime Sludge	0.9863
(Fikret Kurnaz and Kaya 2019)	158	Grain size distribution, LL, PL, PI, MDD, and OMC.	0.9570
(Salahudeen et al.	72	Grain size distribution, LL, PL, PI, MDD and	0.9972

2019)		OMC.	
(Taha et al. 2019)	207	Grain size distribution, LL, PL, PI, MDD, OMC, SG, LS, Cu, and Cc.	0.97
(Alam et al. 2020)	42	SG, Cu, Cc, LL, PL, PI, MDD and OMC.	0.996
(Tenpe and Patel 2020a)	389	Grain size distribution, LL, PL, PI, MDD, and OMC.	0.894
(Nagaraju et al. 2021)	480	Gravel, Sand and Fines, LL, PL, OMC and MDD	0.91906
(Onyelowe et al. 2021)	121	LL, PL, and PI, MDD, OMC, and clay activity are used for predicting the CBR value of hydrated–lime activated rice husk ash treated soil.	0.95
(Raja et al. 2022)	97	Grain size distribution, LL, PL, PI, MDD, OMC, tensile strength of geosynthetic reinforcement, number of reinforcement layers, position of the first reinforcement layer and position of the subsequent reinforcement layers.	0.944
(Othman and Abdelwahab 2022)	77	Grain size distribution, LL, PL and PI, MC and MDD.	0.945
(de Souza et al. 2022)	1790	Grain size distribution, LL, PL, PI, MDD and OMC.	0.9435
(Khasawneh et al. 2022)	110	OMC, MDD, LL, PL and PI, density, gradation parameter (percent of materials retained on sieve #200 (R200), and percent of materials retained on sieve #10 (R10))	0.9461

2.10 Literature Gap

Within the scope of our review of related works, it has become evident that there exist critical research gaps in the realm of estimating California Bearing Ratio (CBR). The identification of these gaps serves as a catalyst for further investigation aimed at refining outcomes and enhancing our comprehension of CBR estimation applications. The following research gaps have been discerned:

1. Limited Application of ANN Software in CBR Studies in Addis Ababa

A noteworthy gap in the existing body of research pertains to the underutilization of Artificial Neural Network (ANN) software for resolving CBR-related challenges specific to Addis Ababa. Previous studies have not extensively explored the potential of ANN in this context, leaving ample room for its application and exploration.

2. Need for Enhanced Methodology and Dataset

Prior research conducted by Yared Laliso focused on CBR prediction using a dataset consisting of a mere 41 observations. This relatively small dataset size raises concerns about the robustness of regression analyses. Furthermore, the reliance on SPSS software, which may not be optimally suited for engineering purposes, underscores the necessity for employing more suitable tools, such as MATLAB 2018, for both simple and multiple regression analyses.

3. Absence of Developed ANN Models for Addis Ababa's Fine-Grained Soils

A striking research gap exists concerning the lack of developed ANN models specifically tailored for the fine-grained soils of Addis Ababa. Given the city's substantial infrastructure development projects, the absence of predictive models represents a significant void. This research seeks to address this gap by leveraging a comprehensive dataset encompassing both primary and secondary data sources.

4. Need for Comparative Analysis with Traditional Empirical Methods

While the potential of ANN models for predicting CBR in subgrade soils has been demonstrated in previous studies, a gap remains regarding their comparative assessment against traditional empirical methods. Discrepancies in data quantity, data quality, neural network architecture, and other variables have the potential to influence results significantly. Consequently, it is essential to refrain from direct result comparisons across different studies. Instead, this research employs identical datasets for simple regression, multiple regression, and ANN analyses, allowing for an accurate evaluation of accuracy and effectiveness in practical applications. Such an approach will offer valuable insights into the performance of ANN models relative to traditional methods in the context of CBR prediction.

CHAPTER THREE

RESEARCH METHODOLOGY

3.1 Introduction

This chapter provides a comprehensive overview of the specific materials and methods utilized in the research process, including the identification, selection, processing, and analysis of data. The chapter delves into the various topics in detail, such as research design, sampling techniques, data collection methods, data analysis procedures, fieldwork processes, and all other related procedures involved in the research. By providing a detailed account of the research methodology, the chapter enables other researchers to replicate the study and validate the findings.

3.2 Study Area

The study area considered in this research is Addis Ababa, the capital city of Ethiopia. Addis Ababa is located at $9^{o}1'48''$N, 38^{o} $44'24''$E, with an average altitude of 2400 meters above sea level. The city's temperature ranges between 23°c and 11°c throughout the year. According to the 2007 E.C census, the population of Addis Ababa was 3,273,000, making it the largest city in the country in terms of population. The current population of the city is estimated to be around 5 million while the annual population growth rate is estimated to be 2.1%. Addis Ababa takes up 3.6% of the national population and 18% of the urban population in Ethiopia (Abnet Gezahegn Berhe 2020).

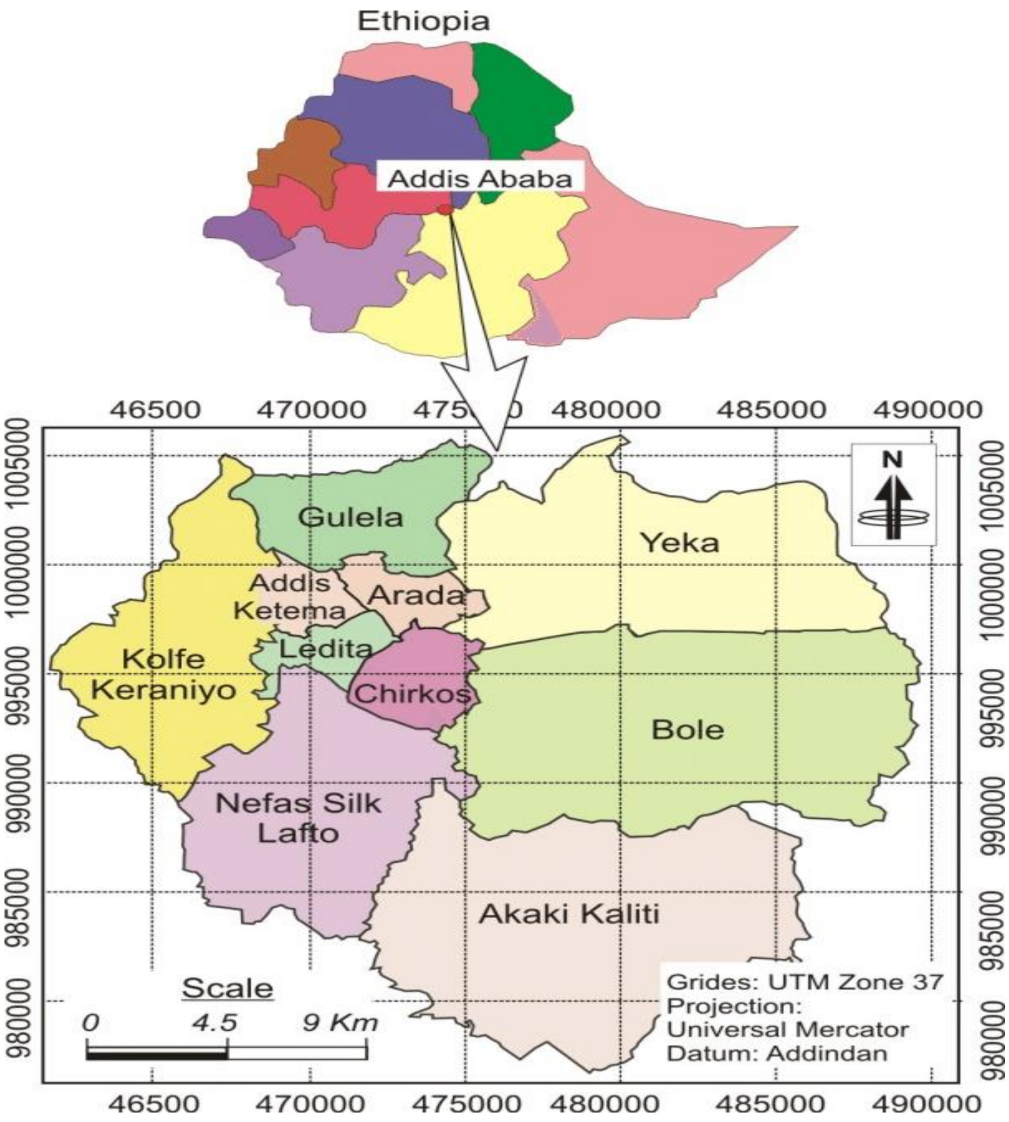

Figure 3. 1 Map of Addis Ababa City Administration

3.2.1 Geology of the Study Area

Addis Ababa is located on the western edge of the main Ethiopian rift valley, where the margin exhibits Mio-Pliocene volcanic activity and is characterized by normal faults that extend towards the rift. The upper boundary of this margin is denoted by a large fault that runs east-west, just north of the Addis Ababa-Ambo road. Meanwhile, the lower boundary runs parallel to the principal systems of fissures on the rift-floor, stretching from Nazareth to the Awash station. Various researchers, such as Haile and Getaneh (1989), have proposed geological and volcanic stratigraphic sequences for the Addis Ababa area. According to Haile and Getaneh (1989), the suggested volcanic succession, from bottom to top, is Alaji Basalts, Entoto silicics, Addis Ababa Basalts, Nazareth Group, and Bofa Basalts, spanning the Miocene-Pleistocene period.

3.2.2 Soil Distribution in Addis Ababa

The development of soil in the Addis Ababa area is primarily a result of the physical disintegration and chemical decomposition of volcanic rocks. The weathering products can either remain in place and form residual soils or be transported and deposited in low-lying flat lands and depressions, as noted by (Alemayehu et al. 2003). Detrital materials from high areas, such as Entoto, Furi, Wechecha, and Yerer, are carried along stream courses and deposited in the piedmont area. In the central, western, and southwestern parts of Addis Ababa, old rocks (both acidic and basic) contribute to the formation of thick soil profiles through weathering. However, in locations where welded tuffs and young basalt are present, the thickness of soil cover is reduced (Alemayehu et al. 2003).

According to Tsehayu and Hailemariam (1990), the engineering geological soil units in the Addis Ababa area can be classified into five groups: alluvial, alluvial fan, lacustrine, colluvial, and residual soils. Alluvial soils consist of channel and terrace deposits that can be observed in certain locations along the Kebena and Akaki rivers. These soils comprise stratified deposits of clay and gravel that are transported by stream. Meanwhile, alluvial fan deposits occur in areas where there is a decrease in gradient from a hill to a plain along a river section. The soil becomes coarser near the mouth of the river and finer towards the outer edges. This type of soil is found in the Entoto region, which is dissected by deep gullies (Tsehayu and Hailemariam 1990).

In the Addis Ababa area, lacustrine soils, also referred to as black cotton soils, are located in flat and relatively low-lying regions. These soils exhibit extremely high plasticity and are highly prone to swelling in comparison to other soil types found in the area. Black cotton soils are prevalent in low-lying areas of Addis Ababa, such as Mekanisa, Ayertena, Akaki, Kality, Lideta, and Bole. The thickness of these soils varies from 2 to 10 meters, with the thickest layers located in the Bole and Beklo Bet regions at around 5 meters thick, as noted by Tsehayu and Hailemariam (1990) and shown in figure 3.2.

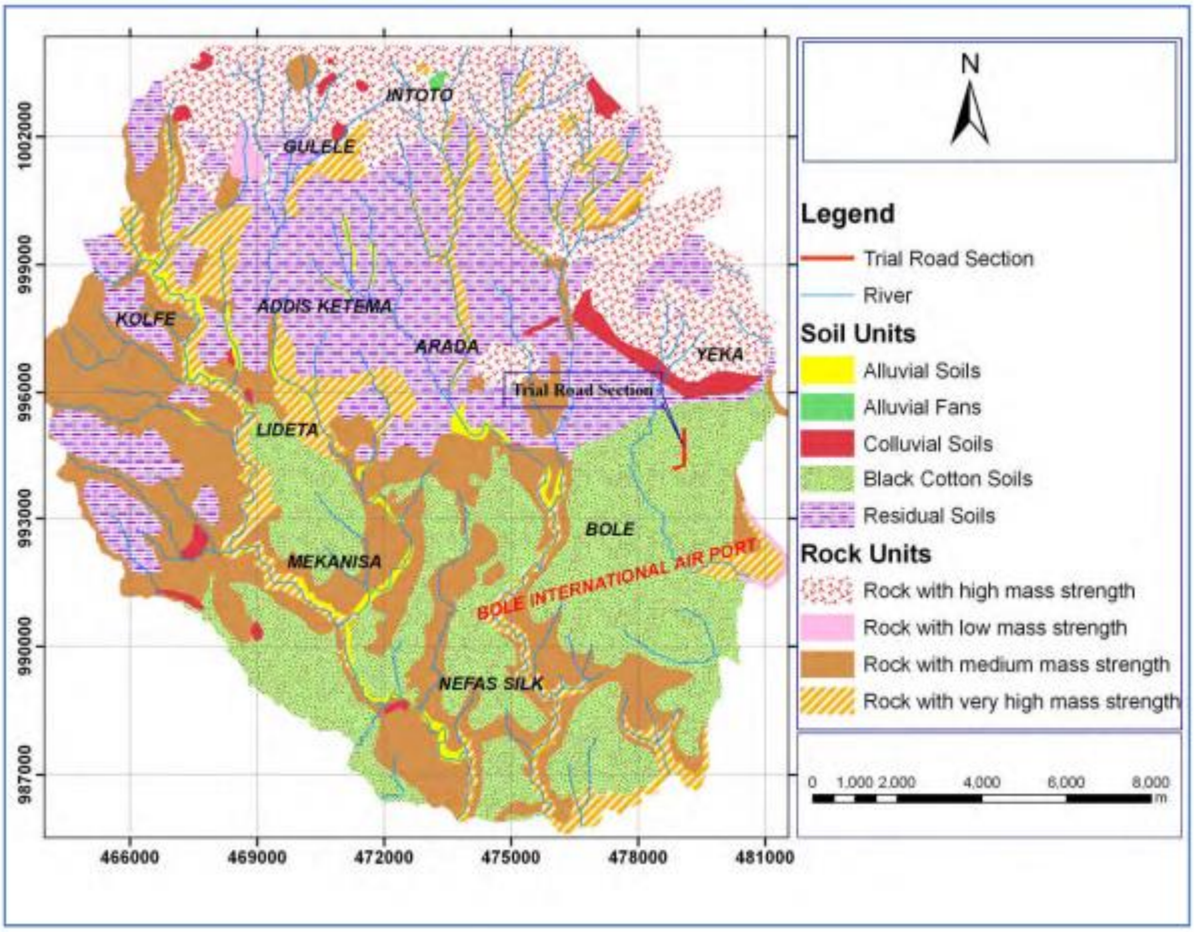

Figure 3. 2 Engineering Geological Map of Addis Ababa

3.3 Study design

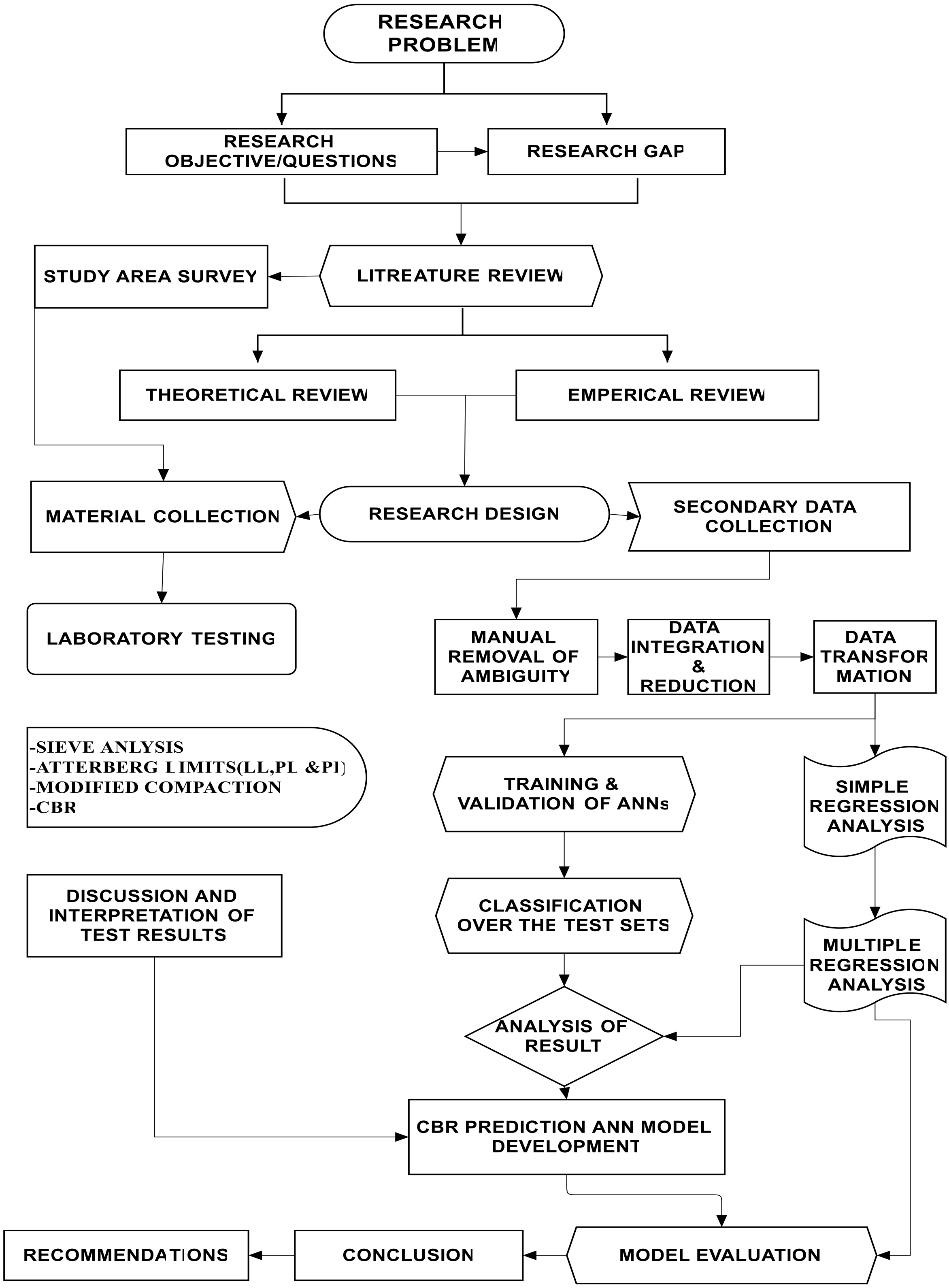

Figure 3. 3 Study Design

3.4 Data collection and Sample size

In this research, a total of 318 soil sample test results were utilized, which was based on the training requirements of the artificial neural network. It is advisable to employ a larger number of data points to develop an artificial neural network to enhance its generalization potential and minimize errors. Among the 318 data sets, 302 were secondary data to train the ANN models, while the remaining 16 were primary data (i.e. determined in the laboratory) were used to validate the neural networks. The secondary data were sourced from the Addis Ababa Construction and Road Authority (AACRA).

3.4.1 Primary Data Collection

To validate the developed models, primary data was obtained by conducting soil laboratory tests on randomly collected soil samples from various locations in Addis Ababa. The samples were collected to ensure that the established neural networks could be applied to any type of soil found in the city.

The number of soil samples to be collected was determined based on the necessary sample size required for statistical analysis, which primarily depends on the maximum statistical uncertainty u of the average (equation 3-1) (Madsen 2016).

$$\left(2\frac{\sigma}{u}\right)^2 \qquad 3.1$$

As per Madsen's recommendation and as Gashaw et al. (2022) implemented, it is not necessary to specify both the standard deviation σ and the statistical uncertainty u. Instead, specifying the desired ratio between σ and u is sufficient. Hence, in the absence of knowledge of the standard deviation, the required sample size can be determined based on the maximum statistical uncertainty, which is half of the standard deviation obtained. To ensure that $\frac{\sigma}{u}$ is at least 2, sixteen soil samples were collected from known areas of Addis Ababa as determined by equation 3.1 with $\frac{\sigma}{u} = 2$.

3.4.2 Sampling Area

To select the locations for primary data samples, a visual site investigation was conducted, and relevant information regarding soil type and distribution throughout Addis Ababa was gathered. The field identification of soils was conducted in accordance with ASTM D 2488 (Standard Practice for Description and Identification of Soil). The selected sample locations were chosen to characterize the soil types in the city, and test pits were excavated to obtain the samples. Sixteen soil samples were collected from known areas of Addis Ababa where, including Gofa camp, Delber, Addisu Gebeya, Megnagna, Winget, Ayer Tena, Bethel, Shgole, Kore Adebabay, Lideta, Leghar, Tikur Anbesa, Shiromeda, Akaki, and Koye fech,as shown in Figure 3.2. This table summarizes the specific location and depth of the samples taken for primary data.

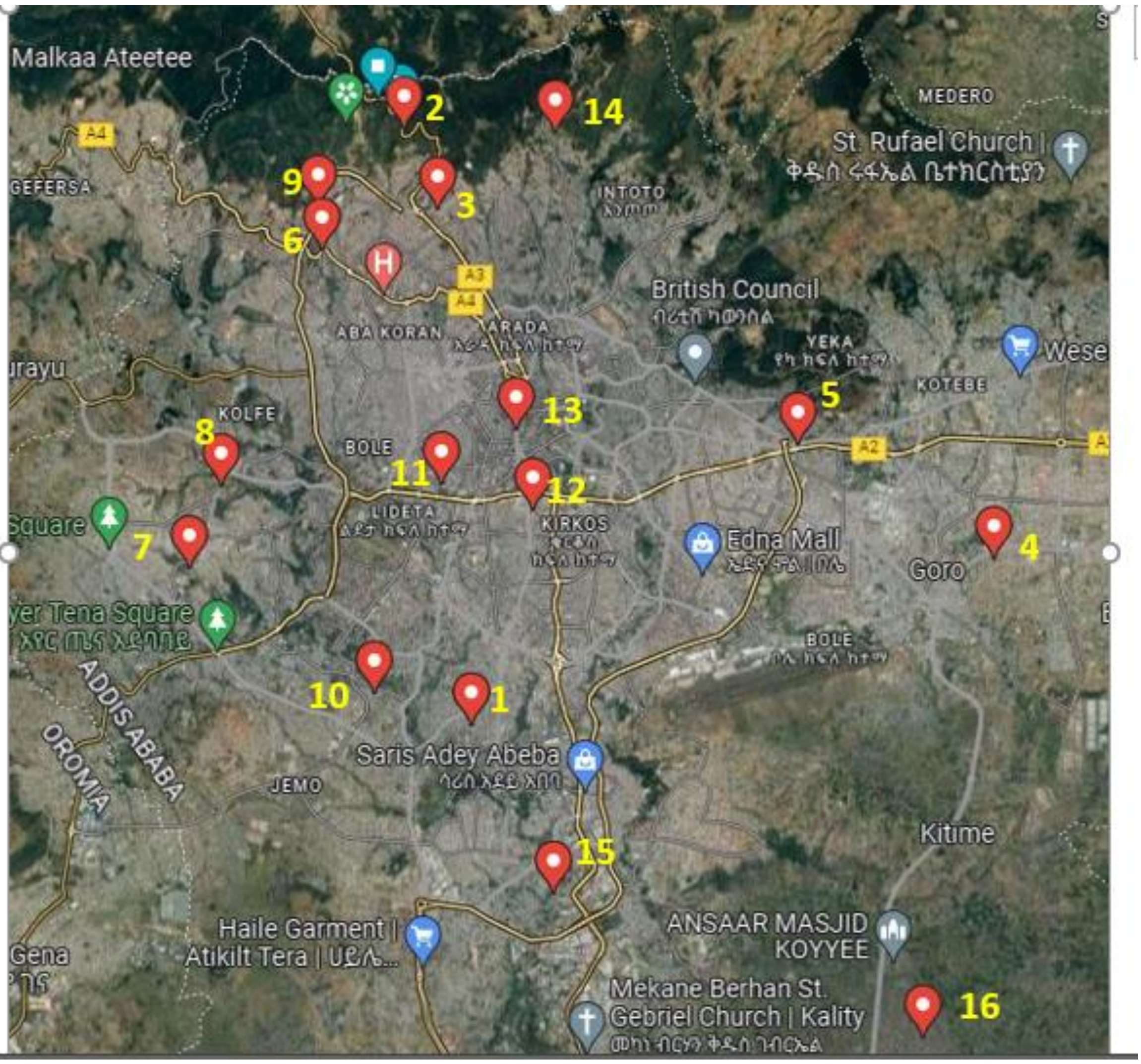

Figure 3. 4 Google locations of sampling test pits

Table 3. 1 Location and Depth of Soil Samples for Primary Data

NO.	Sample Name	Location	Latitude	Longitude	Sample Depth (m)
1	Sample 1	Gofa Camp	8.9695695	38.7439795	1.5
2	Sample 2	Delber	9.078056	38.731496	1.5
3	Sample 3	Addisu Gebeya	9.063333	38.737778	1.5
4	Sample 4	Goro	9.0000547	38.8400869	1.5
5	Sample 5	Megnagna	9.020731	38.8040915	1.5
6	Sample 6	Winget	9.05594221	38.7164744	1.5
7	Sample 7	Ayer Tena	8.998056	38.691944	1.5
8	Sample 8	Bethel	9.0131447	38.6979849	1.5
9	Sample 9	Shgole	9.0636093	38.7157384	1.5
10	Sample 10	Kore Adebabay	8.975556	38.726111	1.5
11	Sample 11	Lideta	9.013333	38.738333	1.5
12	Sample 12	Leghar	9.008889	38.755278	1.5
13	Sample 13	Tikur Anbesa	9.023333	38.752222	1.5
14	Sample 14	Shiromeda	9.077222	38.759444	1.5
15	Sample 15	Akaki	8.939089	38.7591322	1.5
16	Sample 16	Koye Fech	8.912962	38.826913	1.5

3.5 Input and Output Variables Description

The initial stage of the research involved collecting and reviewing previous publications related to the study. Previous studies have shown that California bearing ratio (CBR) is significantly correlated with various index properties of soils (Othman and Abdelwahab 2022; Tenpe and Patel 2020a), the most important factors representing the behavior of CBR were identified based on the literature review discussed in chapter two. Using this information, different combinations of input parameters were proposed, and finally, Liquid

Limit (LL), Plastic Limit (PL), Plasticity Index (PI), Gravel % (GP), Fine % (FP), Maximum Dry Density (MDD), and Optimum Moisture Content (OMC) were selected as the optimal input parameters for this study. It is crucial to select the appropriate input variables that are well-correlated with the desired outputs to achieve good prediction accuracy in a neural network. The input variables must have a clear and direct relationship with the output variables to influence the output's result. To ensure the correlation between the suggested input parameters and the desired output variables, a sensitive analysis was employed. The sensitivity analysis displays the relationship between dependent and independent variables (Raja et al. 2022; Suthar and Aggarwal 2018; Trong et al. 2021). The input variables were used as independent variables, and the output variables were used as dependent variables. The correlation between the input and output variables was used to decide which variables to use as input parameters that have a significant effect on the output results.

3.6 Regression Analysis

3.6.1 Scatter plot

A Scatter plot is defined as a visual method used to display the relationship between two Variables. In carrying out the statistical analysis, MS excel spreadsheet is used to determine the scatter plot, correlation and regression. The MS excel spread sheet is manageable tool f or scatter plot analysis and determination of correlation between two variables.

3.6.2 Simple Regression Analysis

In this study, CBR value are the dependent variables whereas the LL, PL, PI, MDD, OMC, PF and PS are regressor/predictor variables. To carry out statistical analysis, MATLAB 2018 used. A total of 302 numbers of samples are used in correlating CBR with LL, PL, PI, MDD, OMC, PS and PF. While caring out the statistical analysis different regression models are used and those models with a higher value of coefficient of determination are accepted.

3.6.3 Multiple Regression Analysis

Multiple Regressions Analysis Using MATLAB 2018.A regression model that contains more than one predictor variable is called multiple regression models. The multiple regression equations take the form y=b1x1+b2x2+-----+c. The b’s are the regression coefficients, representing the amount the dependent variable changes when the independent changes 1unit. The c is the constant, where the regression line intercepts the y axis; representing the amount, the dependent y will be when all the independent variables are 0. Multiple Correlations is a technique that allows additional factors to enter the analysis separately so that the effect of each can be estimated using one model equations. It is valuable for quantifying the impact of various simultaneous influences upon a single dependent variable. Furthermore, because of omitted variables bias with single regression, multiple regression is often essential even when the investigator is only interested in the effects of one of the independent variables. The regression coefficients are then calculated using MATLAB 2018. Within this study, diverse combinations are employed to execute multiple regression analysis, including Fine and PI, Gravel, Sand, and PI, as well as Fine, LL, and MDD. The selection of these combinations is based on findings from simple regression analyses.

3.7 Modeling Tools

In this study, MATLAB 2018, a programming language that is widely used for data analysis, algorithm development, and model building, was utilized to construct neural networks. MATLAB offers a range of toolboxes that are designed to address specific problems, including the neural network toolbox, which was employed in this research. The neural networks were modeled using both direct coding and the "nftool" neural network fitting application. The "nftool" is a powerful tool that is specially designed to solve complex data fitting problems with consistency and accuracy. By utilizing this tool, it is possible to construct neural networks that were capable of solving data fitting problems effectively.

Additionally, script authoring was used to provide more flexibility in modeling the neural networks. This approach enabled the researchers to customize the architecture, training algorithm, learning methods, and other aspects of the model to improve its performance. Script authoring also allowed for the incorporation of specialized functions and techniques that are not available in the neural network toolboxes.

3.8 Data Preprocessing

Data quality is a critical factor in machine learning, and it is essential to ensure that the data used in the algorithm is of high quality. To achieve this, data preprocessing is necessary as the first step before utilizing the raw data for any machine learning task. There are several techniques available for data preprocessing, and in this study, data integration, data cleaning, data reduction, and data transformation were the primary data analysis methods used before developing the neural networks.

3.8.1 Data Integration, Cleaning and Reduction

Achieving high data quality requires crucial first steps such as data integration, data cleaning, and data reduction. Data integration involves merging data collected from various sources into a consistent format. This was a significant challenge in this study as the collected data was structured differently and in a large-sized format. Despite the effort required, data integration helped to avoid inconsistencies in the dataset.

In situations where the collected data had missing values, data cleaning is performed. Data cleaning can be used to either eliminate or fill in missing data (Dong and Rekatsinas 2018). In this case, since filling in missing data could potentially reduce data quality and lead to incorrect values, all incomplete data were removed. Data reduction is used to eliminate redundancy from the dataset (Alasadi and Bhaya 2017). This required a careful examination of each line of data. In this study, all data integration, data cleaning, and data reduction were performed manually using MS-Excel.

3.8.2 Data Transformation

Data transformation is a crucial process in machine learning that involves scaling data into a uniform range and giving equal weight to all data with different measurement units. Failure to transform the data can result in inaccurate model results, especially when dealing with different measurement units. Normalization is a common data transformation method that is particularly useful in neural networks. Once the data is normalized, the type of unit used no longer affects the result (Bardhan et al. 2021; Khasawneh et al. 2022). In this study, all data were standardized to eliminate the models' dependence on the unit of measure. Among the various data transformation methods, Min-max normalization was chosen because it ensures that all features are scaled within the same range and receive equal attention during neural network training.

Normalization or scaling data within a uniform range helps to prevent larger values from overpowering smaller ones and ensures that all data values are independent of their unit. In this research, data normalization was performed using MATLAB. The map min-max normalization method using equation 3.2 was employed, whereby the minimum value of each feature is transformed into -1, the maximum value into 1, and every other value into a decimal between -1 and 1 (Khasawneh et al. 2022).

$$x' = \frac{x - x\min}{x\max - x\min}\left(New\max - New\min\right) + New\min \qquad 3.2$$

where X is the original value, Xmin is the minimum value of the feature being normalized, Xmax is the maximum value of the feature being normalized, X' is the normalized value, and newmin and newmax are the desired minimum and maximum values of the normalized data range, respectively.

3.9 Neural Network Model Development

During the development of the ANN models, the subsequent procedures were executed.

3.9.1 Data Division

A total of 302 secondary data were split into three distinct sets, namely training, validation, and test sets. To determine the appropriate proportion of data to use for each set, a trial and error approach was employed. The aim was to find the proportion that would result in the best neural network performance. The best proportion was determined by selecting the ratio that minimized the mean squared error (MSE) and maximized the correlation coefficient R. After conducting several experiments, it was found that the optimal proportion for training, validation, and test sets was 70%, 15%, and 15%, respectively. And this proportion is used by different previous studies Fikret Kurnaz and Kaya (2019); Salahudeen et al. (2019); Suthar and Aggarwal (2018); Tenpe and Patel (2020b) This proportion was determined to be the most effective in yielding the best neural network performance for the given dataset with the minimum MSE and the highest correlation coefficient R.

3.9.2 Define Neural Network Architecture

For the prediction models, a two-layered feed-forward network architecture was employed. This type of neural network consists of an input layer, a single hidden layer, and an output layer. The input layer simply introduces the input data, and there is no calculation performed in the input layer neurons. Information flows in the forward direction, and there is no backward travel in a feed-forward neural network. The number of input neurons was equal to the number of input variables, while the number of output neurons was equal to the number of output variables.

To determine the optimal number of hidden layer nodes, various methods proposed by different scholars were used. The best approach, according to Hecht-Nielsen (1992), is to start with the minimum number of nodes and stop when there is no significant improvement in the model's performance. Therefore, to incorporate all the approaches, the minimum node was set to 6, and the minimum upper limit was set to 50. The ANN model structure was then checked with nodes greater than 50 until no significant improvement was recorded. Finally, the best-performing model was selected.

3.9.3 Neural Network Training

To train both neural network models, a supervised learning method was utilized. During this process, both the input and corresponding output values were provided to the neural network. The Levenberg-Marquardt algorithm, also known as the trainlm training function, was utilized for training the neural networks. This algorithm is a type of backpropagation algorithm and is known to be the fastest backpropagation algorithm. It is often suggested as the first choice for supervised learning algorithms (Tenpe and Patel 2020a). Although this training function requires more memory than other methods, it was chosen due to its fast computation ability.

In the hidden neurons, the tangent hyperbolic sigmoid activation function was used, while a linear activation function was utilized in the output neurons. The tangent hyperbolic sigmoid activation function was preferred because it is differentiable and produces outputs within a fixed range between -1 and 1 (Kayadelen et al. 2009; Tenpe and Patel 2020a). Overall, these activation functions were chosen to optimize the performance of the neural network models.

3.10 Model Performance Measures

According to Salahudeen et al. (2019), statistical measures such as the correlation coefficient (R), the mean absolute error (MAE), and the root mean square error (RMSE) are commonly used to evaluate neural network performance and indicate error rates. Similarly, Rezazadeh Eidgahee et al. (2019) and Shahin (2013) suggested that the lowest MSE values and the highest R values are the best measures for evaluating the performance of developed ANN models. Fikret Kurnaz and Kaya (2019) utilized MSE, RMSE, and determination coefficient (R) as performance measures, while Ali, Belal, Rahman and

Rafizul (2016) evaluated ANN models based on MAE and regression (R). In contrast, Naderpour et al. (2010) used only MSE values as a measurement parameter.

Anupama. U (2016) suggested that the performance of the ANN model is considered to be good if it has high correlation coefficients (R approximately 1) and low mean squared errors (MSE approximately 0) between the measured and predicted output variables for all data sets (i.e., training, testing, and validation). The model performance was evaluated based on the best validation performance and the correlation coefficient between measured and predicted CBR values, as noted by the authors. For each ANN modeling structure, the training results of MSE, RMSE, MAE, and R-value were analyzed, and the better ANN model structure that provides better prediction was selected. Once the better ANN model structure was selected, mathematical formula development was conducted based on the model training weight and bias results.

These measuring parameters are calculated by the following equations:

$$R = \frac{\sum_{i=1}^{n}(X_i - \bar{X}_i)\left(X'_i - \bar{X}'_i\right)}{\sqrt{\sum_{i=1}^{n}(X_i - \bar{X}_i)^2 \sum_{i=1}^{n}(X'_i - \bar{X}'_i)^2}} \tag{3.3}$$

$$MSE = \frac{1}{n}\sum_{i=1}^{n}(X_i - X'_i)^2 \tag{3.4}$$

$$RMSE = \sqrt{\frac{1}{n}\sum_{i=1}^{n}(X_i - X'_i)^2} \tag{3.5}$$

$$MAE = \frac{1}{n}\sum_{i=1}^{n}\left|X_i - X'_i\right| \tag{3.6}$$

Where Xi is Actual CBR value, X'i is Predicted CBR value, $\bar{\bar{X}}$i is the average value of actual CBR, $\bar{\bar{X}}$’i is the average value of predicted CBR and n is the total number of observations.

3.11 Model Validation

The developed neural network models were validated using primary soil laboratory test results. The soil laboratory tests include grain size analysis, Atterberg limit and modified compaction. tests were done in AASTU (Addis Ababa Science and Technology University) geotechnical laboratory. The tests were done according to the ASTM manual.

3.11.1 Grain Size Analysis

According to the ASTM manual D 422 standard test methods for the amount of material in soils finer than No. 200 (75-µm), the grain size analysis was conducted. The process involved soaking the samples to determine the original size of soil grains while preventing finer particles from sticking to larger ones. The samples were then washed on sieve No. 200 and dried in an oven at 105°C. Finally, a stack of successive sieves (2mm,425mic and 75mic) was used to sieve the samples.

3.11.2 Atterberg Limit

To conduct the Atterberg limit tests, soil samples were utilized, which were made up of material that passed a No. 40 (425µm) test sieve. The samples were prepared for each test using either wet or dry methods, as specified in the relevant standards. To adjust the moisture content in the test specimens, water was added, and the mixture was stirred with a spatula, after which it was left to condition for at least 16 hours.

I. The measurement of Liquid Limit (LL) involves spreading a portion of the soil sample in the brass cup of a liquid limit machine and dividing it using a grooving tool. The point at which the groove closes for 1/2 inch (13mm) after 25 drops of the cup is considered to be the moisture content corresponding to the Liquid Limit. The test methods used for this measurement are ASTM D 4318.

II. To determine the Plastic Limit (PL), a small ball of moist plastic soil is repeatedly remolded and manually rolled out into a 1/8-inch (3mm) thread. The point at which the thread crumbles before being completely rolled out is taken as the moisture content corresponding to the Plastic Limit. The standard test methods used for this purpose are ASTM D4318.

III. The Plasticity Index (PI) of the soil can be calculated by subtracting the Plastic Limit (PL) from the Liquid Limit (LL).

3.11.3 Compaction

In accordance with the ASTM D 698 standard test methods for laboratory compaction characteristics of soil using modified effort (56,000 ft-lb/ft3 (2,700 kN-m/m^3)), the compaction test was conducted. Prior to the test, the soil samples were allowed to air dry. A mold size of 101 mm (4 in) diameter with a volume of 944 cu.cm was used for implementing both test methods A and B. Each soil sample was compacted in five separate layers.

3.11.4 California Bearing Ratio

In this study, the California bearing ratio (CBR) test was performed to determine the strength characteristics of the soil. The Modified AASHTO T-180 method was used to obtain the soaked CBR value, which was calculated for 10, 30, and 65 blows. To ensure accurate results, three specimens were compacted to attain a range of 95% (or lower) to 100% (or higher) of the maximum dry density. The process involved clamping the mold to the base plate, attaching the extension collar, and adding 5 kg weight along with a spacer disk. Filter paper was placed on top of the spacer disk and the soil mixture was added with sufficient water to achieve the optimum moisture content. The soil-water mixture was then compacted in the mold in three equal layers to achieve a total compacted depth of about 127mm. The extension collar was removed, and the top surface of the mold was trimmed with a straightedge to remove any irregularities. The spacer disk was removed, and a filter paper was placed on the perforated base plate. The mold was inverted, and the soil was compacted onto the filter paper. The specimen, along with the mold, was weighed, and a tripod with a dial indicator was placed on top of the mold to take the initial dial reading. The mold was then immersed in water for 96 hours to allow free access of water to both the top and bottom of the specimen. After 96 hours, a final reading was taken on the soaked specimen. The percentage swell was then calculated using the difference between the initial and final dial readings.

$$Percent\ \text{swell} = \frac{Change\ \text{in length}}{116.5mm} * 100 \qquad 3.7$$

After removing the specimen from the soaking tank and draining the water off the top, the surcharge weights and perforated plates were removed. The next step involved placing a surcharge of annular and slotted weights that were equal to the weight used during soaking on top of the specimen. The penetration piston was then seated, with one surcharge weight placed on the specimen and the remaining surcharge weight placed around the piston. The penetration piston was seated with a 44 N load, and both the penetration dial indicator and the load indicator were set to zero. The load was then applied to the penetration piston at a rate of 1.3mm per minute, and the load was recorded when the penetration was 0.64, 1.27, 1.91, 2.54, 3.18, 3.81, 4.45, and 5.08 mm. The corrected values were then determined for each specimen at 2.54- and 5.08-mm penetration. The California bearing ratio values were obtained as a percentage by dividing the corrected load values at 2.54- and 5.08-mm penetration and multiplying the result by 100.

$$CBR = \frac{\text{Corrected load value}}{\text{Standard value}} * 100 \tag{3.8}$$

CHAPTER 4

RESULTS AND DISCUSSION

4.1 General

This chapter comprises 5 main sections. The first section provides a descriptive statistical analysis of both primary and secondary data. The second section presents the laboratory test results for primary data. The third section encompasses a statistical analysis, which includes scatter plots, simple regression, and multiple regressions. The fifth section delves into the entire ANN model, including prediction, validation, and model equation performance evaluation. Lastly, the chapter concludes with a comparison of the ANN model with multiple regression analysis.

4.2 Secondary Data Analysis

Table 4. 1 Descriptive Statistics of the Secondary Data Soil Test Results

Parameters	**Gravel %**	**Sand %**	**Fine %**	**LL**	**PL**	**PI**	**OMC**	**MDD**	**CBR**
Mean	10.592	17.946	71.462	56.364	31.318	25.037	20.216	1.648	5.092
Standard Error	0.983	0.704	1.161	0.950	0.416	0.605	0.325	0.010	0.322
Median	2	14.29	76.94	57	32	25	20	1.6	3
Mode	0	11	89	71	34	23	20	2	1
Standard Deviation	17.090	12.229	20.169	16.514	7.234	10.512	5.648	0.166	5.603
Sample Variance	292.060	149.558	406.796	272.698	52.331	110.500	31.905	0.028	31.394
Skewness	1.853	1.535	-0.891	-0.091	-0.003	0.099	0.302	0.633	2.269

Range	71.1	69.2	82.2	73	39	50	26.2	0.776	29.5
Minimum	0	1.8	16	24	14	3	11	1.2	0.5
Maximum	71.1	71	98	97	53	53	37	2	30
Count (N)	302	302	302	302	302	302	302	302	302

As shown in table 4.1, the CBR values had a mean of 5.092 and standard deviation of 5.605. Also, the values are in the range of 0.5 to 30. The fact that the CBR values are within the range of 0.5 to 30 might pose a limitation when predicting values outside this range. In other words, any prediction or estimation made using the data should be considered reliable only within this specified range. Values beyond this range may not be accurately predicted or estimated based on the available data. That might represent a limitation on the prediction of values outside this range.

4.3 Primary Data Analysis

The statistical analysis of the laboratory test results of the primary data is summarized below in Table 4.2. The CBR values are ranged from1.76% to 10% as shown in the table.

Table 4. 2 Descriptive Statistics of the Primary Data Set

Parameters	**Gravel %**	**Sand %**	**Fine %**	**LL**	**PL**	**PI**	**OMC**	**MDD**	**CBR**
Mean	7.821	15.185	76.990	59.44	34.018	25.359	22.365	1.538	6.493
Standard Error	4.749	1.466	4.7127	2.198	1.458	1.822	1.036	0.030	1.335
Median	1.62	13.79	78.85	59.62	34.06	24.58	21.95	1.52	6.75
Mode	0	18.75	78.5		32		21.82	1.49	
Standard Deviation	18.997	5.864	18.850	8.793	5.832	7.290	4.146	0.122	3.272

Sample Variance	360.923	34.397	355.358	77.325	34.012	53.144	17.190	0.015	10.707
Skewness	3.667	-0.103	-2.912	0.039	-0.460	0.334	-0.568	1.769	-0.382
Range	77.2	19.28	82.48	32.4	24.31	26	18.6	0.5	8.24
Minimum	0	4.97	12.55	43	20.29	14	11.7	1.4	1.76
Maximum	77.2	24.25	95.03	75.4	44.6	40	30.3	1.9	10
Count (N)	16	16	16	16	16	16	16	16	16

4.4 Laboratory Test Result and Discussion

The research study involved the utilization of laboratory tests to assess the soil samples' index, compaction characteristics, and California Bearing Ratio (CBR). The primary dataset comprised 16 soil samples on which four specific laboratory tests were conducted, namely grain size analysis, Atterberg limit, Modified compaction test, and CBR assessment. These tests were executed following the guidelines outlined in the ASTM and AASHTO manuals.

4.4.1 Grain Size Distribution

The analysis of grain size distribution reveals how different-sized particles are distributed within the soil. This helps classify soil as either coarse-grained or fine-grained, depending on the amount passing through a small sieve (No. 200 sieve with a size of 0.075µm). In this research, larger particles like gravel and sand labeled as "coarse materials," while the smaller silt and clay particles grouped as "fine materials." Using the USCS classification system, the percentage distribution of these particle sizes in soil samples calculated as follows:

%Gravel =%Soilpassing 75mm sieve - %Soilpassing 4.75mmsieve 4.1

%Sand=%Soilpassing 4.75mmsieve-% Soil passing 0.075 mm sieve 4.2

%Fine=%Soilpassing0.075mmsieve 4.3

The grain size distribution of the soil samples is summarized on Table 4.3. As can be seen from Table 4.3, out of the 16 samples 1 sample was coarse grained soil whereas the remaining 15 samples were found to be fine grained soils.

Table 4. 3 Grain Size Distribution of Primary Data

S.NO	**Sample Name**	**Gravel%**	**Sand%**	**Fine%**	**Soil Classification**
1	Sample 1	0.27	12.69	87.04	Fine Grained
2	Sample 2	0	22	78.0	Fine Grained
3	Sample 3	0	9	91.0	Fine Grained
4	Sample 4	12.5	21.7	65.8	Fine Grained
5	Sample 5	0.5	13.4	86.1	Fine Grained
6	Sample 6	0	12.7	87.3	Fine Grained
7	Sample 7	2.75	18.75	78.5	Fine Grained
8	Sample 8	0	4.97	95.03	Fine Grained
9	Sample 9	2.75	18.75	78.5	Fine Grained
10	Sample 10	3.07	11.96	84.97	Fine Grained
11	Sample 11	0	20.8	79.2	Fine Grained
12	Sample 12	77.2	10.25	12.55	Coarse Grained
13	Sample 13	8.75	20.49	70.76	Fine Grained
14	Sample 14	12.18	14.18	73.64	Fine Grained
15	Sample 15	0	24.25	75.75	Fine Grained
16	Sample 16	5.17	7.07	87.71	Fine Grained

4.4.2 Atterberg Limits

From the Atterberg limit test the liquid limit and plastic limit were determined and plasticity index which is the difference of the two was computed. The value of liquid limit, plastic limit and plasticity index of the samples is summarized on Table 4.4.

Table 4. 4 Atterberg Limit Test Result for Primary Data

S.NO	Sample Name	LL	PL	PI
1	Sample 1	72	32	40
2	Sample 2	61	40	21
3	Sample 3	54	32	22
4	Sample 4	69.7	39.7	30
5	Sample 5	43	29	14
6	Sample 6	52	33	19
7	Sample 7	65.3	36	29.3
8	Sample 8	60	28.3	31.7
9	Sample 9	65.26	35.99	28.27
10	Sample 10	55.95	20.29	35.66
11	Sample 11	55	30	25
12	Sample 12	47.01	31.29	15.72
13	Sample 13	59.25	39.47	19.78
14	Sample 14	61.68	37.52	24.16
15	Sample 15	54.49	35.13	19.36
16	Sample 16	75.4	44.6	30.8

4.4.3 Soil Classification

Using the outcomes of grain size distribution and Atterberg limits, the soil types were categorized employing the Unified Soil Classification System (USCS). For coarse-grained soils, this classification depended on the percentage of larger particles they contained. Furthermore, the plasticity index value or its placement on the plasticity chart was considered as an additional factor, given that the samples included a certain amount of fines. Conversely, fine-grained soils were categorized based on their plasticity Characteristics. The plasticity chart, a graphical representation of liquid limit versus plasticity index, was employed to visually represent the classification of fine-grained soils.

By using the location of soil samples relative to the A line and their value of liquid limit generally fine-grained soils can be classified as CH (high plasticity inorganic clay), OH (high plasticity organic clay), CL (Low plasticity inorganic clay), OL (low plasticity organic clay), MH (high plasticity inorganic silt), OH (high plasticity organic silt), ML (Low plasticity inorganic silt) and OL (low plasticity organic silt).

From the 16 soil samples 1 sample was found to be coarse grained soil based on the grain size distribution result. This sample has a coarse fraction of more than 50% which is larger than the No.4 sieve and was classified as gravel soil. The soil sample also has a fine content of more than 12% so by using the plasticity chart it was further classified as GM (silty gravel). The summary of soil classification of the 16 soil samples used as primary data is presented on Table 4.5.

Table 4. 5 Summary of Soil Classification of Primary Data

S.NO	Sample Name	Soil Classification	
		AASHTO Classification	**USCS Classification**
1	Sample 1	A-7-5 (40)	MH
2	Sample 2	A-7-5 (20)	MH
3	Sample 3	A-7-5 (24)	MH
4	Sample 4	A-7-5 (20)	MH
5	Sample 5	A-7-6 (14)	ML
6	Sample 6	A-7-5 (20)	MH
7	Sample 7	A-7-5 (26)	MH

8	Sample 8	A-7-6 (34)	CH
9	Sample 9	A-7-5 (25)	MH
10	Sample 10	A-7-6 (18)	CH
11	Sample 11	A-7-5 (39)	MH
12	Sample 12	A-2-7 (0)	GM
13	Sample 13	A-7-5 (9)	MH
14	Sample 14	A-7-5 (19)	MH
15	Sample 15	A-7-5 (15)	MH
16	Sample 16	A-7-5 (35)	MH

4.4.4 Modified Proctor

The compaction test was done using modified proctor test method. Using a modified effort on compaction helps to achieve a higher maximum dry density at lower moisture content. The value of the two compaction parameters maximum dry density and optimum moisture content for each sample is summarized on Table 4.6.

Table 4. 6 Modified Proctor Test Result for Primary Data

S.NO	Sample Name	MDD (g/cm3)	OMC (%)
1	Sample 1	1.47	27.14
2	Sample 2	1.57	19
3	Sample 3	1.61	23.4
4	Sample 4	1.49	19.3
5	Sample 5	1.60	21.9
6	Sample 6	1.53	27.6
7	Sample 7	1.41	21.82
8	Sample 8	1.67	22.01
9	Sample 9	1.41	21.82
10	Sample 10	1.55	23.66
11	Sample 11	1.52	23.3
12	Sample 12	1.9	11.7
13	Sample 13	1.52	23.26

14	Sample 14	1.49	21
15	Sample 15	1.48	20.63
16	Sample 16	1.4	30.3

4.4.5 CBR

This table presents the California Bearing Ratio (CBR) values obtained from a series of tests conducted on different soil samples. The CBR values are a measure of the load-bearing capacity of the soil, expressed as a percentage of the load required to penetrate the soil at a certain depth and standard conditions. Each row of the table represents a specific soil sample and its corresponding CBR value is summarized on Table 4.7.

Table 4. 7 CBR Test Results for Primary Data

S.NO	Sample Name	CBR %
1	Sample 1	7.2
2	Sample 2	4.3
3	Sample 3	8.4
4	Sample 4	6
5	Sample 5	10
6	Sample 6	9.4
7	Sample 7	3.2
8	Sample 8	8.9
9	Sample 9	3.2
10	Sample 10	5.8
11	Sample 11	5.1
12	Sample 12	18
13	Sample 13	6.4
14	Sample 14	4.4
15	Sample 15	3.2
16	Sample 16	2.7

4.5 Statistical analyses

4.5.1 Sensitivity Analysis

In the context of sensitivity analysis, a Pearson's correlation matrix was applied to investigate the interrelationships among diverse soil parameters, encompassing %gravel, %sand, %Fine, liquid limit (LL), plastic limit (PL), plasticity index (PI), optimum moisture content (OMC %), maximum dry density (MDD) in g/cm3, and California Bearing Ratio (CBR%), as presented in Table 4.8. Of particular note is the prominent correlation observed between liquid limit and plastic limit, underscoring a consistent co-fluctuation between these variables. In the pursuit of robust model performance and enhanced interpretability of explanatory variables, deliberate steps were taken to mitigate concerns related to multicollinearity during the parameter selection process. In contrast, the outcomes of the correlation analysis cast light upon the relatively subdued associations involving CBR% and the other soil parameters. As a result, conventional regression analysis was deemed potentially inadequate for precise CBR% modeling. In this regard, artificial neural networks (ANNs) emerged as a more suitable avenue, offering tailored modeling alternatives that align more effectively with the complexity of the data relationships.

Table 4. 8 Pearson’s Correlation Matrix of the Variables

	%gravel	**%sand**	**%Fine**	**LL**	**PL**	**PI**	**OMC %**	**MDD g/cm^3**	**CBR %**
%gravel	1								
%sand	-0.08331	1							
%Fine	-0.79681	-0.53575	1						
LL	-0.2169	-	0.3689	1					

	1	0.3053	05						
PL	-0.15974	-0.19099	0.251159	0.896124	1				
PI	-0.23023	-0.35009	0.407351	0.952376	0.720586	1			
OMC %	-0.20883	-0.2277	0.315012	0.656182	0.618062	0.606475	1		
MDD	0.183359	0.199369	-0.27625	-0.74494	-0.72059	-0.67815	-0.84304	1	
CBR %	0.423824	0.463604	-0.64022	-0.44142	-0.32563	-0.47228	-0.30298	0.335085	1

4.5.2 Scatter Plot

In the present study, The California Bearing Ratio (CBR) serves as the dependent variable, while independent variables consist of percent fine, percent sand, percent gravel, liquid limit, plastic limit, plasticity index, maximum dry density, and optimum moisture content. By applying an Excel Spreadsheet, we construct scatter diagrams to explore the intricate relationships between the dependent variable and the regressor variables. This enables us to ascertain the most suitable model for representing the test results. To this end, we present the series of scatter plots in Figure 4.1. The incorporation of sensitivity analysis enriches our understanding of the model's behavior and its responses to variations in the independent variables, thus enhancing the robustness and applicability of our predictions.

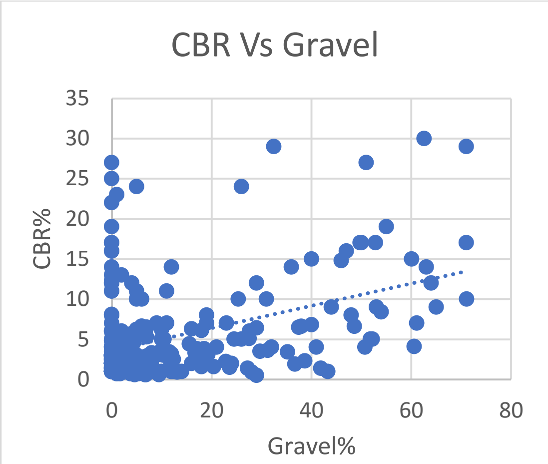
CBR Vs Gravel
CBR%
35
30
25
20
15
10
5
0
0
20
40
60
80
Gravel%

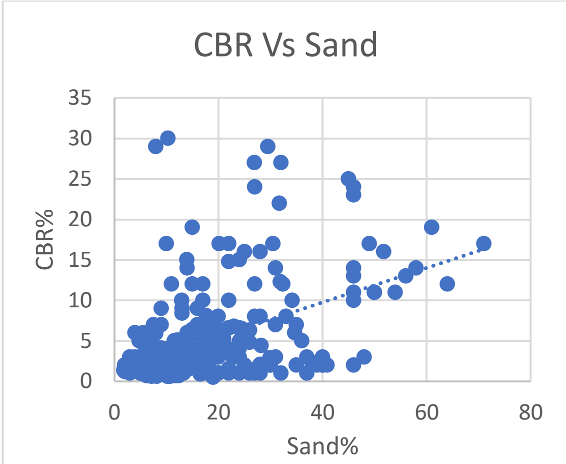
CBR Vs Sand
CBR%
35
30
25
20
15
10
5
0
0
20
40
60
80
Sand%

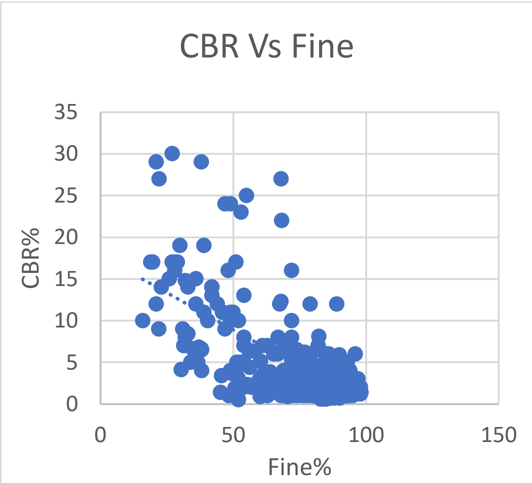
CBR Vs Fine
CBR%
35
30
25
20
15
10
5
0
0
50
100
150
Fine%

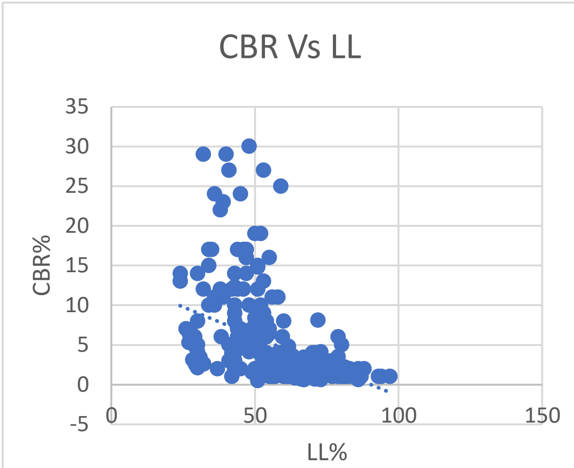
CBR Vs LL
CBR%
35
30
25
20
15
10
5
0
-5
0
50
100
150
LL%

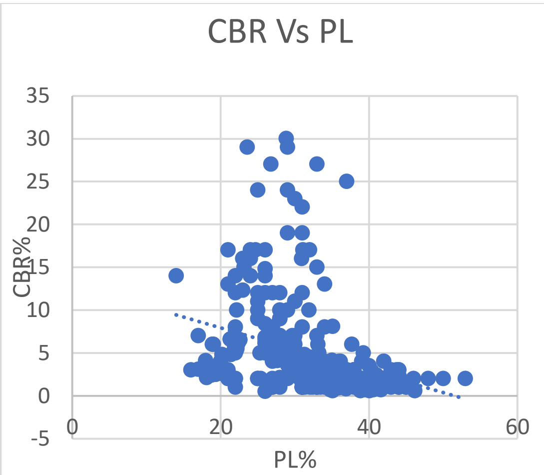
CBR Vs PL
CBR%
35
30
25
20
15
10
5
0
-5
0
20
40
60
PL%

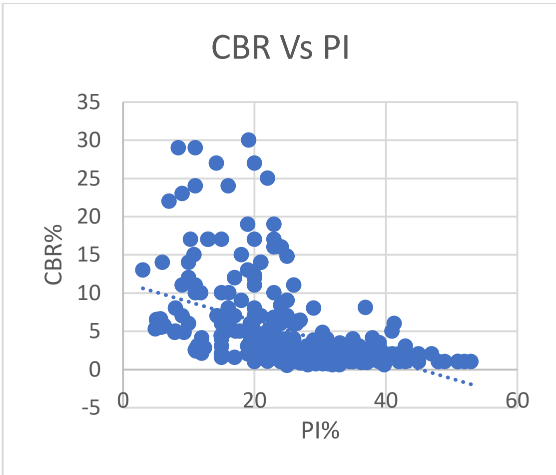
CBR Vs PI
CBR%
35
30
25
20
15
10
5
0
-5
0
20
40
60
PI%

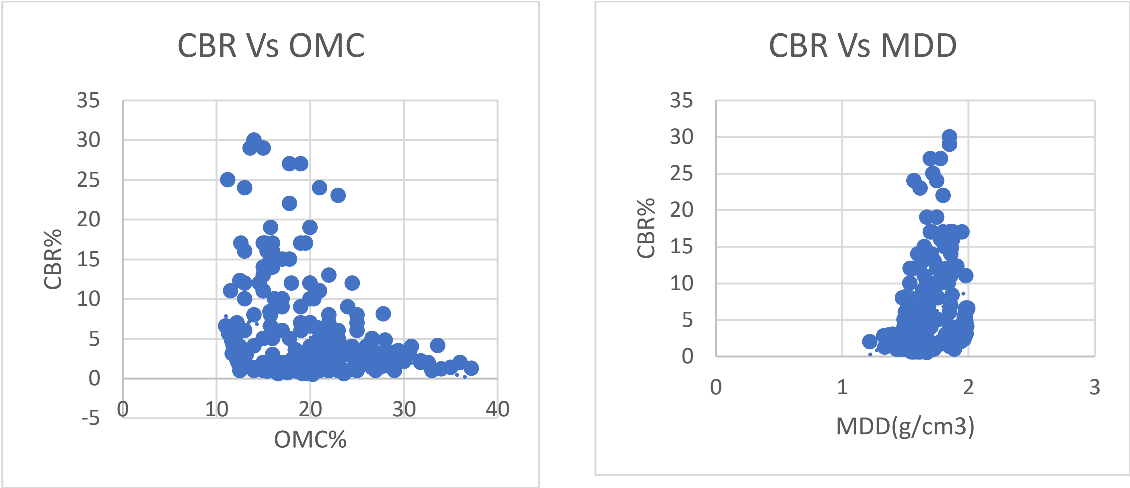

Figure 4. 1 Scatter Plots of the Variables Vs CBR

4.5.3 Results of Simple regression analysis (SRA)

Prior to delving into more complex analyses, a preliminary step involved employing simple regression analysis. This preliminary exploration aimed to discern input parameters that hold significance in predicting the soaked California Bearing Ratio (CBR) of fine-grained soils. This initial stage served a dual purpose: firstly, to pinpoint pertinent input parameters, and secondly, to exclude input parameters that exhibited weak correlations, thereby reducing the likelihood of neural networks converging towards local minima during subsequent neural network analyses.

In this study, a comprehensive analysis was conducted to explore the relationships between various soil properties and the California Bearing Ratio (CBR) of fine-grained soils. The dataset encompassed eight independent parameters: Gravel percentage (G), Sand percentage (S), Fine percentage (F), Liquid Limit (LL), Plastic Limit (PL), Plastic Index (PI), Optimum Moisture Content (OMC), and Maximum Dry Density (MDD). Through a series of regression analyses, both simple quadratic regression and multiple regressions, we aimed to determine the most influential parameters on the soaked CBR of fine-grained soils. Initially, a simple quadratic regression was performed for each independent parameter against the dependent variable, CBR. The regression coefficient values provided insights into the individual impact of these parameters on CBR. Notably, the Fine percentage (F) displayed the highest regression coefficient value of 0.66, indicating a relatively strong positive relationship with soaked CBR. Additionally, the Plastic Index (PI) exhibited a substantial influence with a coefficient value of 0.47.

The findings of the simple regression analyses are presented in Figure 4.2. notably, the results unequivocally highlight the influential roles of Fine Percentage (F) and Plastic Index (PI) in determining soaked CBR. This prominence is evident from their higher regression coefficients in comparison to other parameters such as MDD and OMC. This insight underscores the significance of soil composition and plasticity in the context of load-bearing capacity.

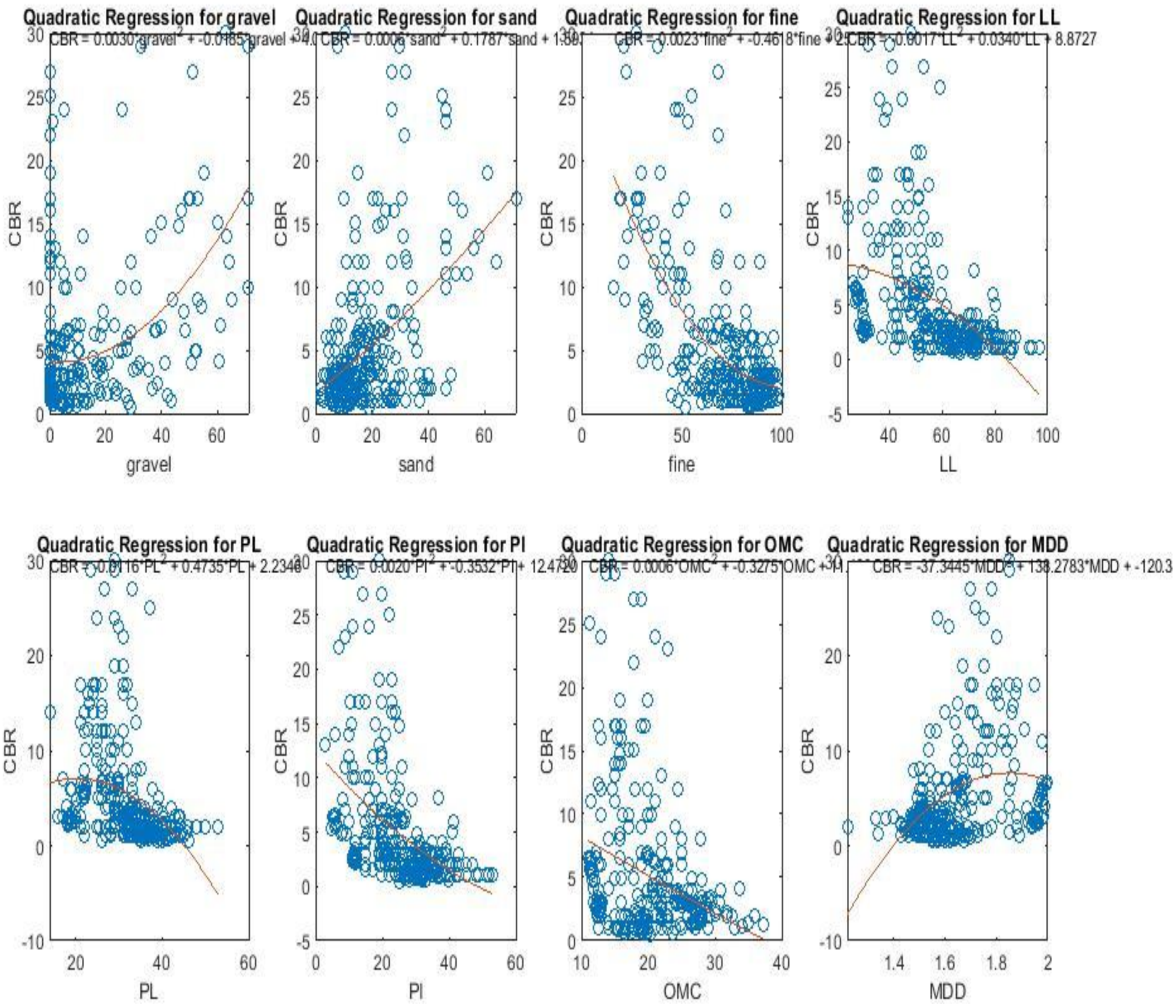

Figure 4. 2 Graphs of Simple Quadratic Regression

To further encapsulate the relationships identified through simple regression analyses, equations representing the soaked CBR were derived and are detailed in Table 4.9. These equations encapsulate the influences of the identified parameters on soaked CBR, providing a foundation for understanding their relative contributions.

Table 4. 9 Simple Regression Analyses Results

Inputs	R - value	Equation
Gravel %(G)	0.45	CBR = 0.003*Gravel^2+(-0.0185*Gravel)+40
Sand %(S)	0.46	CBR = -0.0006*Sand^2+(-0.1535*Sand)+1.59
Fine %(F)	0.66	CBR = -0.0023*Fine^2+(-0.1535*Fine)+25
Liquid Limit (LL)	0.45	CBR = -0.0017*LL^2 +(-0.1535*LL) +8.8727
Plastic Limit (PL)	0.35	CBR = -0.0116*PL^2+(-0.1535*PL)+2.2346
Plastic Index (PI)	0.47	CBR = -0.002*PI^2+(-0.3532*PI)+12.472
OMC	0.4	*CBR* = -0.0006*OMC^2+(-0..3275*OMC)+11
MDD	0.4	CBR = -37.3445*MDD^2+ 138.2783*MDD -120.3

4.5.4 Results of Multiple regression analysis (MRA)

Further investigation was carried out through multiple regression analyses to understand the combined effects of these parameters on CBR. Four different combinations were explored: Fine and PI, Gravel, Sand, and PI, Fine, LL, and MDD, and Gravel, Fine, Sand, and PI. The multiple regression models were evaluated using the coefficient of determination (R-squared) value, which indicates the proportion of the dependent variable's variability explained by the independent variables. Among these combinations, the model incorporating Gravel, Fine, Sand, and PI exhibited the highest R-squared value of 0.7593 as shown in table 4.10 and figure 4.3. This indicates that this particular combination of parameters provided the best fit for predicting the variability in soaked CBR values. The close relationship between CBR and these parameters suggests that they collectively contribute significantly to the load-bearing capacity of fine-grained soils.

Table 4. 10 Results from Multiple Regression

Combination	Equation	R-value	MAE	MSE
Fine and PI	CBR= 0 + (-0.1888)F + (-0.0064)PI	0.6808	2.6269	17.6501
Gravel, Sand and PI	CBR= 0 + (-0.1888)G + (-0.0064)S +(-0.8562)PI	0.6888	5.5894	56.4754
Fine, LL and	CBR= 0 + -(0.1888)F + (-0.0064)LL + (-	0.6773	2.7295	19.8227

MDD	0.8562)MDD			
	CBR = 19.7479 +(-0.1535) *Fine +(-0.0775) *LL + 0.4141*MDD			
Gravel, Fine, Sand and PI	CBR = 0 + (-0.1888)G + (-0.0064)S + (-0.0002)F^2 + (-0.0009)PI^2	0.7593	2.8075	12.6967

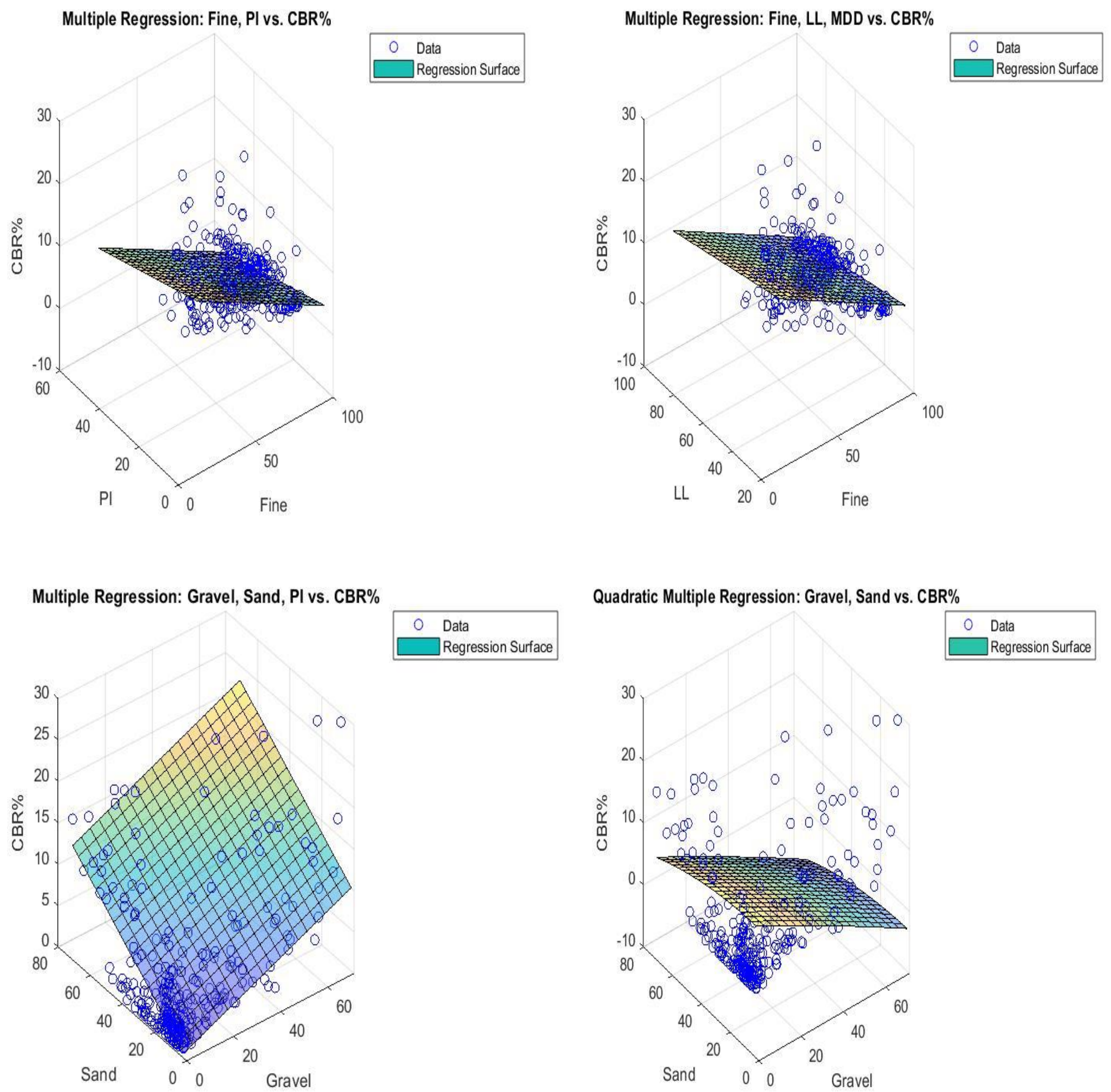

Figure 4. 3 Graphs from Multiple Regression

Interestingly, the combination of Fine and PI yielded an R-squared value of 0.6808, indicating a substantial predictive power. This confirms the initial observation that both

Fine percentage and Plastic Index have a strong influence on CBR individually, and their combined effect strengthens their predictive capabilities. Furthermore, the combination of Gravel, Sand, and PI resulted in an R-squared value of 0.6888. While these coarse-grained components (Gravel and Sand) might not seem as intuitive predictors for fine-grained soil behavior, their influence on CBR emphasizes the interplay between different soil constituents and their impact on overall stability.

4.6 ANN Prediction Model

Predictive modeling is a machine learning technique that uses existing data to predict expected future outcomes. It works by analyzing current and existing data and projecting what it learns on a model generated to forecast expected outcomes. A predictive model works on anything with a numerical value based on learning process. In this research predictive models were developed that can be used to forecast the value of California bearing ratio, using an artificial neural network. The total data set was 302 soil samples. Then ANN prediction models were developed.

After input and output data gathered and structured; training and test sets were established. A total of 302 secondary data were used to develop the models in this study, 70% used for the training, 15% for test and 15% for validation. After the models developed the 1 primary data used for cross validation of the selected best model. The general characteristic of the developed models is presented in the table below.

Table 4. 11 Summary of the Developed Neural Network Models Characteristics

Parameters	Descriptions
Input parameters	Gravel%, Sand%, Fine%, LL, PL, PI, OMC, MDD
Output parameters	CBR
Number of hidden neurons	Trial and error (from 6 to 20)
Number of hidden layers	1
Learning method	Supervised learning
Network type	Feed forward Back propagation
Architecture	Multilayer Perceptron (MLP)
Data division	Random (dividerand)
Hidden layer activation function	Hyperbolic tangent Sigmoid Function (tansig)

Output layer activation function	Linear function (purelin)
Training function	Levenberg-Marquardt (trainlm)
Performance function	R and MAE

4.6.1 Model Input Parameters

The selection of model input parameters is based on prior sensitivity analysis. The findings indicate that certain parameters exhibit a strong correlation with CBR (California Bearing Ratio), while others display a weaker connection. However, in this study, all eight input parameters are considered. This decision stems from the advantageous nature of incorporating both less influential and more potent input parameters in neural network analysis. This approach contrasts with conventional statistical methods, which carry higher risks and potential drawbacks.

The utilization of various input parameters to predict the dependent variable doesn't necessarily require each parameter to exert an equal and significant influence on the outcome when employing Artificial Neural Networks (ANN). Conversely, this strategy might not consistently yield favorable outcomes when employing multiple regression models. By introducing additional input parameters, the neural network gains access to more information, thereby enhancing its overall performance. In comparison to multiple regression models, ANN models excel at detecting subtle relationships between the dependent variable and weaker independent variables.

It is advisable to exclude only exceedingly weak parameters in neural network analysis. Conversely, relying solely on less impactful parameters within ANN models is unlikely to yield positive results. Given the intricate nature of soil behaviors, ensuring the reliability of prediction models for soil properties warrants the incorporation of a greater number of influential parameters. This can be safely achieved using neural networks. Additionally, simple laboratory tests that yield moderately correlated data with the predicted variable can also enhance prediction outcomes through inclusion in the neural network analysis.

4.6.2 Prediction Model

To predict cohesion values, a set of 20 models were created. In this scenario, various structures were formulated for neurons within a single hidden layer. Initially, the configuration encompassed 8 neurons in a three-layer architecture (input layer, hidden layer, output layer). Subsequently, the number of neurons in the hidden layer was incrementally raised to explore the impact of this augmentation on each architecture. Table 4.12 provides an overview of the diverse neural structures along with their corresponding accuracies, as measured by correlation coefficient (R), mean squared error (MSE), Root mean square error (RMSE) and mean absolute error (MAE) values.

Table 4. 12 Prediction Models Developed for CBR

Model No.	Network	Correlation Coefficient, R				MSE	RMSE	MAE
		Training	Validation	Test	All			
1	8-5-1	0.75861	0.73397	0.74689	0.75426	26.26	5.12	3.12
2	8-7-1	0.80825	0.76565	0.76395	0.79491	11.55	3.40	2.11
3	8- 8-1	0.84342	0.80577	0.79135	0.80238	19.60	4.43	2.39
4	8-10-1	0.89373	0.72619	0.70203	0.80655	11.87	3.45	2.52
5	8-12-1	0.94251	0.83731	0.62982	0.81351	6.95	2.64	1.50
6	8-14-1	0.85482	0.84588	0.72216	0.81338	15.55	3.94	2.62
7	8-15-1	0.83461	0.84857	0.79091	0.81017	5.53	2.35	1.64
8	8-16-1	0.90481	0.70368	0.86178	0.85331	15.74	3.97	2.58
9	8-18-1	0.94686	0.80457	0.70969	0.87306	5.67	2.38	1.83
10	8-20-1	0.93771	0.63261	0.75584	0.84629	7.76	2.79	2.07
11	8-22-1	0.93411	0.78253	0.63787	0.82031	20.58	4.54	2.47
12	8-24-1	0.91691	0.83066	0.71903	0.86422	9.22	3.04	1.98
13	8-25-1	0.86179	0.81737	0.74685	0.81788	41.61	6.45	3.76
14	8-28-1	0.92199	0.65272	0.72269	0.85817	12.29	3.51	2.57
15	8-30-1	0.84612	0.76674	0.85249	0.79931	8.93	2.99	1.89
16	8-32-1	0.94153	0.62745	0.64752	0.85538	9.93	3.15	2.07
17	**8-35-1**	**0.99636**	**0.70095**	**0.59241**	**0.90028**	**26.85**	**5.18**	**3.22**
18	8-40-1	0.93412	0.59352	0.84352	0.82891	16.51	4.06	3.04
19	8-45-1	0.92911	0.58799	0.79399	0.82949	70.48	8.40	5.57
20	8-50-1	0.96073	0.68842	0.78905	0.86456	40.32	6.35	4.35

The training, validation and testing accuracies in terms of R values observed across different models are as follows: 0.75 to 0.99 for training 0.58 to 0.84 for validation and 0.59 to 0.86 for testing. R value close to 1 and MAE and MSE value near zero indicates a predicting capability. So a stable architecture can be reported among these architectures. Accordingly, a robust model selected among 20 architectures developed is model 17 of network 8-35-1. The neural network is shown in figure 4.4.

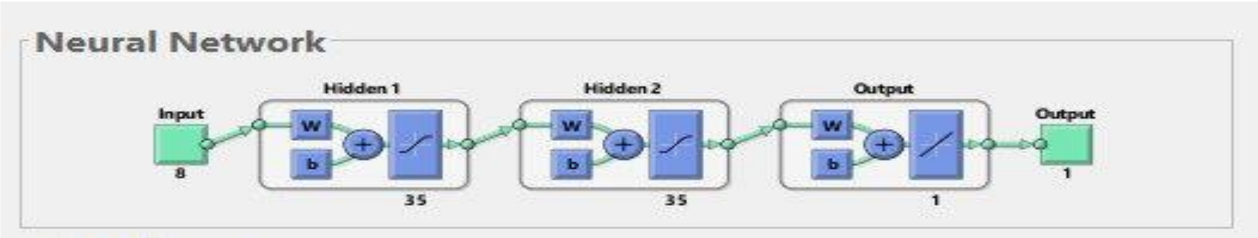

Figure 4. 4 Neural Network Architecture Sample of model 17

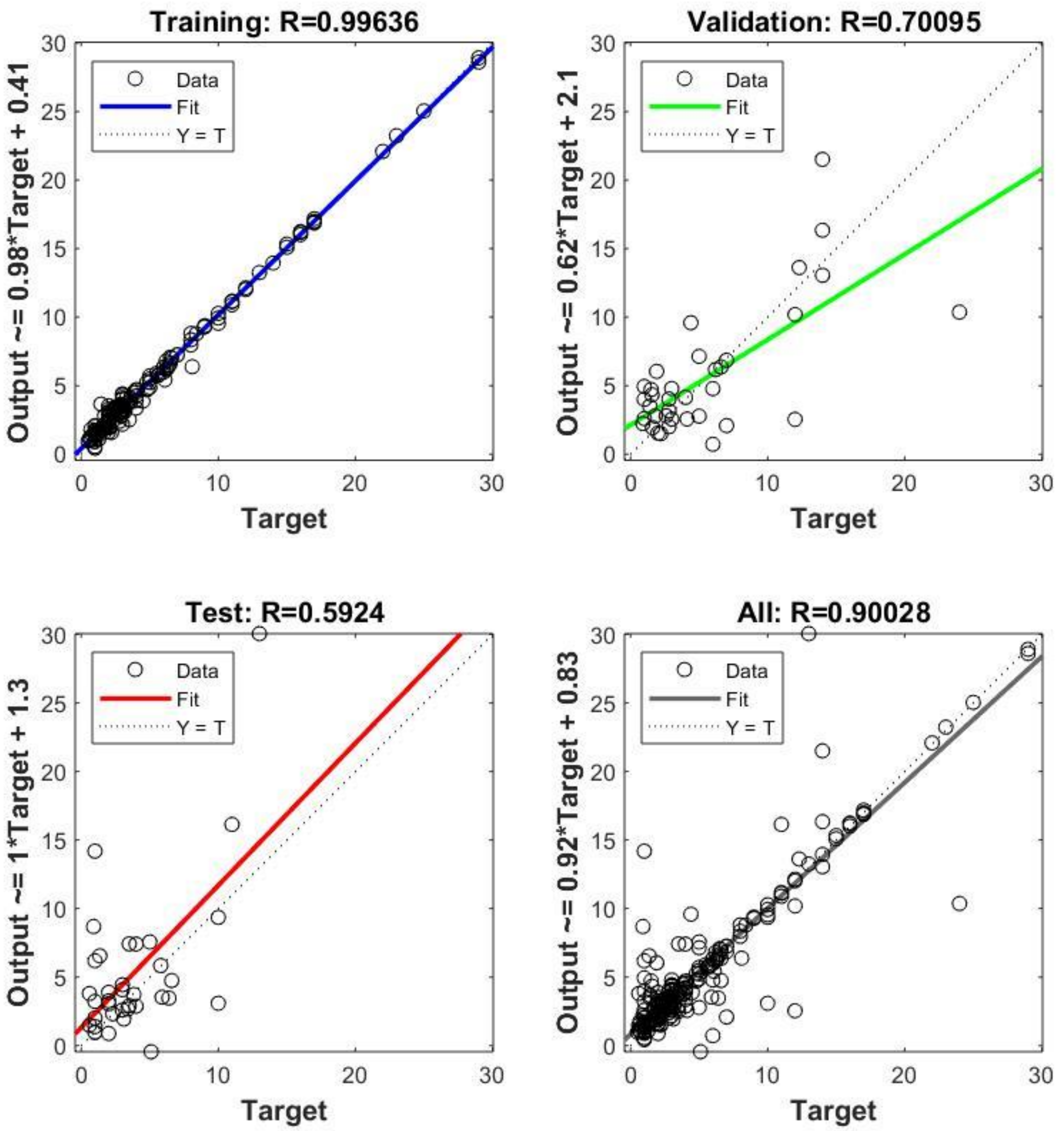

Figure 4. 5 Regression plot of Model 17

The regression plot describes the relationship between the response (output) variable, and the predictor (input) variables; also, relationship between the actual (target) value and the predicted (output) value. As shown in Table 4.12 and Figure 4.5, Model 17 was determined to be the best structure to solve this problem. In order to examine the relationship between the values obtained as a result of the network and the actual values, the regression plot generated at the end of the process is looked at. In this study, R values were calculated as 0.996 for the training, 0.7009 for the validation, 0.5924 for the test, and 0.9002 for all data as shown in Figure 4.5.

4.7 ANN Model Validations

The neural network prediction models were validated using experimental laboratory test results. The actual modified compaction test results were compared with the predicted values using the selected neural networks. According to Table 4.13, the error of the developed ANN models, for predicting California bearing ratio of soils on the primary data, ranges from 2.7 to 18 with a mean squared error of 4.573. This indicates that the developed neural networks can predict the value of California bearing ratio of soil from soil index properties in a good precision with the actual value.

Table 4. 13 Actual Vs Predicted CBR

S.No	Sample Name	Actual CBR%	Predicted CBR%	Error %	Squared Error
1	Sample 1	7.2	6.3037	0.896	0.803
2	Sample 2	4.3	7.2068	2.907	8.449
3	Sample 3	8.4	8.4793	0.079	0.006
4	Sample 4	6	6.1908	0.191	0.036
5	Sample 5	10	11.6982	1.698	2.884
6	Sample 6	9.4	6.7169	2.683	7.199
7	Sample 7	3.2	6.2570	3.057	9.34
8	Sample 8	8.9	8.2101	0.689	0.476
9	Sample 9	3.2	6.2708	3.071	9.429
10	Sample 10	5.8	7.5801	1.780	3.169
11	Sample 11	5.1	7.1220	2.022	4.088

12	Sample 12	18	16.6052	1.395	1.945
13	Sample 13	6.4	6.2332	0.167	0.028
14	Sample 14	4.4	6.3974	1.997	3.999
15	Sample 15	5.2	7.9453	2.745	7.536
16	Sample 16	2.7	6.4136	3.714	13.791
					MSE =4.573

The regression graph in Figure 4.6 shows that, the data points are scattered near the line Y=T. the correlation coefficient R= 0.99581 indicates very good correlation between the actual and the predicted values of the primary data set of CBR values.

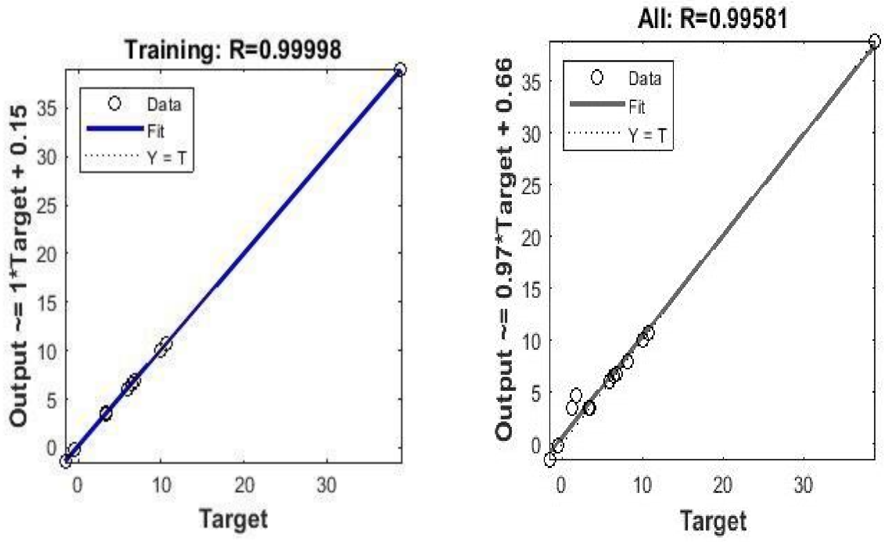

Figure 4. 6 Regression Plot of Prediction of CBR Value for Primary Data Set

4.8 ANN Model Equations Model Performance Evaluation

The model performance was evaluated by the coefficient of correlation (R) values of the test data and the combined data, Error histogram of the combined data and also MSE & RMSE values. The selected model, Model 17 (network 8-35-1) showed R value of 0.5924 and 0.9002 for testing and combined data sets respectively; also, minimum values of MSE and MAE, 26.85 and 3.22 respectively. The correlation coefficient R= 0.9002 of the combined data indicates very good correlation between the actual and the predicted values of the entire data. R = 0.5924 of the test data also indicates the performance of the model on new data sets. The comparison between the actual and predicted value of CBR using model 17, is plotted on Figure 4.8. The plot indicates good fitting and accuracy between experimental and predicted CBR values.

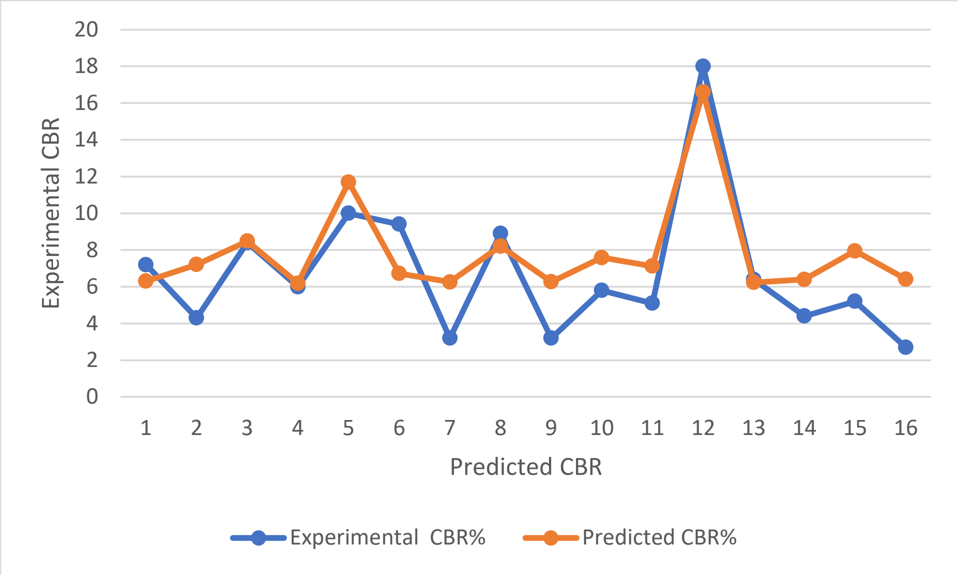

Figure 4. 7 Comparison of measured and predicted CBR value of model 17

Error histogram indicates the errors between target values and predicted values of the model. As these error values indicate how predicted values are differing from the target values, hence these can be negative.

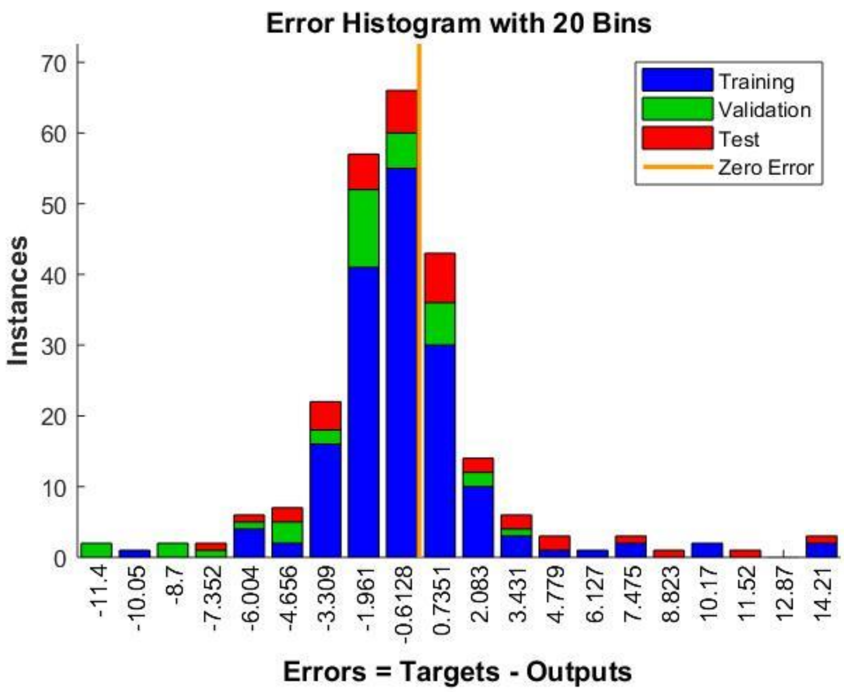

Figure 4. 8 Error Histogram of Model 17 for Prediction of CBR

Error distribution of the entire data using model 17 is plotted on an error histogram graph of Figure 4.8. A significant concentration of error is seen at 0. The error histogram also shows that instances near zero error are higher than the rest indicating a minimum difference between actual and predicted values.

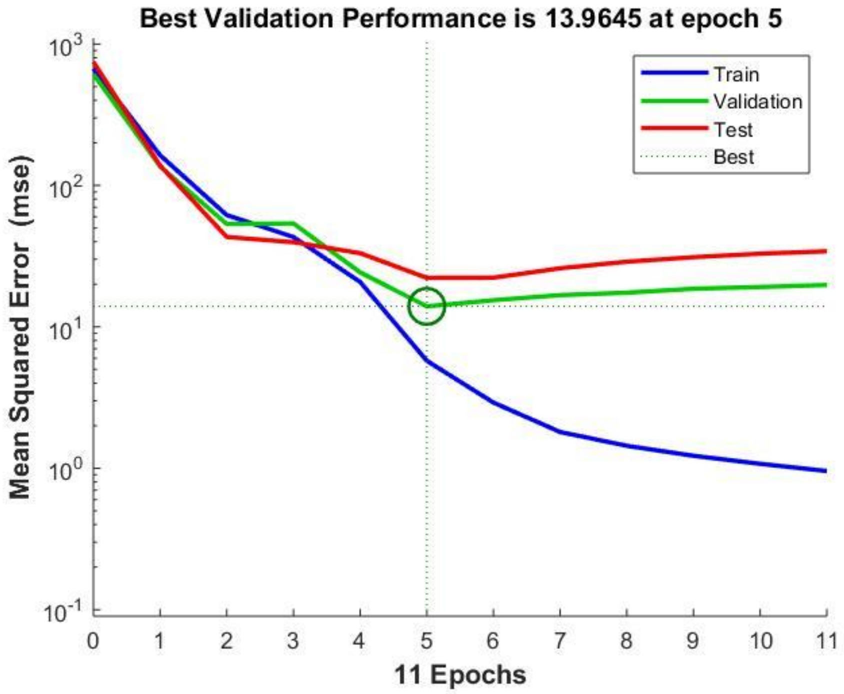

Figure 4. 9 MSE value of the selected ANN model

4.8.1 Model Equation for CBR

A transfer function is an essential component in neural networks that maps input values to output values. The sigmoid function is a commonly used transfer function due to its differentiable nature, which allows for the mapping of desirable nonlinear input-output relations. However, other differentiable nonlinear functions can also be used for this purpose. In this particular study, the hyperbolic tangent sigmoid function (tansig) was chosen as the transfer function in the hidden neurons. Equation 4.4 represents the mathematical formulation of this function.

$$F\ tansig = f(x) = \frac{2}{1+e^{2x}} - 1 \qquad 4.4$$

Among the different models and architectures tested, Model 17 of the 8-35-1 neural network architecture was found to be the most effective in predicting CBR values. The model equation can be derived from the weights and biases between input-hidden and hidden-output neurons, as described in the study. Table 4.14 presents the weight and bias matrices for this model.

Table 4. 14 Weights and Biases of Model 17 (Network 8-35-1) for c Prediction

	Connection Weights (wih)									Biases	
h	G(X1)	S(X2)	F(X3)	LL(X4)	PL(X5)	PI(X6)	OMC (X7)	MDD (X8)	Vh	bh	b0
1	0.118	0.084	-0.642	0.004	0.216	0.496	-0.421	-0.180	-1.851	-0.718	1.077
2	-0.549	-0.251	-0.687	-0.099	0.685	0.171	-0.449	0.343	-1.678	-0.865	
3	-0.469	-0.124	-0.103	-0.169	0.485	-0.197	-0.323	-0.393	1.406	0.742	
4	-0.338	0.434	-0.632	0.519	-0.052	-0.659	0.646	0.096	-1.171	-1.091	
5	-0.266	-0.157	-0.368	0.586	-0.676	-0.076	0.254	-0.188	0.926	1.056	
6	-0.160	-0.026	0.588	0.499	0.781	0.271	0.215	-0.122	0.644	-0.124	
7	-0.621	-0.657	-0.326	-0.480	-0.118	-0.551	0.061	0.183	0.397	0.877	
8	-0.061	0.358	0.372	-0.330	0.454	0.546	0.12	0.424	-0.056	0.649	
9	-0.157	0.368	-0.577	0.681	-0.165	-0.763	0.010	0.019	0.102	0.433	
10	-0.391	-0.209	-0.438	0.178	-0.257	-0.789	0.278	-0.182	-0.353	0.051	

11	-0.313	0.280	-0.018	0.422	0.174	0.654	0.131	0.291	-0.636	0.098
12	-0.274	0.593	-0.480	-0.311	0.592	-0.484	-0.468	-0.172	0.902	0.662
13	-0.350	0.364	0.330	0.281	0.191	-0.512	-0.725	-0.199	-1.147	0.199
14	-0.399	0.604	0.265	-0.563	-0.564	-0.187	0.193	0.230	1.911	0.873
15	-0.08	0.276	-0.153	-0.059	0.606	0.653	-0.164	0.342	-1.67	-0.477
16	-0.730	0.068	-0.151	-0.132	-0.578	0.594	0.553	-0.148	1.93	0.916
17	-0.506	-0.293	-0.395	0.449	0.177	-0.299	0.045	0.245	-1.636	-0.144
18	-0.572	0.006	0.511	-0.498	-0.593	0.538	-0.387	-0.375	1.414	0.486
19	-0.520	-0.583	-0.430	0.577	0.136	-0.509	-0.487	0.061	1.191	-0.884
20	0.340	-0.383	-0.026	-0.468	-0.233	-0.395	0.176	0.533	1.022	-0.161
21	0.425	-0.206	0.551	-0.637	0.514	0.237	-0.303	0.472	0.721	1.144
22	-0.656	0.147	-0.136	0.043	-0.180	-0.440	0.518	-0.340	0.563	0.325
23	-0.526	0.519	-0.204	0.425	0.311	-0.544	0.109	-0.133	0.318	0.656
24	0.52	0.295	-	-0.383	-0.467	-0.518	-	0.501	0.115	-

			0.376				0.301			0.136
25	-0.267	0.320	-0.448	0.209	0.330	-0.576	-0.653	0.099	-0.097	0.705
26	-0.400	0.494	-0.215	-0.624	0.279	0.139	0.113	0.636	-0.327	-1.157
27	0.457	-0.293	0.537	-0.068	-0.614	0.277	-0.698	0.329	0.545	0.133
28	0.169	-0.024	-0.081	0.717	0.680	-0.122	-0.011	-0.028	-0.777	1.052
29	-0.067	-0.485	0.466	0.110	-0.450	-0.756	-0.191	0.062	-0.976	-0.397
30	0.033	0.380	-0.555	0.376	-0.274	-0.373	0.514	-0.539	1.182	-0.745
31	0.520	-0.377	0.260	0.350	-0.506	-0.402	-0.402	0.482	-1.407	-0.350
32	0.243	-0.363	0.551	0.544	0.335	-0.287	-0.507	0.014	1.618	0.271
33	1.109	0.072	-1.110	0.199	-0.587	-0.384	0.163	0.991	-0.52	-0.790
34	0.082	0.905	-0.034	-0.762	0.787	1.134	0.660	-0.058	-0.707	0.728
35	-1.193	-0.690	-0.223	-1.118	0.147	0.424	0.227	-0.529	-0.586	0.761

Wih is a 35 by 8 connection weight between the input and hidden neurons; since i represent the input variables which is equal to 8, and 35 represents the number of hidden neurons that is equal to 35. Vh is a 35 by 1 connection weight between hth hidden layer and output layer of h equal to 35 hidden neurons, and 1 represents the number of output layer.bh is bias at the hth neuron of hidden layer and b0 is a bias at output layer with one output CBR . The weighted sum, wh for each hidden neurons is calculated as:

$$\mathrm{wh} = \mathrm{bh} + \sum \mathrm{pi} = 1\ (\mathrm{wih} * \mathrm{xi}) \qquad 4.5$$

Xi represents the normalized value of the input variables. Min, max normalization was used in this research, given by:

$$\mathrm{Xi} = \left(\frac{Xnorm, max - Xnorm, min}{Xmax - Xmin}\right)(x - xmin) + xnorm, \min \qquad 4.6$$

Where, Xmin is the minimum value of each input variables of the entire data set; Xmax is the maximum value of each input variables of the entire data set; Xnorm,min is the minimum value of the normalized data range; and Xnorm,max is the maximum value of the normalized data range. The values used for normalizing each input variables are tabulated below in Table 4.15.

Table 4. 15 Normalizing Values for Input Variables of CBR

$xmin$	$\left(\frac{Xnorm, max - Xnorm, min}{Xmax - Xmin}\right)$	$xnorm, min$
29	0.0301	-1
8	0.0477	
3.2	0.0708	
1	0.0890	
30.91	0.1188	

The resulted value of a 35 by 1 weighted sum (wh), calculated by using Equation 4.7 was then inserted into the hyperbolic tangent sigmoid transfer function in Equation 4.7.

$$Th = Ftansig\ (wh) = \frac{2}{1 + e^{-2wh}} - 1 \qquad 4.7$$

The summation of the resulted a 35 by 1 matrix value of Th multiplied with corresponding values of vh 35 by 1 matrixes was then added with b0 value as shown in Equation 4.8 resulting normalized CBR value.

$$CBRnorm = b0 + \sum_{h=1}^{n} (Vh * Th) \qquad 4.8$$

Finally, the real values of CBR then can be obtained by deformalizing the normalized CBR values with respect to the values given in Table 4.16 and by using Equation 4.9.

$$CBR = \frac{CBRnorm - Ynormmin}{\frac{(Ynorm,max - Ynorm,min)}{Ymax - Ymin}} + Ymin \quad 4.9$$

Table 4. 16 Normalizing Values for Output Variable c

Ynorm,min	-1
$\frac{Ynorm,max \; - \; Ynorm,min}{Ymax \; - \; Ymin}$	0.0311
Ymin	8

The formulation of CBR, based on the ANN result is as given in Equation 4.4 to 4.9. Using these mathematical equations output can be derived from input variables.

4.9 Comparison of ANN Models with Regression Analysis

This study aims to compare the performance of ANN models and multiple regression analysis in assessing the alignment of analytical values. The evaluation metrics employed for this purpose are the Mean Absolute Error (MAE) and the Correlation Coefficient (R) of the predicted values. The results for the prediction of California Bearing Ratio (CBR) in fine-grained soils using both multiple regression analysis and neural network analysis are presented in Table 4.17. The effectiveness of these models in predicting soaked CBR is also summarized in the same table.

Table 4. 17 Comparison of ANN models with multiple regressions

Models	Input	Output	Equations	R	MAE	MSE
Multiple Regression	Fine and PI	CBR	CBR= 0 + (-0.1888)F + (-0.0064)PI 0.6808	0.6808	2.63	17.65
	Gravel, Sand and PI		CBR= 0 + (-0.1888)G + (-0.0064)S +(-0.8562)PI	0.6888	5.59	56.47
	Fine,LL and MDD		CBR= 0 + -(0.1888)F + (-0.0064)LL + (-0.8562)MDD	0.6773	2.73	19.82
	Gravel, Fine,Sand and		CBR= 0 + (-0.1888)G + (-0.0064)S + (-0.0002)F^2	0.7593	2.81	12.69

	PI	+ (-0.0009)PI^2			
ANN	All	CBR = 19.7479 +(-0.1535) *Fine +(-0.0775) *LL + 0.4141*MDD	0.9002	3.22	26.85

The findings demonstrate that when predicting the soaked CBR of fine-grained soils, multiple regression analysis provides strong agreement between predicted and experimental values, particularly when using four variables: Gravel, Sand, Fine, and PI. Additionally, fairly accurate predictions of soaked CBR can be made using two (Fine and PI) or three (Gravel, Sand, and PI, and Fine, LL, and MDD) strong parameters, where multiple regression models continue to exhibit accuracy. But ANN yields more accurate prediction than multiple regressions. All input parameters (Gravel, Sand, Fine, LL, PL, PI, OMC, and MDD) were utilized in the ANN prediction model. Notably, the accuracy of the neural network model significantly improved with the inclusion of additional input parameters, while the impact on the multiple regression models was marginal. The enhanced accuracy of CBR prediction using the neural network model with additional parameters is clearly evident in the individual results of validation data, as illustrated in the error plots. This suggests that, in the context of neural network analysis, combining less influential input parameters with stronger ones is advantageous a contrast to conventional statistical methods, which may not yield such benefits and could even have detrimental effects.

The results indicate that in neural network analysis, the inclusion of relatively weaker independent variables alongside stronger ones can yield positive outcomes. However, in the case of multiple regression models, this approach may not consistently produce favorable results. The augmentation of input parameters enhances the information available to neural networks, thereby improving their performance. Neural network models excel in capturing subtle relationships between dependent and weak independent variables compared to multiple regression models. In neural network analysis, only very weak parameters should be avoided. Nevertheless, relying solely on less influential parameters in ANN models may not yield favorable outcomes.

The behavior of soils is inherently complex, and to ensure the reliability of prediction models for soil properties, it is advisable to incorporate a greater number of influential parameters. Neural networks facilitate this, allowing for the safe inclusion of more influential parameters. Furthermore, parameters that can be easily determined through simple laboratory tests, even if they exhibit moderate correlation with the predicted variable, can be beneficially integrated into neural network analysis to enhance prediction accuracy.

The study underscores the superior performance of neural network models, especially when dealing with a greater number of influential parameters. This approach aligns well with the intricacies of soil behavior, providing a more reliable means of predicting soil properties compared to traditional regression analysis.

CHAPTER FIVE

CONCLUSION AND RECOMMENDATION

5.1 Conclusion

The primary objective of this study is to investigate reliable Artificial Neural Network (ANN) model that can estimate/ predict the California Bearing Ratio (CBR) value for fine-grained soil based on their index properties. It was found that the optimum architecture for the ANN network for cohesion was found to be 8-35-1 (Eight inputs, thirty five hidden layer nodes, and one output node) with a correlation coefficient of R=0.9002 for testing data MAE=3.22 and MSE=26.85 by using 302 secondary data.

The second objective of this study is to conduct sensitivity analysis to see the most efficient input parameter for output CBR value of fine-grained soil in ANN model. It was executed by scatter plot and quadratic simple regression and the results show the influential roles of Fine Percentage (F) and Plastic Index (PI) with R value of 0.46 and 0.45 in determining soaked CBR. This prominence is evident from their higher regression coefficients in comparison to other parameters such as MDD and OMC. This insight underscores the significance of soil composition and plasticity in the context of load-bearing capacity.

The third objective is to compare the developed ANN model with a multiple regression model. The influential input parameters are taken from the sensitivity analysis and it was found that the model incorporating Gravel, Fine, Sand, and PI exhibited the highest R-squared value of 0.7593. This indicates that this particular combination of parameters provided the best fit for predicting the variability in soaked CBR values. The combination of Fine and PI yielded an R-squared value of 0.6808, indicating a substantial predictive power. This confirms the initial observation that both Fine percentage and Plastic Index have a strong influence on CBR individually, and their combined effect strengthens their predictive capabilities. Furthermore, the combination of Gravel, Sand, and PI resulted in an R-squared value of 0.6888.these multiple regression results compared with ANN prediction model gave weak correlation. The overall results obtained demonstrated that the ANN method outperforms the empirical methods considered.

The fourth objective is to validate the ANN prediction model using primary data. The result shows that the developed ANN models, for predicting California bearing ratio of soils on the primary data is with a mean squared error of 4.573. This indicates that the developed neural networks can predict the value of California bearing ratio of soil from soil index properties in a good precision with the actual value. The data points are also scattered near the line Y=T. the correlation coefficient R= 0.99581 indicates very good correlation between the actual and the predicted values of the primary data set of CBR values.

5.2 Recommendation

While this research contributes valuable insights, it is essential to acknowledge its limitations and propose avenues for further investigation to advance the field of California Bearing Ratio (CBR) estimation. The following recommendations are offered for future research endeavors:

To enhance the accuracy and generalization capacity of CBR predictions, it is recommended to expand the size and diversity of the training dataset. This expansion can be achieved by acquiring data from a wider spectrum of soil types, geological formations, and geographical regions. A more extensive and varied dataset can lead to more robust CBR models capable of accommodating a broader range of soil conditions.

While this study primarily focused on utilizing index properties as input parameters, future research should explore the inclusion of additional relevant factors that influence CBR. Parameters such as organic content and stress history represent potential contributors to the predictive capabilities of ANN models. Incorporating these variables may lead to a more comprehensive understanding of the intricate relationships affecting CBR values.

This study exclusively considered soils from Addis Ababa city. Future investigations should broaden their geographical scope to encompass a more diverse range of locations and soil properties. Given the spatial and temporal variations in soil characteristics, regular soil studies across different regions are advisable. This approach ensures that CBR prediction models remain adaptable and representative of real-world scenarios.

In the pursuit of refining CBR prediction techniques, future studies should delve into comparative analyses involving various artificial neural network architectures. Such analyses can unveil the specific strengths and weaknesses of different network types in the context of CBR estimation. By identifying and understanding these nuances, researchers can make informed decisions regarding the selection and optimization of neural network structures for enhanced predictive accuracy.

REFERENCES

AASHTO. 2001. A Policy on Geometric Design of Highways and Streets. Am. Assoc. State Highw. Transp. Off.

Abnet Gezahegn Berhe. 2020. “Household Energy Management in Informal Settlements of Addis Ababa.”

Agarwal, K. B., and K. D. Ghanekar. 1970. “Prediction of CBR from plasticity characteristics of soil.” Proceeding 2nd south-east Asian Conf. soil Eng. Singapore, 571–576.

Al-Refeai, T., and A. Al-Suhaibani. 1997. “Prediction of CBR Using Dynamic Cone Penetrometer.” J. King Saud Univ. - Eng. Sci., 9 (2): 191–203. Elsevier. https://doi.org/10.1016/S1018-3639(18)30676-7.

Alam, S. K., A. Mondal, and A. Shiuly. 2020. “Prediction of CBR Value of Fine Grained Soils of Bengal Basin by Genetic Expression Programming, Artificial Neural Network and Krigging Method.” J. Geol. Soc. India, 95 (2): 190–196. https://doi.org/10.1007/s12594-020-1409-0.

Alasadi, S. A., and W. S. Bhaya. 2017. “Review of data preprocessing techniques in data mining.” J. Eng. Appl. Sci., 12 (16): 4102–4107.

Alavi, A. H., A. H. Gandomi, A. Mollahassani, A. A. Heshmati, and A. Rashed. 2010. “Modeling of maximum dry density and optimum moisture content of stabilized soil using artificial neural networks.” J. Plant Nutr. Soil Sci., 173 (3): 368–379. https://doi.org/10.1002/jpln.200800233.

Alawi, M. H., and M. I. Rajab. 2013. “Prediction of California bearing ratio of subbase layer using multiple linear regression models.” Road Mater. Pavement Des., 14 (1): 211–219. https://doi.org/10.1080/14680629.2012.757557.

Alemayehu, T., T. Ayenew, D. Legesse, Y. Tadesse, S. Waltenigus, and N. Mohammed. 2003. “Ground Water Vulnerability Mapping of the Addis Ababa Water Supply Aquifers.” Sci. Report, Addis Ababa, Ethiop.

Ali, Belal, Rahman, A., and I. M. Rafizul. 2016. “Prediction of California Bearing Ratio of Stabilized Soil Using.” 3th Int. Conf. Civ. Eng. Sustain. Dev., (February): 978–984.

Almeida, J. S. 2002. “Predictive non-linear modeling of complex data by artificial neural networks." Curr. Opin. Biotechnol., 13 (1): 72–76. Elsevier.

Anupama. U, H. H. N. 2016. "Prediction of CBR Value of Coarse Grained Soils by Soft Computing Techniques." 4 (4): 545–550.

Arora, K. R. 2004. Arora, KR,'Soil mechanics and foundation engineering.' Standard Publishers Distributors, New Delhi.

Banimahd, M., S. S. Yasrobi, and P. K. Woodward. 2005. "Artificial neural network for stress–strain behavior of sandy soils: Knowledge based verification." Comput. Geotech., 32 (5): 377–386. Elsevier.

Bardhan, A., C. Gokceoglu, A. Burman, P. Samui, and P. G. Asteris. 2021. "Efficient computational techniques for predicting the California bearing ratio of soil in soaked conditions." Eng. Geol., 291: 106239. Elsevier. https://doi.org/10.1016/J.ENGGEO.2021.106239.

Barza, S., M. Johansson, and L. E. Persson. 2005. "A Sawyer duality principle for radially monotone functions in ℝn." J. Inequalities Pure Appl. Math., 6 (2): 36–46.

Bendana, R., A. del Cano, and M. Pilar De La Cruz. 2008. "Contractor selection: fuzzy-control approach." Can. J. Civ. Eng., 35 (5): 473–486.

Berke, L., and P. Hajela. 1993. "Application of neural nets in structural optimization." Optim. Large Struct. Syst., 731–745. Springer.

Bhatt, S., P. K. Jain, and M. Pradesh. 2014. "Prediction of California Bearing Ratio of Soils Using Artificial Neural Network." Am. Int. J. Res. Sci. Technol. Eng. Math., 156–161.

Bienen, B., C. Gaudin, M. J. Cassidy, L. Rausch, O. A. Purwana, and H. Krisdani. 2012. "Numerical modelling of a hybrid skirted foundation under combined loading." Comput. Geotech., 45: 127–139. Elsevier Ltd. https://doi.org/10.1016/j.compgeo.2012.05.009.

Black, W. P. M. 1962. "A Method of Estimating the California Bearing Ratio of Cohesive Soils from Plasticity Data." Géotechnique, 271–282. Thomas Telford Ltd.

Bowles, J. E. 1992. Engineering properties of soils and their measurement. McGraw-Hill, Inc.

Cebrián, D. 2021. “An Introduction to Artificial Neural Networks.” (5): 11843. https://doi.org/10.3390/mol2net-07-11843.

Chandrakar, V., and R. K. Yadav. 2016. “Study of correlation of CBR value with engineering properties and index properties of coarse grained soil .”.” Int. Res. J. Engieneerign Technol., 3 (11): 772–778.

Cheng, Q., C.-S. Tang, H. Zeng, C. Zhu, N. An, and B. Shi. 2020. “Effects of microstructure on desiccation cracking of a compacted soil.” Eng. Geol., 265: 105418. Elsevier.

Das, B. M. 2011. Principles of Foundation Engineering. (T. A. Gowans Hilda, ed.). Global Engineering: Christopher M. Shortt.

Das, B. M. 2015. Fundamentals of Geotechnical Engineering. (H. Gowans, ed.). Chris Carson.

Desalegn, Y. 2012. “Developing correlation between dcp and cbr for locally used subgrade materials.” (June).

Diallo, M. C., L. Z. Cheng, E. Rosa, C. Gunther, and M. Chouteau. 2019. “Integrated GPR and ERT data interpretation for bedrock identification at Cléricy, Québec, Canada.” Eng. Geol., 248: 230–241. Elsevier.

Dong, X. L., and T. Rekatsinas. 2018. “Data integration and machine learning: A natural synergy.” Proc. 2018 Int. Conf. Manag. data, 1645–1650.

Dongare, A. D., R. R. Kharde, and A. D. Kachare. 2012. “Introduction to Artificial Neural Network (ANN) Methods.” Int. J. Eng. Innov. Technol., 2 (1): 189–194.

El-Shahat, A. 2018. “Introductory Chapter: Artificial Neural Networks.” Adv. Appl. Artif. Neural Networks, 1–10. https://doi.org/10.5772/intechopen.73530.

Elmas, Ç. 2007. “Artificial intelligence applications.” Seckin, Ankara (in Turkish).

Erzin, Y., and D. Turkoz. 2016. “Use of neural networks for the prediction of the CBR value of some Aegean sands.” Neural Comput. Appl., 27 (5): 1415–1426. Springer London. https://doi.org/10.1007/s00521-015-1943-7.

Fatehnia, M., and G. Amirinia. 2018. “A review of Genetic Programming and Artificial Neural Network applications in pile foundations.” Int. J. Geo-Engineering, 9 (1).

Springer Singapore. https://doi.org/10.1186/s40703-017-0067-6.

Fatehnia, M., K. Tawfiq(Dongare et al. 2012), and M. Ye. 2016. "Estimation of saturated hydraulic conductivity from double-ring infiltrometer measurements." Eur. J. Soil Sci., 67 (2): 135–147. Wiley Online Library.

Fikret Kurnaz, T., and Y. Kaya. 2019. "Prediction of the California bearing ratio (CBR) of compacted soils by using GMDH-type neural network." Eur. Phys. J. Plus, 134 (7). https://doi.org/10.1140/epjp/i2019-12692-0.

Gallo, C. 2015. "Artificial neural networks tutorial. Encyclopedia of Information Science and Technology." Dostupno na https//www. Res. net/publication/261392616_Artificial_Neural_Networks_tutori al [pristupljeno 21.05. 2022.].

Gashaw, N. A., E. Assefa, and C. Sachpazis. 2022. "Consolidation parameters conceptualization using regression analysis and genetic programming for Addis Ababa's red clay soils." Model. Earth Syst. Environ., 8 (1): 1087–1098. Springer International Publishing. https://doi.org/10.1007/s40808-021-01127-2.

González Farias, I., W. Araujo, and G. Ruiz. 2018. "Prediction of California Bearing Ratio from Index Properties of Soils Using Parametric and Non-parametric Models." Geotech. Geol. Eng., 36 (6): 3485–3498. Springer. https://doi.org/10.1007/s10706-018-0548-1.

De Graft-Johnson, J. W., H. S. Bhatia, and D. M. Gidigasu. 1969. "The engineering characteristics of the laterite gravels of Ghana." Soil Mech Fdn Eng Conf Proc/Mexico/.

Haile, S. G., and A. Getaneh. 1989. "The Addis Ababa-Nazret volcanics: a Miocene-Pleistocene volcanic succession in the Ethiopian Rift." Sinet, 12 (1): 1–24.

Han, J., M. Kamber, and J. Pei. 2011. "Concepts and Techniques-Cha pter 2."

Hassan, J., B. Alshameri, and F. Iqbal. 2021. "Prediction of California Bearing Ratio (CBR) Using Index Soil Properties and Compaction Parameters of Low Plastic Fine-Grained Soil." Transp. Infrastruct. Geotechnol., 764–776. Springer US. https://doi.org/10.1007/s40515-021-00197-0.

Haupt, F. J., and F. Netterberg. 2021. "Prediction of California Bearing Ratio and compaction characteristics of Transvaal soils from indicator properties." J. South African Inst. Civ. Eng., 63 (2): 47–56. https://doi.org/10.17159/2309-8775/2021/v63n2a6.

Haykin, S., and N. Network. 2004. "A comprehensive foundation." Neural networks, 2 (2004): 41.

Hecht-Nielsen, R. 1992. Theory of the Backpropagation Neural Network**Based on "nonindent" by Robert Hecht-Nielsen, which appeared in Proceedings of the International Joint Conference on Neural Networks 1, 593–611, June 1989. © 1989 IEEE. Neural Networks Percept. Academic Press, Inc.

Hn, H., and S. Naagesh. 2014. "Predicting Cbr of Fine Grained Soils By Artificial Neural Network and Multiple Linear Regression." Int. J. Civ. Eng. Technol., 5 (2): 119–126.

Huang, R., Y. Li, K. Qu, and K. Wang. 2013. "Engineering geological assessment for route selection of railway line in geologically active area: A case study in China." J. Mt. Sci., 10 (4): 495–508. Springer.

Ibrahim, F. K. 2017. "Application of Soft Computing Techniques and Multiple Regression Models for CBR prediction of Soils." (5): 1552–1561.

Islam, M. R., and A. C. Roy. 2020. "Prediction of California Bearing Ratio of Fine-Grained Soil Stabilized With Admixtures Using Soft Computing Systems." J. Civ. Eng. Sci. Technol., 11 (1): 28–44. https://doi.org/10.33736/jcest.2035.2020.

Janjua, Z. S., and J. Chand. 2016. "Correlation of CBR with index properties of soil." Int. J. Civ. Eng. Technol., 7 (5): 57–62.

Karsoliya, S. 2012. "Approximating Number of Hidden layer neurons in Multiple Hidden Layer BPNN Architecture." Int. J. Eng. Trends Technol., 3 (6): 714–717.

Katte, V. Y., S. M. Mfoyet, B. Manefouet, A. S. L. Wouatong, and L. A. Bezeng. 2019. "Correlation of California Bearing Ratio (CBR) Value with Soil Properties of Road Subgrade Soil." Geotech. Geol. Eng., 37 (1): 217–234. Springer International Publishing. https://doi.org/10.1007/s10706-018-0604-x.

Kayadelen, C., O. Günaydın, M. Fener, A. Demir, and A. Özvan. 2009. "Modeling of the angle of shearing resistance of soils using soft computing systems." Expert Syst. Appl., 36 (9): 11814–11826. Elsevier.

Khasawneh, M. A., H. I. Al-Akhrass, S. R. Rabab'ah, and A. O. Al-sugaier. 2022. "Prediction of California Bearing Ratio Using Soil Index Properties by Regression and Machine-Learning Techniques." Int. J. Pavement Res. Technol., (0123456789). Springer Nature Singapore. https://doi.org/10.1007/s42947-022-00237-z.

Kim, P. 2017. "MATLAB Deep Learning." MATLAB Deep Learn., 81–102. https://doi.org/10.1007/978-1-4842-2845-6.

Kin, M. W. 2006. "California bearing ratio correlation with soil index properties." Master degree Proj. Fac. Civ. Eng. Univ. Technol. Malaysia.

Korde, M., and P. R. K. Yadav. 2015. "A Study of Correlation between CBR Value and Physical Properties of Some Soils." Int. J. Emerg. Technol. Adv. Eng., 5 (7): 237–239.

Kumar, S. A., J. P. Kumar, and J. Rajeev. 2013. "Application Of Machine Learning Techniques To Predict Soaked CBR Of Remolded Soils." 2 (6): 3019–3024.

LEE, T. Y. K. and S. H. 2012. "Combustion and Emission Characteristics of Wood Pyrolysis Oil-Butanol Blended Fuels in a Di Diesel Engine." Int. J. …, 13 (2): 293–300. https://doi.org/10.1007/s12239.

Leonardo et al. 2015. "regression analysis between properties of subgrade lateritic soils in Osogbo town of southwestern Nigeria." J. Sci., (July-December): 99–108.

Madsen, B. S. 2016. Statistics for Non-Statisticians. Berlin, Heidelberg: Springer Berlin Heidelberg.

Maind, S. B., and P. Wankar. 2014. "Research paper on basic of artificial neural network." Int. J. Recent Innov. Trends Comput. Commun., 2 (1): 96–100.

Mathur, U., N. Kumar, N. T. Pandey, and A. Choudhary. 2017. "Study of index properties of the soil." Ijariie, 3: 656–661.

McCulloch, W. S., and W. Pitts. 1943. "A logical calculus of the ideas immanent in nervous activity." Bull. Math. Biophys., 5: 115–133. Springer.

Mishra, A., and P. J. P. Tegar. 2019. "Correlation of CBR with Index Properties of Soil of Kolar Region (Bhopal) using Regression Analysis." (July): 3603–3612.

Mohammad, L. N., B. Huang, A. J. Puppala, and A. Allen. 1999. "Regression model for resilient modulus of subgrade soils." Transp. Res. Rec., 1687 (1): 47–54. SAGE Publications Sage CA: Los Angeles, CA.

Molla, S. 2019. "Jimma Institute of Technology School of Graduate Studies Faculty of Civil and Environmental Engineering Geotechnical Engineering Stream." Jimma University.

Muni Budhu. 2011. SOIL MECHANICS AND FOUNATIONS. JOHN WilEY SONS, INC., (A. S. Welter Jennifer, ed.).

V. Murthy. 2002. "Geotechnical Engineering Principles and Practices of Soil Mechanics and Foundation Engineering." New York Marcel Dekker, 53.

Naderpour, H., A. Kheyroddin, and G. G. Amiri. 2010. "Prediction of FRP-confined compressive strength of concrete using artificial neural networks." Compos. Struct., 92 (12): 2817–2829. Elsevier Ltd. https://doi.org/10.1016/j.compstruct.2010.04.008.

Nagaraju, T. V., R. Gobinath, P. Awoyera, and M. A. H. Abdy Sayyed. 2021. "Prediction of California Bearing Ratio of Subgrade Soils Using Artificial Neural Network Principles." Commun. Intell. Syst., 133–146. Springer Singapore. https://doi.org/10.1007/978-981-16-1089-9_12.

Nawari, N. O., R. Liang, and J. Nusairat. 1999. "Artificial intelligence techniques for the design and analysis of deep foundations." Electron. J. Geotech. Eng., 4 (1): 1–21.

NCHRP. 2004. "Cold Regions Research." Director, (September).

NCHRP 1-37A. 2004. "Guide for Mechanistic–Empirical Design of New and Rehabilitated Pavement Structures (Final Report)." Natl. Coop. Highw. Res. Progr. , Washington, DC Transp. Res. Program, Natl. Res. Counc., (February): 1–219.

De Oliveira, R. M. S., R. C. F. Araújo, F. J. B. Barros, A. P. Segundo, R. F. Zampolo, W. Fonseca, V. Dmitriev, and F. S. Brasil. 2017. "A system based on artificial neural networks for automatic classification of hydro-generator stator windings partial discharges." J. Microwaves, Optoelectron. Electromagn. Appl., 16 (3): 628–645. https://doi.org/10.1590/2179-10742017v16i3854.

Onyelowe, K. C., M. Iqbal, F. E. Jalal, M. E. Onyia, and I. C. Onuoha. 2021. "Application of 3-algorithm ANN programming to predict the strength performance of hydrated-lime activated rice husk ash treated soil." Multiscale Multidiscip. Model. Exp. Des., 4

(4): 259–274. Springer. https://doi.org/10.1007/s41939-021-00093-7.

Othman, K., and H. Abdelwahab. 2022. "The application of deep neural networks for the prediction of California Bearing Ratio of road subgrade soil." Ain Shams Eng. J., (xxxx): 101988. THE AUTHORS. https://doi.org/10.1016/j.asej.2022.101988.

Park, Y.-S., S. Lek, and S. Walczak. 2015. "Artificial Neural Network Ecological Model Types Artificial Neural Networks." J. Environ. Manage.

Patel, M. a, and H. S. Patel. 2012. "Laboratory Assessment To Correlate DCP And Optimum Moisture Content With Strength Characteristic Of Subgrade." Int. J. Eng. Res. Appl., 2 (6): 800–805.

Patel, R. S., and M. D. Desai. 2010. "CBR Predicted by Index Properties for Alluvial Soils of South Gujarat." Indian Geotech. Conf., 79–82.

Puri, N., and A. Jain. 2015. "Correlation Between California Bearing Ratio and Index Properties of Silt and Clay of Low Compressibility." 5th Indian Young Geotech. Eng. Conf., (March 2020).

Raja, M. N. A., S. K. Shukla, and M. U. A. Khan. 2022. "An intelligent approach for predicting the strength of geosynthetic-reinforced subgrade soil." Int. J. Pavement Eng., 23 (10): 3505–3521. https://doi.org/10.1080/10298436.2021.1904237.

Rezazadeh Eidgahee, D., A. Haddad, and H. Naderpour. 2019. "Evaluation of shear strength parameters of granulated waste rubber using artificial neural networks and group method of data handling." Sci. Iran., 26 (6): 3233–3244. https://doi.org/10.24200/sci.2018.5663.1408.

Roksana, K., and A. Muqtadir. 2018. "Relationship between CBR and soil index properties of bangladesh soil samples Journal of Modern Science and Technology Relationship between CBR and Soil Index Properties of Bangladesh Soil Samples Kaniz Roksana , Tabassum Islam and Abdul Muqtadir." J. Mod. Sci. Technol., 6 (August): 1–9. https://doi.org/10.13140/RG.2.2.32196.94084.

Sabat, A. K. 2015. "Prediction of california bearing ratio of a stabilized expansive soil using artificial neural network and support vector machine." Electron. J. Geotech. Eng., 20 (3): 981–991.

Sadrossadat, E., A. Heidaripanah, and B. Ghorbani. 2018. "Towards application of linear genetic programming for indirect estimation of the resilient modulus of pavements subgrade soils." Road Mater. Pavement Des., 19 (1): 139–153. Taylor & Francis. https://doi.org/10.1080/14680629.2016.1250665.

Salahudeen, A. B., J. Afar, and A. Sadeeq. 2019. California bearing ratio prediction of modified black clay using artificial neural networks.

Salchenberger, L. M., E. M. Cinar, and N. A. Lash. 1992. "Neural Networks: A New Tool for Predicting Thrift Failures." Decis. Sci., 23 (4): 899–916. https://doi.org/10.1111/j.1540-5915.1992.tb00425.x.

Sarstedt, M., and E. Mooi. 2014. "A concise guide to market research." Process. Data, 12. Springer.

Shahin, M. A. 2013. Artificial Intelligence in Geotechnical Engineering: Applications, Modeling Aspects, and Future Directions. Metaheuristics Water, Geotech. Transp. Eng. Elsevier Inc.

Shahin, M. A. 2016. "State-of-the-art review of some artificial intelligence applications in pile foundations." Geosci. Front., 7 (1): 33–44. Elsevier Ltd. https://doi.org/10.1016/j.gsf.2014.10.002.

Shahin, M. A., M. B. Jaksa, and H. R. Maier. 2001. "Artificial neural network applications in geotechnical engineering." Aust. Geomech. J., 36 (1): 49–62.

Sharma, H., M. Kumar, G. G. S. Tomar, and W. Lipo. 2020. Lecture Notes in Networks and Systems 204 Communication and Intelligent Systems Proceedings of ICCIS 2020.

Smith, G., and I. Simth. 1988. "Elements of soil mechanics Smith."

de Souza, W. M., A. J. A. Ribeiro, and C. A. U. da Silva. 2022. "Use of ANN and visual-manual classification for prediction of soil properties for paving purposes." Int. J. Pavement Eng., 23 (5): 1482–1490. Taylor & Francis. https://doi.org/10.1080/10298436.2020.1807546.

Stephens, D. J. 1992. "Variation of the California bearing ratio in some synthetic clayey soils." Civ. Eng. Siviele Ingenieurswese, 1992 (11): 379–380. South African Institution Of Civil Engineering (SAICE).

Stoltzfus, J. C. 2011. "Logistic regression: A brief primer." Acad. Emerg. Med., 18 (10):

1099–1104. https://doi.org/10.1111/j.1553-2712.2011.01185.x.

Strajhar, P., Y. Schmid, E. Liakoni, P. C. Dolder, K. M. Rentsch, D. V. Kratschmar, A. Odermatt, M. E. Liechti, R. Ac, N. No, C. No, C. V. Oramas, D. J. Langford, A. L. Bailey, M. L. Chanda, S. E. Clarke, T. E. Drummond, S. Echols, S. Glick, J. Ingrao, T. Klassen-Ross, M. L. Lacroix-Fralish, L. Matsumiya, R. E. Sorge, S. G. Sotocinal, J. M. Tabaka, D. Wong, A. M. J. M. Van Den Maagdenberg, M. D. Ferrari, K. D. Craig, and J. S. Mogil. 2016. "comparison of correlation development in Ethiopia and TRL, overseas road note 8 betweeen DCP and CBR for locally used subgrade materials." Nat. Methods.

Suthar, M., and P. Aggarwal. 2018. "Predicting CBR Value of Stabilized Pond Ash with Lime and Lime Sludge Using ANN and MR Models." Int. J. Geosynth. Gr. Eng., 4 (1): 6. Springer. https://doi.org/10.1007/s40891-017-0125-3.

Taha, S., A. Gabr, and S. El-Badawy. 2019. "Regression and Neural Network Models for California Bearing Ratio Prediction of Typical Granular Materials in Egypt." Arab. J. Sci. Eng., 44 (10): 8691–8705. Springer Berlin Heidelberg. https://doi.org/10.1007/s13369-019-03803-z.

Tai, B., J. Liu, and D. Chang. 2020. "Experimental and numerical investigation on the sunny-shady slopes effect of three cooling embankments along an expressway in warm permafrost region, China." Eng. Geol., 269: 105545. Elsevier B.V. https://doi.org/10.1016/j.enggeo.2020.105545.

Talukdar, D. K. 2014. "A Study of Correlation Between California Bearing Ratio (CBR) Value With Other Properties of Soil." Int. J. Emerg. Technol. Adv. Eng. Website www.ijetae.com, 9001 (1): 1–4.

Taskiran, T. 2010. "Prediction of California bearing ratio (CBR) of fine grained soils by AI methods." Adv. Eng. Softw., 41 (6): 886–892. Elsevier Ltd. https://doi.org/10.1016/j.advengsoft.2010.01.003.

Teferra, A., and M. Leikun. 1999. "Soil mechanics." Addis Ababa Addis Ababa Univ.

Tenpe, A. R., and A. Patel. 2020a. "Application of genetic expression programming and artificial neural network for prediction of CBR." Road Mater. Pavement Des., 21 (5): 1183–1200. Taylor & Francis. https://doi.org/10.1080/14680629.2018.1544924.

Tenpe, A. R., and A. Patel. 2020b. "Utilization of Support Vector Models and Gene Expression Programming for Soil Strength Modeling." Arab. J. Sci. Eng., 45 (5): 4301–4319. Springer Berlin Heidelberg. https://doi.org/10.1007/s13369-020-04441-6.

Terzaghi Karl, R. B. P. andGholamreza M. 1996. Soil mechanics in engineering practice. JOHN WILEY & SONS, INC.

Tesfaye, B., and A. M. Potdar. 2020. "Prediction of California Bearing Ratio of a Black Cotton Soil Stabilized With Waste Glass and Eggshell Powder Using." J. Xi'an Univ. Archit. Technol., XII (Ix): 805–812. https://doi.org/10.20372/nadre/20116.

Tien Bui, D., V. H. Nhu, and N. D. Hoang. 2018. "Prediction of soil compression coefficient for urban housing project using novel integration machine learning approach of swarm intelligence and Multi-layer Perceptron Neural Network." Adv. Eng. Informatics, 38 (April): 593–604. Elsevier. https://doi.org/10.1016/j.aei.2018.09.005.

Trong, D. K., B. T. Pham, F. E. Jalal, M. Iqbal, P. C. Roussis, A. Mamou, M. Ferentinou, D. Q. Vu, N. Duc Dam, Q. A. Tran, and P. G. Asteris. 2021. "On Random Subspace Optimization-Based Hybrid Computing Models Predicting the California Bearing Ratio of Soils." Materials (Basel)., 14 (21): 6516. Multidisciplinary Digital Publishing Institute. https://doi.org/10.3390/ma14216516.

Tsehayu, K., and T. Hailemariam. 1990. "Engineering geological map of Addis Ababa." Ethiop. Inst. Geol. Surv. Addis Ababa.

Varghese, V. K., S. S. Babu, R. Bijukumar, S. Cyrus, and B. M. Abraham. 2013. "Artificial Neural Networks: A Solution to the Ambiguity in Prediction of Engineering Properties of Fine-Grained Soils." Geotech. Geol. Eng., 31 (4): 1187–1205. https://doi.org/10.1007/s10706-013-9643-5.

Venkatramaiah, C. 1995. Geotechnical engineering. New Age International.

Verma, G., and B. Kumar. 2022. "Application of multi-expression programming (MEP) in predicting the soaked California bearing ratio (CBR) value of fine-grained soil." Innov. Infrastruct. Solut., 7 (4): 1–16. Springer International Publishing. https://doi.org/10.1007/s41062-022-00858-0.

Vujičić, T., T. Matijević, and Z. Ševarac. 2016. "Comparative Analysis of Methods for

Determining Number of Hidden Neurons in Artificial Neural Network.” Cent. Eur. Conf. Inf. Intell. Syst., 219–223.

Wang, H. L., and Z. Y. Yin. 2020. “High performance prediction of soil compaction parameters using multi expression programming.” Eng. Geol., 276: 105758. Elsevier B.V. https://doi.org/10.1016/j.enggeo.2020.105758.

Yildirim, B., and O. Gunaydin. 2011. “Estimation of California bearing ratio by using soft computing systems.” Expert Syst. Appl., 38 (5): 6381–6391. Elsevier Ltd. https://doi.org/10.1016/j.eswa.2010.12.054.

Yoder, E. J., and M. W. Witczak. 1991. Principles of pavement design. John Wiley & Sons.

APPENDIX

APPENDIX A: DETAILS OF SECONDARY DATA

Percent of Grain Size Distribution Property			Atterberg Limits			Modified Proctor		
% Gravel	%sand	%Fine	liquid limit (LL)	plastic limit (PL)	plastic index (PI)	Optimum moisture content (OMC %)	Maximum Dry Density (g/cm3)	CBR%
29.00	19.00	52.00	51.00	26.00	25.00	20.30	1.67	0.50
9.48	7.15	83.36	86.00	46.19	39.81	16.60	1.62	0.60
6.73	8.18	85.09	73.00	40.05	32.95	19.20	1.60	0.60
6.85	10.17	82.99	67.00	35.09	31.91	19.80	1.55	0.60
4.57	10.72	84.70	67.00	38.86	28.14	23.60	1.57	0.60
0.98	12.41	86.61	71.00	39.41	31.59	17.60	1.57	0.70
1.66	11.76	86.57	66.00	34.77	31.23	19.00	1.63	0.70
3.75	6.17	90.08	71.00	41.63	29.37	20.00	1.59	0.70
5.38	6.55	88.07	71.00	40.57	30.43	20.00	1.55	0.70
4.42	11.75	83.83	64.00	36.92	27.08	16.40	1.64	0.80
28.03	11.77	60.20	73.00	36.67	36.33	15.40	1.70	0.90
13.10	16.51	70.39	65.00	35.40	29.60	18.60	1.62	0.90
3.31	10.13	86.56	73.00	35.86	37.14	19.40	1.60	0.90
0.00	20.00	80.00	42.00	22.00	20.00	12.50	1.89	1.00
7.00	12.00	81.00	51.00	27.00	24.00	14.00	1.89	1.00
0.00	32.00	68.00	63.00	36.00	27.00	15.00	1.67	1.00
1.29	9.52	89.19	64.00	36.37	27.63	15.40	1.60	1.00
0.00	20.00	80.00	68.00	37.00	31.00	16.00	1.68	1.00
43.28	8.38	48.34	61.00	31.33	29.67	16.60	1.73	1.00
6.00	9.00	85.00	63.00	31.00	32.00	17.00	1.64	1.00
0.00	18.00	82.00	79.00	40.00	39.00	18.00	1.54	1.00
8.48	19.75	71.78	62.00	32.07	29.93	18.00	1.60	1.00
10.00	27.00	63.00	57.00	31.00	26.00	18.00	1.53	1.00
11.89	10.91	77.20	60.00	32.43	27.57	18.60	1.65	1.00
0.00	17.00	83.00	70.00	40.00	30.00	19.00	1.57	1.00
0.00	37.00	63.00	55.00	27.00	28.00	19.00	1.65	1.00
2.00	7.00	91.00	82.00	31.00	51.00	19.00	1.51	1.00
14.00	8.00	78.00	66.00	33.00	33.00	19.00	1.54	1.00
6.29	13.35	80.35	61.00	35.95	25.05	19.60	1.65	1.00
1.00	5.00	94.00	71.00	31.00	40.00	20.00	1.60	1.00
1.00	11.00	88.00	86.00	33.00	53.00	20.00	1.60	1.00
4.00	6.00	90.00	86.00	35.00	51.00	20.00	1.49	1.00
0.00	9.00	91.00	83.00	38.00	45.00	21.00	1.52	1.00
0.00	8.00	92.00	87.00	44.00	43.00	21.00	1.53	1.00

0.00	7.00	93.00	80.00	31.00	49.00	21.00	1.57	1.00
0.00	28.00	72.00	71.00	40.00	31.00	21.00	1.60	1.00
1.00	6.00	93.00	81.00	33.00	48.00	21.00	1.56	1.00
4.00	3.00	93.00	56.00	28.00	28.00	21.00	1.56	1.00
0.00	13.00	87.00	86.00	44.00	42.00	22.00	1.43	1.00
0.00	26.00	74.00	74.00	39.00	35.00	22.00	1.55	1.00
0.00	11.00	89.00	77.00	42.00	35.00	22.00	1.56	1.00
0.00	20.00	80.00	66.00	34.00	32.00	22.00	1.56	1.00
12.26	16.86	70.89	68.00	33.45	34.55	22.00	1.60	1.00
0.00	24.00	76.00	73.00	42.00	31.00	23.00	1.56	1.00
0.00	18.00	82.00	72.00	39.00	33.00	24.00	1.54	1.00
0.00	6.00	94.00	97.00	45.00	52.00	25.00	1.50	1.00
0.00	8.00	92.00	93.00	45.00	45.00	25.00	1.51	1.00
0.00	9.00	91.00	94.00	43.00	51.00	27.00	1.52	1.00
0.00	5.00	95.00	77.00	40.00	37.00	29.00	1.46	1.00
0.00	13.00	87.00	81.00	36.00	45.00	33.00	1.46	1.00
0.00	22.00	78.00	56.00	34.00	22.00	17.80	1.69	1.03
0.00	2.00	98.00	72.00	34.00	38.00	34.00	1.49	1.20
0.00	27.60	72.40	82.00	43.10	38.90	37.20	1.34	1.27
0.00	25.60	74.40	51.80	28.00	23.80	24.80	1.59	1.30
0.00	16.50	83.50	70.00	33.90	36.10	26.60	1.50	1.35
0.00	11.30	88.70	80.30	44.50	35.80	13.90	1.85	1.36
0.00	1.80	98.20	80.40	45.60	34.80	35.00	1.45	1.38
41.92	12.84	45.24	60.00	33.55	26.45	18.60	1.65	1.40
27.23	9.54	63.23	70.00	37.62	32.38	19.80	1.65	1.40
0.00	13.90	86.10	75.00	38.60	36.40	27.50	1.48	1.41
0.00	5.30	94.70	65.00	31.00	34.00	26.80	1.59	1.43
0.00	10.90	89.10	71.00	37.00	34.00	26.60	1.52	1.44
0.00	10.90	89.10	67.00	37.00	30.00	27.00	1.49	1.44
23.63	14.20	62.17	70.00	34.52	35.48	17.40	1.66	1.50
0.00	26.00	74.00	65.00	34.00	31.00	19.50	1.71	1.50
0.00	22.00	78.00	49.00	34.00	15.00	19.60	1.76	1.56
0.00	17.00	83.00	51.00	34.00	17.00	23.00	1.73	1.57
18.00	12.69	69.31	65.00	31.97	33.03	19.60	1.62	1.60
20.45	10.25	69.29	62.00	32.75	29.25	20.00	1.66	1.60
1.00	3.00	96.00	73.00	37.00	36.00	28.00	1.46	1.60
0.00	15.00	85.00	64.00	35.00	29.00	18.40	1.63	1.65
4.00	7.00	89.00	71.00	36.00	35.00	27.60	1.46	1.65
2.00	6.00	92.00	71.00	36.00	35.00	27.70	1.46	1.70
1.00	8.00	91.00	71.00	36.00	35.00	27.80	1.46	1.70
0.00	16.00	84.00	68.00	40.00	28.00	22.00	1.72	1.75
17.76	14.29	67.96	60.00	31.68	28.32	22.00	1.60	1.80
6.00	7.00	87.00	71.00	36.00	35.00	27.40	1.47	1.80
36.69	12.66	50.65	70.00	35.57	34.43	22.00	1.62	1.90

8.00	16.00	76.00	43.00	21.00	22.00	12.30	1.94	2.00
0.00	14.00	86.00	71.00	39.00	32.00	13.00	1.58	2.00
1.00	11.00	88.00	44.00	21.00	23.00	13.00	1.88	2.00
0.00	7.00	93.00	79.00	48.00	31.00	15.00	1.69	2.00
0.00	30.00	70.00	65.00	42.00	23.00	16.00	1.64	2.00
0.00	2.00	98.00	37.00	22.00	15.00	16.50	1.78	2.00
0.00	11.00	89.00	81.00	34.00	47.00	17.00	1.58	2.00
0.00	6.00	94.00	50.00	25.00	25.00	18.00	1.55	2.00
0.00	28.00	72.00	80.00	38.00	42.00	19.00	1.62	2.00
16.00	18.00	66.00	43.00	28.00	15.00	19.00	1.60	2.00
0.00	40.90	59.10	43.00	22.00	21.00	19.60	1.63	2.00
5.01	15.73	79.26	63.00	31.92	31.08	19.60	1.52	2.00
0.00	18.00	82.00	73.00	41.00	32.00	20.00	1.57	2.00
0.00	40.00	60.00	59.00	33.00	26.00	20.00	1.57	2.00
0.00	40.00	60.00	75.00	46.00	29.00	21.00	1.52	2.00
5.01	16.72	78.27	60.00	36.24	23.76	21.00	1.59	2.00
0.00	35.00	65.00	45.00	25.40	19.60	22.80	1.49	2.00
0.00	2.00	98.00	55.00	29.00	26.00	22.80	1.59	2.00
11.81	5.28	82.91	62.00	36.92	25.08	22.80	1.45	2.00
0.00	11.00	89.00	81.00	40.00	41.00	23.00	1.53	2.00
1.00	9.00	90.00	64.00	27.00	37.00	23.00	1.49	2.00
4.00	39.00	57.00	66.00	33.00	33.00	23.00	1.48	2.00
24.00	12.00	64.00	58.00	34.00	24.00	23.00	1.45	2.00
3.45	11.91	84.64	68.00	35.51	32.49	26.00	1.47	2.00
0.00	11.00	89.00	88.00	43.00	45.00	27.00	1.49	2.00
0.00	11.00	89.00	75.00	39.00	36.00	27.00	1.60	2.00
0.00	18.00	82.00	82.00	42.00	40.00	27.80	1.50	2.00
0.00	25.00	75.00	71.00	38.00	33.00	28.00	1.50	2.00
0.00	30.00	70.00	69.00	35.00	34.00	29.20	1.50	2.00
0.00	6.00	94.00	83.00	53.00	30.00	29.20	1.50	2.00
0.00	8.00	92.00	44.00	25.00	19.00	31.80	1.50	2.00
0.00	9.00	91.00	77.00	34.00	43.00	32.60	1.50	2.00
0.00	46.00	54.00	86.00	50.00	36.00	36.00	1.22	2.00
0.00	7.00	93.00	30.10	18.10	12.00	12.30	1.94	2.10
0.94	16.53	82.53	63.00	30.58	32.42	19.40	1.59	2.10
0.00	28.00	72.00	51.00	28.00	23.00	30.00	1.56	2.10
22.85	11.25	65.91	65.00	40.08	24.92	18.40	1.59	2.20
0.00	14.30	85.70	81.30	44.10	37.20	31.80	1.43	2.20
0.00	9.00	91.00	29.80	18.10	11.70	12.70	1.97	2.30
38.68	5.78	55.53	77.00	40.13	36.87	18.00	1.65	2.30
0.00	38.00	62.00	61.00	32.00	29.00	28.00	1.57	2.32
0.00	9.00	91.00	29.90	18.80	11.10	12.60	1.96	2.40
0.00	9.00	91.00	72.00	41.00	31.00	30.00	1.43	2.40
0.00	10.00	90.00	31.20	19.30	11.90	12.20	1.95	2.50

0.00	10	90.00	31.2	19.3	11.9	12.70	1.95	2.50
0.00	14	86	29.4	18.4	11	13.00	1.92	2.50
12.37	6.14	81.48	60.00	36.54	23.46	22.00	1.54	2.50
2.00	7.00	91.00	63.00	32.00	31.00	27.10	1.47	2.50
0.00	9.00	91.00	32.20	20.10	12.10	12.10	1.96	2.60
0.00	8.00	92.00	31.20	19.30	11.90	12.30	1.96	2.60
0.26	5.82	93.92	68.85	38.00	30.85	21.96	1.55	2.60
0.00	10.00	90.00	74.00	37.00	37.00	28.60	1.50	2.60
5.00	8.00	87.00	65.00	33.00	32.00	26.60	1.48	2.65
0.00	11.00	89.00	30.20	18.10	12.10	12.20	1.98	2.80
0.00	13	87.00	29.8	18.6	11.2	12.30	1.93	2.80
0.00	10	90.00	31.1	18.7	12.4	12.40	1.96	2.80
0.00	12.00	88.00	64.00	34.00	30.00	25.00	1.33	2.80
0.00	12.00	88.00	64.00	34.00	30.00	25.00	1.33	2.80
7.78	14.68	77.55	55.00	34.39	20.61	25.00	1.53	2.80
0.00	8.00	92.00	59.00	30.00	29.00	26.20	1.48	2.80
0.00	11	89	30.5	18.8	11.7	12.40	1.95	2.90
0.00	12	88.00	29.9	18.4	11.5	12.80	1.93	2.90
8.33	14.20	77.47	57.00	35.17	21.83	24.20	1.48	2.90
7.00	7.00	86.00	61.00	31.00	30.00	26.00	1.48	2.90
5.00	9.00	86.00	63.00	32.00	31.00	26.30	1.48	2.90
2.29	29.90	67.81	60.00	40.35	19.65	26.60	1.37	2.90
5.00	20.00	75.00	41.00	20.00	21.00	12.50	1.95	3.00
0.00	11	89.00	30.4	18.8	11.6	12.70	1.94	3.00
0.00	37.00	63.00	31.00	16.00	15.00	13.00	1.82	3.00
2.00	17.00	81.00	43.00	21.00	22.00	13.20	1.88	3.00
0.00	31.00	69.00	79.00	43.00	36.00	16.00	1.51	3.00
0.00	40.00	60.00	58.00	38.00	28.00	19.00	1.53	3.00
0.00	48.00	52.00	53.00	34.00	19.00	20.00	1.59	3.00
10.29	19.51	70.20	60.00	31.11	28.89	21.40	1.61	3.00
2.00	19.00	79.00	54.00	31.00	23.00	22.00	1.48	3.00
2.00	7.00	91.00	62.00	34.00	28.00	24.00	1.52	3.00
19.23	9.28	71.49	69.00	43.74	25.26	24.00	1.40	3.00
0.00	7.60	92.40	67.00	34.00	33.00	24.50	1.40	3.00
0.00	23.00	77.00	74.00	44.00	30.00	25.00	1.50	3.00
0.00	14.00	86.00	62.00	37.00	25.00	25.20	1.50	3.00
0.00	4.00	96.00	72.00	37.00	35.00	25.70	1.60	3.00
0.00	3.00	97.00	60.00	32.00	28.00	26.00	1.48	3.00
0.00	7.00	93.00	75.00	32.00	43.00	26.40	1.50	3.00
0.00	5.00	95.00	73.00	44.00	29.00	27.00	1.52	3.00
0.00	3.00	97.00	69.00	38.00	31.00	28.00	1.48	3.00
0.00	6.00	94.00	70.00	38.00	32.00	28.00	1.58	3.00
0.00	6.00	94.00	74.00	36.00	38.00	28.60	1.48	3.00
0.00	24.00	76.00	77.00	38.00	39.00	29.60	1.53	3.00

0.00	7.00	93.00	59.00	33.00	26.00	30.60	1.50	3.00
0.00	12.00	88.00	28.40	17.00	11.40	11.70	1.98	3.10
19.29	10.58	70.13	54.00	34.97	19.03	21.40	1.57	3.10
10.00	14.00	76.00	68.00	34.00	34.00	25.80	1.49	3.10
12.00	15.00	73.00	71.00	36.00	35.00	25.50	1.49	3.18
8.00	18.00	74.00	67.00	34.00	33.00	25.30	1.49	3.30
16.70	6.85	76.45	54.00	29.86	24.14	29.00	1.47	3.30
0.00	10	90.00	30.9	19.1	11.8	12.40	1.96	3.40
35.20	19.25	45.56	54.00	33.84	20.16	21.00	1.62	3.40
11.53	16.77	71.70	54.00	33.12	20.88	28.00	1.52	3.40
10.00	22.00	68.00	67.00	34.00	33.00	24.90	1.50	3.44
29.73	9.02	61.24	56.00	35.23	20.77	20.60	1.59	3.50
0.79	6.00	93.20	54.00	32.41	21.59	22.60	1.53	3.50
0.00	12.00	88.00	79.00	40.00	39.00	29.40	1.54	3.50
31.24	18.93	49.83	55.00	29.03	25.97	18.40	1.68	3.60
18.00	19.00	63.00	60.00	30.00	30.00	24.30	1.52	3.60
10.00	21.00	69.00	63.00	32.00	31.00	24.60	1.50	3.62
18.48	12.69	68.83	52.00	32.59	19.41	23.80	1.56	3.80
17.00	19.00	64.00	59.00	30.00	29.00	24.20	1.52	3.83
3.00	18.00	79.00	43.00	20.00	23.00	12.50	1.92	4.00
2.00	22.00	76.00	59.00	33.00	26.00	20.00	1.62	4.00
50.71	11.09	38.20	59.00	36.12	22.88	20.60	1.58	4.00
3.00	15.00	82.00	58.00	33.00	25.00	22.00	1.49	4.00
21.00	10.00	69.00	54.00	31.00	23.00	22.00	1.54	4.00
41.00	8.00	51.00	53.00	29.00	24.00	22.00	1.52	4.00
32.00	19.00	49.00	42.00	27.00	15.00	23.00	1.70	4.00
0.00	11.00	89.00	73.00	42.00	31.00	24.50	1.60	4.00
0.00	10.00	90.00	70.00	39.00	31.00	26.00	1.51	4.00
0.00	11.00	89.00	71.00	36.00	35.00	26.50	1.50	4.00
0.00	6.00	94.00	59.00	34.00	25.00	30.80	1.50	4.00
0.00	24.00	76.00	30.00	18.00	12.00	11.80	1.99	4.10
60.56	8.97	30.47	48.00	27.63	20.37	14.00	1.85	4.10
0.00	13.00	87.00	73.00	35.00	38.00	33.60	1.51	4.12
15.57	28.18	56.24	48.00	33.05	14.95	20.60	1.66	4.40
4.36	18.77	76.88	52.00	32.00	20.00	21.40	1.54	4.50
0.00	26.00	74.00	29.50	20.20	9.30	11.60	1.98	4.80
3.00	17.00	80.00	29.30	21.40	7.90	12.00	1.96	4.80
0.00	12.80	87.20	61.70	31.30	30.40	28.00	1.51	4.80
10.00	36.00	54.00	30.00	22.00	8.00	15.00	1.71	5.00
51.80	11.54	36.66	41.00	25.33	15.67	15.00	1.76	5.00
26.00	21.00	53.00	51.00	28.00	23.00	16.00	1.64	5.00
24.51	24.11	51.38	51.00	33.24	17.76	17.80	1.54	5.00
52.20	13.77	34.03	47.00	29.83	17.17	21.91	1.75	5.00
10.52	4.76	84.72	80.19	39.23	40.97	22.00	1.60	5.00

1.00	13.00	86.00	51.00	29.00	22.00	23.00	1.66	5.00
0.00	7.00	93.00	46.00	26.00	20.00	26.60	1.49	5.00
27.56	12.08	60.35	49.00	29.06	19.94	21.00	1.67	5.10
7.00	21.00	72.00	27.00	22.10	4.90	11.50	1.97	5.30
4.00	19.00	77.00	28.00	22.20	5.80	11.80	1.97	5.50
5.00	18.00	77.00	28.20	21.90	6.30	11.30	1.97	5.60
4.00	17.00	79.00	28.20	21.90	6.30	11.30	1.98	5.70
5.00	16.00	79.00	28.30	22.10	6.20	11.40	1.98	5.80
2.00	8.00	90.00	53.00	27.00	26.00	22.70	1.59	5.90
0.00	34.70	65.30	38.30	18.90	19.40	12.60	1.98	6.00
0.00	15.00	85.00	29.00	19.00	10.00	13.00	1.85	6.00
2.00	19.00	79.00	44.00	29.00	15.00	17.00	1.54	6.00
27.62	5.60	66.78	79.00	37.69	41.31	19.03	1.66	6.00
0.56	14.80	84.64	59.59	33.13	26.46	22.60	1.65	6.00
0.00	4.00	96.00	50.00	27.00	23.00	23.00	1.51	6.00
0.00	14.00	86.00	54.00	30.00	24.00	25.00	1.50	6.00
18.00	16.00	66.00	50.00	26.00	24.00	21.00	1.65	6.10
5.00	18.00	77.00	28.10	22.40	5.70	11.40	1.98	6.20
5.00	18.00	77.00	28.10	22.40	5.70	11.40	1.98	6.20
10.00	18.00	72.00	49.00	26.00	23.00	21.10	1.65	6.20
16.00	26.00	58.00	53.00	27.00	26.00	20.80	1.65	6.30
7.00	20.00	73.00	27.20	21.90	5.30	11.20	1.99	6.40
29.00	15.00	56.00	55.00	28.00	27.00	20.70	1.65	6.40
7.00	19.00	74.00	27.70	22.60	5.10	11.40	1.99	6.50
7.00	19.00	74.00	27.70	22.60	5.10	11.40	1.99	6.50
37.44	24.48	38.09	46.00	29.75	16.25	12.20	1.67	6.50
6.00	22.00	72.00	27.00	21.30	5.70	11.00	1.98	6.60
6.00	22.00	72.00	27.00	21.30	5.70	11.00	2.00	6.60
48.59	16.65	34.76	50.00	29.90	20.10	15.80	1.67	6.60
38.00	24.00	38.00	50.00	26.00	24.00	20.00	1.68	6.60
40.00	23.00	37.00	49.00	26.00	23.00	19.80	1.69	6.80
0.00	31.00	69.00	26.00	17.00	9.00	12.20	1.86	7.00
61.09	7.53	31.37	44.00	29.67	14.33	19.00	1.67	7.00
9.00	9.00	82.00	49.00	28.00	21.00	20.00	1.57	7.00
11.00	35.00	54.00	45.00	28.00	17.00	20.00	1.61	7.00
19.00	18.00	63.00	55.00	30.00	25.00	22.00	1.61	7.00
23.00	16.00	61.00	53.00	33.00	20.00	25.00	1.52	7.00
0.00	33.00	67.00	30.00	22.00	8.00	14.00	1.76	8.00
48.00	20.00	32.00	43.00	27.00	16.00	15.80	1.67	8.00
19.00	27.00	54.00	54.00	34.00	20.00	22.00	1.48	8.00
0.00	28.00	72.00	60.00	31.00	29.00	25.00	1.54	8.00
0.00	17.70	82.30	72.00	35.10	36.90	27.80	1.50	8.10
54.00	13.00	33.00	50.00	26.00	24.00	15.70	1.87	8.40
65.00	13.00	22.00	53.00	28.00	25.00	17.00	1.73	9.00

53.00	16.00	31.00	43.00	25.00	18.00	19.00	1.71	9.00
44.00	9.00	47.00	53.00	28.00	25.00	24.00	1.64	9.00
5.00	46.00	49.00	36.00	25.00	11.00	13.00	1.74	10.00
71.09	12.95	15.96	48.00	31.89	16.11	16.20	1.84	10.00
6.00	22.00	72.00	52.00	29.00	23.00	17.00	1.67	10.00
31.00	17.00	52.00	43.00	28.00	15.00	20.00	1.54	10.00
25.37	34.19	40.44	34.00	22.18	11.82	20.40	1.78	10.00
5.00	46.00	49.00	36.00	25.00	11.00	11.50	1.98	11.00
0.00	54.00	46.00	56.00	30.00	20.00	15.00	1.82	11.00
0.00	50.00	50.00	58.00	30.00	26.00	15.00	1.86	11.00
11.00	50.00	39.00	39.00	30.00	9.00	21.00	1.65	11.00
0.00	11.00	89.00	32.00	22.00	10.00	13.00	1.76	12.00
29.00	27.00	44.00	38.00	28.00	10.00	14.60	1.77	12.00
64.00	15.00	21.00	44.00	27.00	17.00	18.00	1.83	12.00
0.00	64.00	36.00	51.00	31.00	20.00	20.00	1.75	12.00
4.00	17.00	79.00	42.00	25.00	17.00	20.00	1.57	12.00
0.00	32.40	67.60	46.00	26.00	20.00	24.50	1.54	12.00
0.00	31.90	68.10	43.00	23.00	20.00	12.50	1.91	12.30
2.00	56.00	42.00	24.00	21.00	3.00	15.00	1.73	13.00
0.00	46.00	54.00	53.00	34.00	19.00	22.00	1.64	13.00
63.00	14.00	23.00	47.00	26.00	21.00	15.00	1.60	14.00
0.00	58.00	42.00	24.00	14.00	10.00	15.50	1.71	14.00
36.00	31.00	33.00	43.00	22.00	21.00	15.90	1.86	14.00
12.00	46.00	42.00	30.00	24.00	6.00	16.00	1.70	14.00
46.00	22.00	32.00	51.00	26.00	25.00	15.70	1.87	14.80
40.00	24.00	36.00	51.00	33.00	18.00	17.00	1.81	15.00
60.05	13.95	26.00	34.00	23.18	10.82	17.80	1.65	15.00
0.00	28.00	72.00	47.00	23.00	24.00	13.00	1.78	16.00
47.00	25.00	28.00	47.00	24.00	23.00	15.40	1.88	16.00
0.00	51.80	48.20	55.00	30.90	24.10	16.00	1.80	16.00
49.80	30.52	19.69	35.00	24.70	10.30	12.60	1.95	17.00
71.00	10.00	19.00	34.00	21.00	13.00	15.00	1.85	17.00
50.00	22.00	28.00	47.00	24.00	23.00	15.20	1.88	17.00
0.00	49.00	51.00	46.00	26.00	20.00	16.00	1.80	17.00
52.83	20.13	27.05	44.00	31.09	12.91	19.00	1.71	17.00
0.00	71.00	29.00	47.00	32.00	15.00	19.50	1.70	17.00
55.00	15.00	30.00	50.00	31.00	19.00	15.80	1.67	19.00
0.00	61.00	39.00	52.00	29.00	23.00	20.00	1.75	19.00
0.00	31.70	68.30	38.00	31.00	7.00	17.80	1.80	22.00
1.00	46.00	53.00	39.00	30.00	9.00	23.00	1.62	23.00
5.00	46.00	49.00	36.00	25.00	11.00	13.00	1.75	24.00
26.00	27.00	47.00	45.00	29.00	16.00	21.00	1.57	24.00
0.00	45.00	55.00	59.00	37.00	22.00	11.20	1.72	25.00
50.96	26.90	22.14	41.00	26.79	14.21	17.80	1.78	27.00

0.00	32.00	68.00	53.00	33.00	20.00	19.00	1.70	27.00
32.45	29.51	38.04	32.00	23.57	8.43	13.60	1.85	29.00
71.00	8.00	21.00	40.00	29.00	11.00	15.00	1.85	29.00
62.56	10.33	27.10	48.00	28.85	19.15	14.00	1.85	30.00

APPENDIX B: DETAILS OF GRAIN SIZE ANALYSIS TEST RESULTS

Location: Delber

Test Method: ASTM D 422

Wet Sieve Analysis					Total mass of sample, 1000g		
Sieve No.	Sieve Opening (mm)	Mass of Sieve (g)	Mass of sieve + Retaine	Mass of Retained soil (g)	Percentage Retained (%)	Cum. Percentage Retained	Percentage Passing (%)
3/4"	19.0	555.4	555.4	0.0	0.0	0.0	100.0
1/2"	12.5	560.7	560.7	0.0	0.0	0.0	100.0
3.8"	9.5	534.8	534.8	0.0	0.0	0.0	100.0
No 4	4.75	571.0	571.0	0.0	0.0	0.0	100.0
No 8	2.36	533.4	533.4	0.0	0.0	0.0	100.0
No 10	2	529.2	560.2	31.0	2.5	2.5	97.5
No 40	0.425	432.8	503.8	71.0	5.7	8.3	91.7
No 200	0.075	391.3	554.3	163.0	13.2	21.5	78.5
pan	-------	410.0	1380.0	970.0	78.5	100.0	0.0
				1235.0	82.33333333		

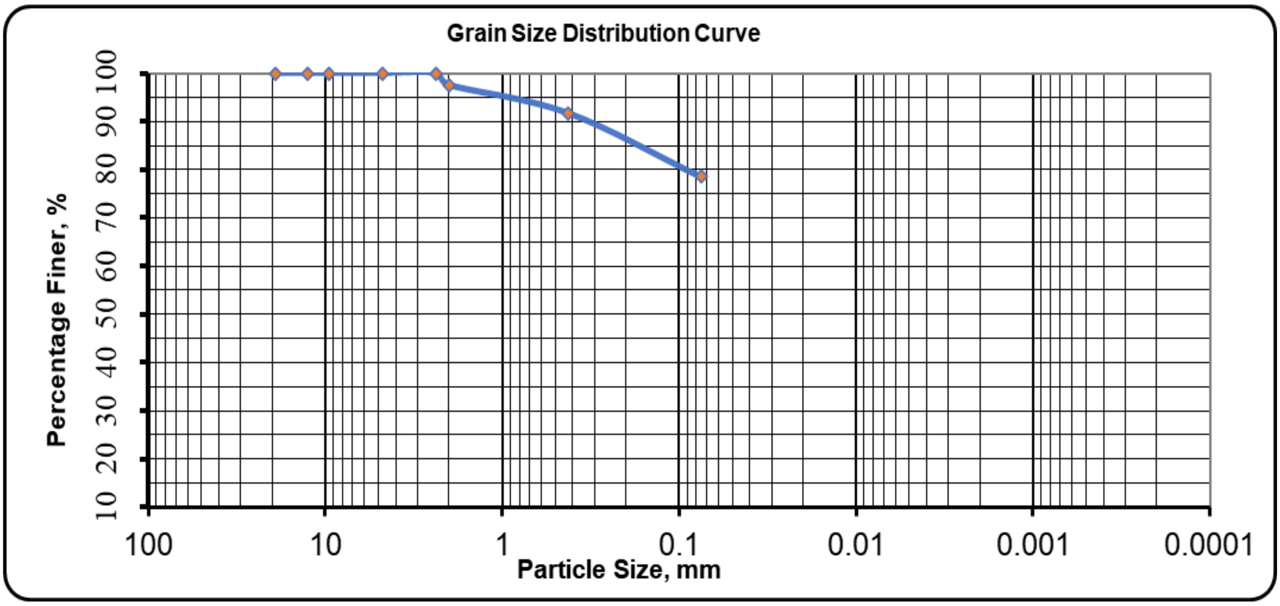

Location: Adisu Gebiya

Test Method: ASTM D 422

Wet Sieve Analysis					Total mass of sample, 1000g		
Sieve No.	Sieve Opening (mm)	Mass of Sieve (g)	Mass of sieve + Retaine	Mass of Retained soil (g)	Percentage Retained (%)	Cum. Percentage Retained	Percentage Passing (%)
3/4"	19.0	555.4	555.4	0.0	0.0	0.0	100.0
1/2"	12.5	560.7	560.7	0.0	0.0	0.0	100.0
3.8"	9.5	534.8	534.8	0.0	0.0	0.0	100.0
No 4	4.75	571.0	571.0	0.0	0.0	0.0	100.0
No 8	2.36	533.4	533.4	0.0	0.0	0.0	100.0
No 10	2	529.2	529.2	0.0	0.0	0.0	100.0
No 40	0.425	432.8	456.8	24.0	3.0	3.0	97.0
No 200	0.075	391.3	439.3	48.0	6.0	9.0	91.0
pan	-------	410.0	1140.0	730.0	91.0	100.0	0.0
				802.0	53.46666667		

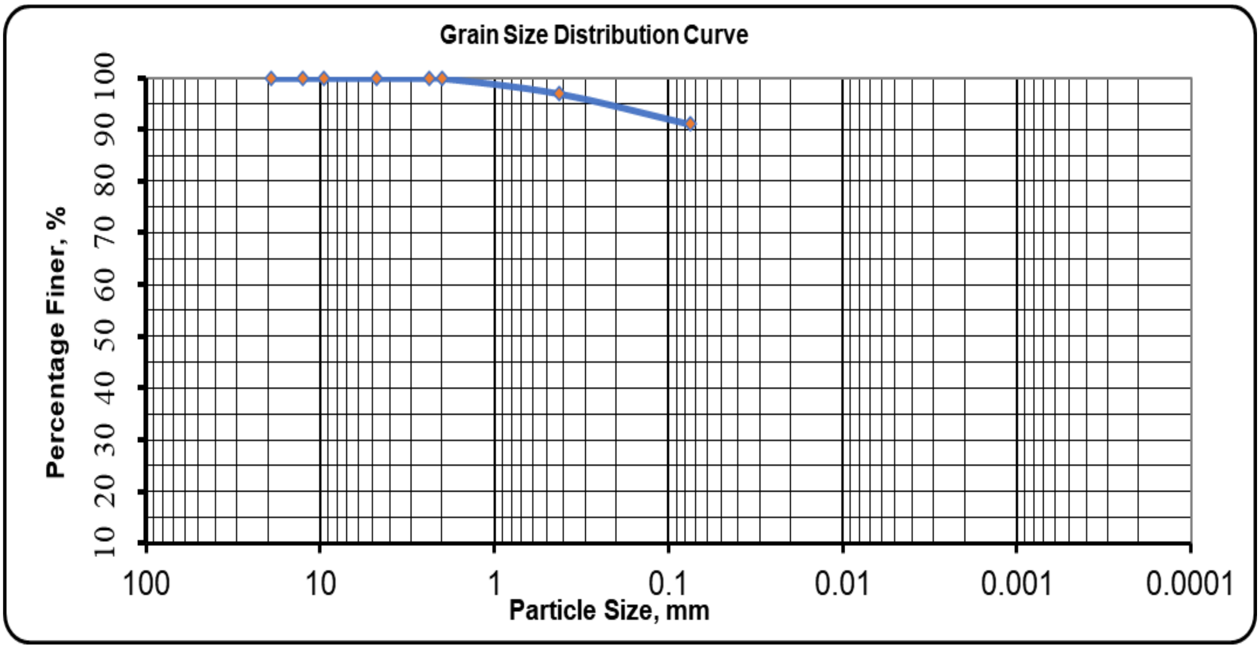

Location: Goro

Test Method: ASTM D 422

Wet Sieve Analysis					Total mass of sample,		
Sieve No.	Sieve Opening (mm)	Mass of Sieve (g)	Mass of sieve + Retaine	Mass of Retained soil (g)	Percentage Retaine	Cum. Percentage	Percentage Passing
3/4''	19.0	555.4	555.4	0.0	0.0	0.0	100.0
1/2"	12.5	560.7	560.7	0.0	0.0	0.0	100.0
3.8"	9.5	534.8	534.8	0.0	0.0	0.0	100.0
No 4	4.75	571.0	646.0	75.0	12.5	12.5	87.5
No 8	2.36	533.4	593.4	60.0	10.0	22.5	77.5
No 16	1.18	503.5	528.5	25.0	4.2	26.7	73.3
No 30	0.6	452.2	452.2	0.0	0.0	26.7	73.3
No 40	0.425	432.8	452.8	20.0	3.3	30.0	70.0
No 100	0.15	403.3	418.3	15.0	2.5	32.5	67.5
No 200	0.075	391.3	401.3	10.0	1.7	34.2	65.8
pan	-------	410.0	805.0	395.0	65.8	100.0	0.0
				600.0	40		

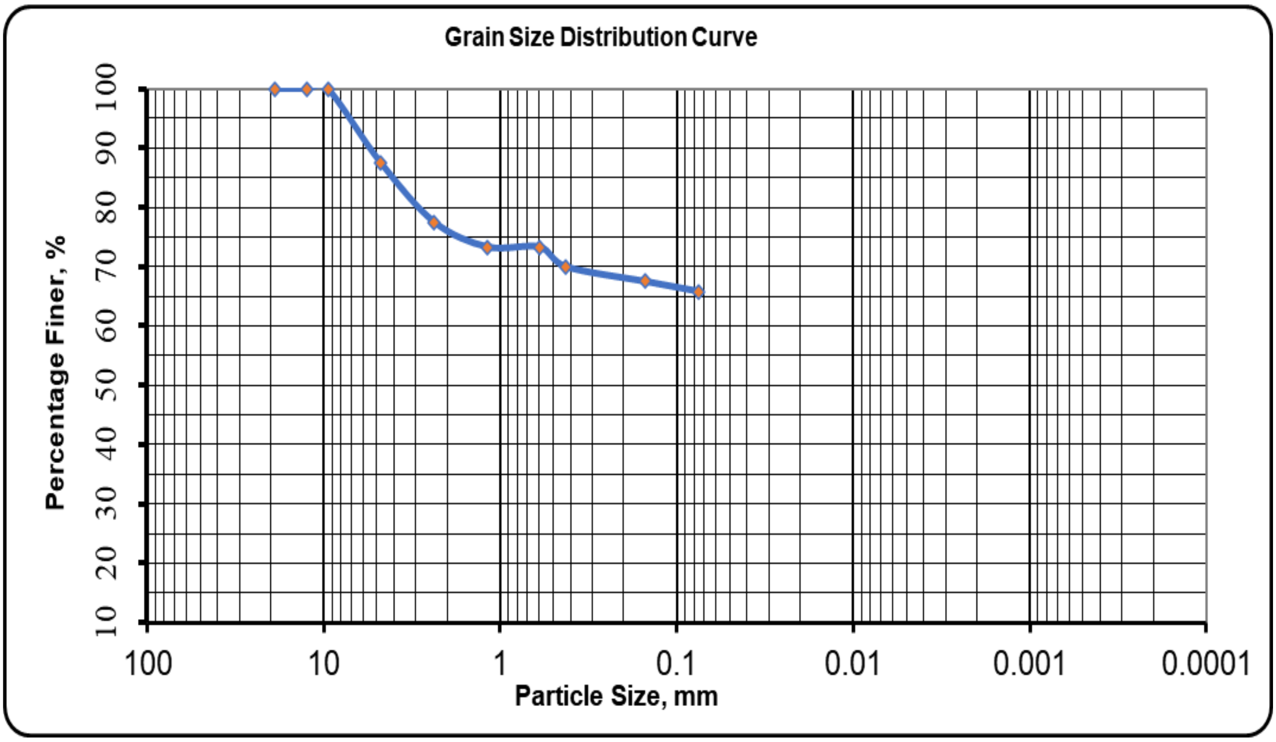

Location: Megenagna

Test Method: ASTM D 422

Wet Sieve Analysis					Total mass of sample, 1000g		
Sieve No.	Sieve Opening (mm)	Mass of Sieve (g)	Mass of sieve + Retaine	Mass of Retained soil (g)	Percentage Retained (%)	Cum. Percentage Retained	Percentage Passing (%)
3/4"	19.0	555.4	555.4	0.0	0.0	0.0	100.0
1/2"	12.5	560.7	560.7	0.0	0.0	0.0	100.0
3.8"	9.5	534.8	534.8	0.0	0.0	0.0	100.0
No 4	4.75	571.0	571.0	0.0	0.0	0.0	100.0
No 8	2.36	533.4	537.4	4.0	0.5	0.5	99.5
No 10	2	529.2	541.2	12.0	1.4	1.9	98.1
No 40	0.425	432.8	466.8	34.0	3.9	5.8	94.2
No 200	0.075	391.3	461.3	70.0	8.1	13.9	86.1
pan	-------	410.0	1154.0	744.0	86.1	100.0	0.0
				864.0	57.6		

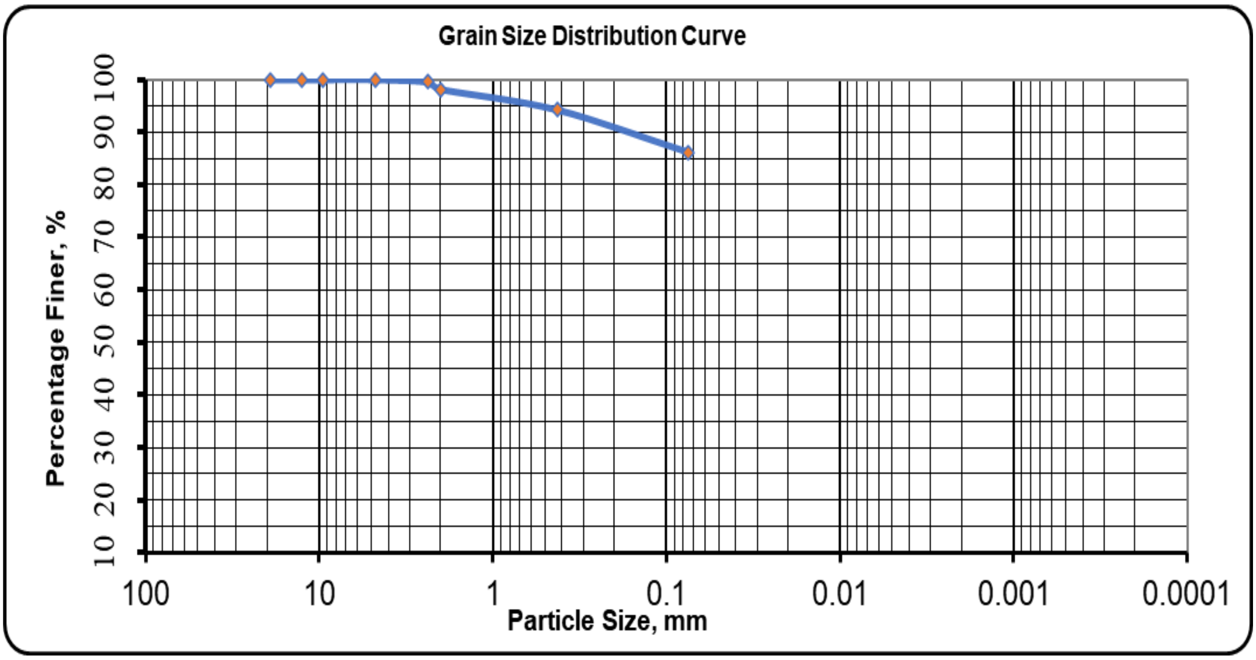

Location: Winget

Test Method: ASTM D 422

Wet Sieve Analysis					Total mass of sample, 1000g		
Sieve No.	Sieve Opening (mm)	Mass of Sieve (g)	Mass of sieve + Retaine	Mass of Retained soil (g)	Percentage Retained (%)	Cum. Percentage Retained	Percentage Passing (%)
3/4"	19.0	555.4	555.4	0.0	0.0	0.0	100.0
1/2"	12.5	560.7	560.7	0.0	0.0	0.0	100.0
3.8"	9.5	534.8	534.8	0.0	0.0	0.0	100.0
No 4	4.75	571.0	571.0	0.0	0.0	0.0	100.0
No 8	2.36	533.4	533.4	0.0	0.0	0.0	100.0
No 10	2	529.2	542.2	13.0	0.8	0.8	99.2
No 40	0.425	432.8	528.8	96.0	5.9	6.7	93.3
No 200	0.075	391.3	490.3	99.0	6.1	12.7	87.3
pan	-------	410.0	1834.0	1424.0	87.3	100.0	0.0
				1632.0	108.8		

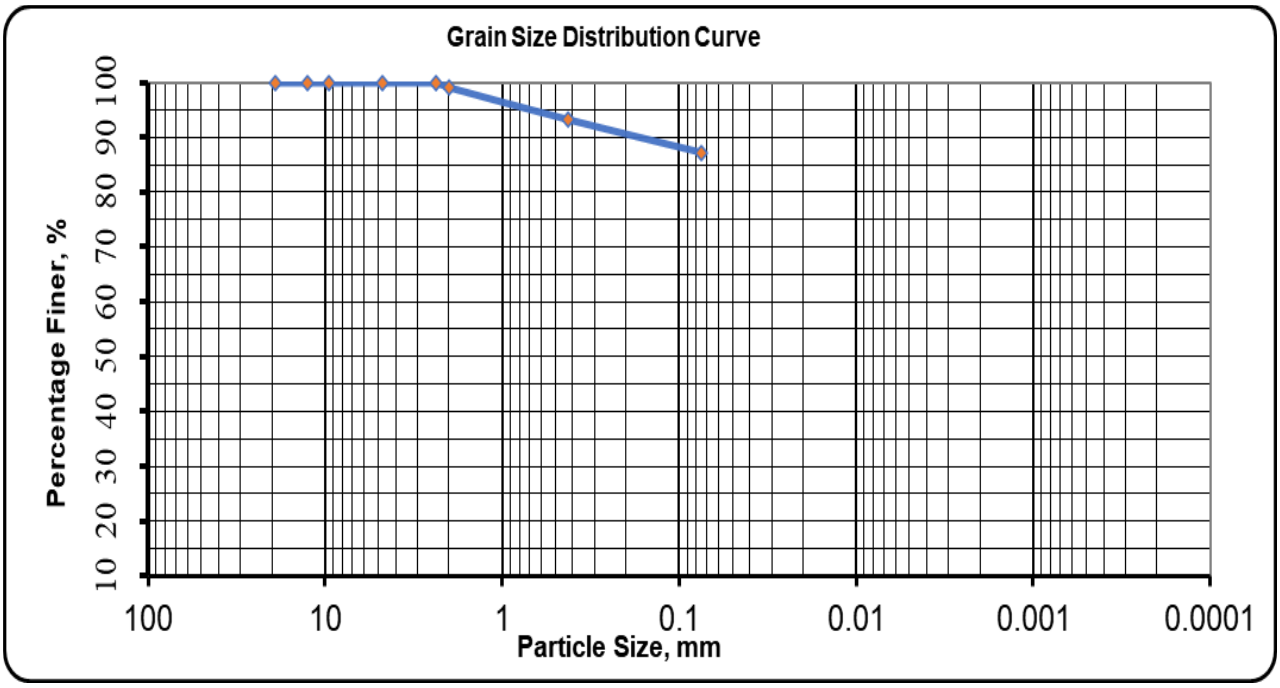

Location: Ayer tena

Test Method: ASTM D 422

Wet Sieve Analysis					Total mass of sample,		
Sieve No.	Sieve Opening (mm)	Mass of Sieve (g)	Mass of sieve + Retaine	Mass of Retaine d soil (g)	Percent age Retaine	Cum. Percent age	Percent age Passing
3/4"	19.0	555.4	555.4	0.0	0.0	0.0	100.0
1/2"	12.5	560.7	625.7	65.0	4.3	4.3	95.7
3.8"	9.5	534.8	654.8	120.0	8.0	12.3	87.7
No 4	4.75	571.0	635.0	64.0	4.3	16.6	83.4
No 8	2.36	533.4	613.4	80.0	5.3	21.9	78.1
No 10	2	529.2	529.2	0.0	0.0	21.9	78.1
No 16	1.18	503.5	538.5	35.0	2.3	24.3	75.7
No 30	0.6	452.2	452.2	0.0	0.0	24.3	75.7
No 40	0.425	432.8	457.8	25.0	1.7	25.9	74.1
No 50	0.3	412.5	412.5	0.0	0.0	25.9	74.1
No 100	0.15	403.3	413.3	10.0	0.7	26.6	73.4
No 200	0.075	391.3	396.3	5.0	0.3	26.9	73.1
pan	-------	410.0	1506.0	1096.0	73.1	100.0	0.0
				1500.0	100		

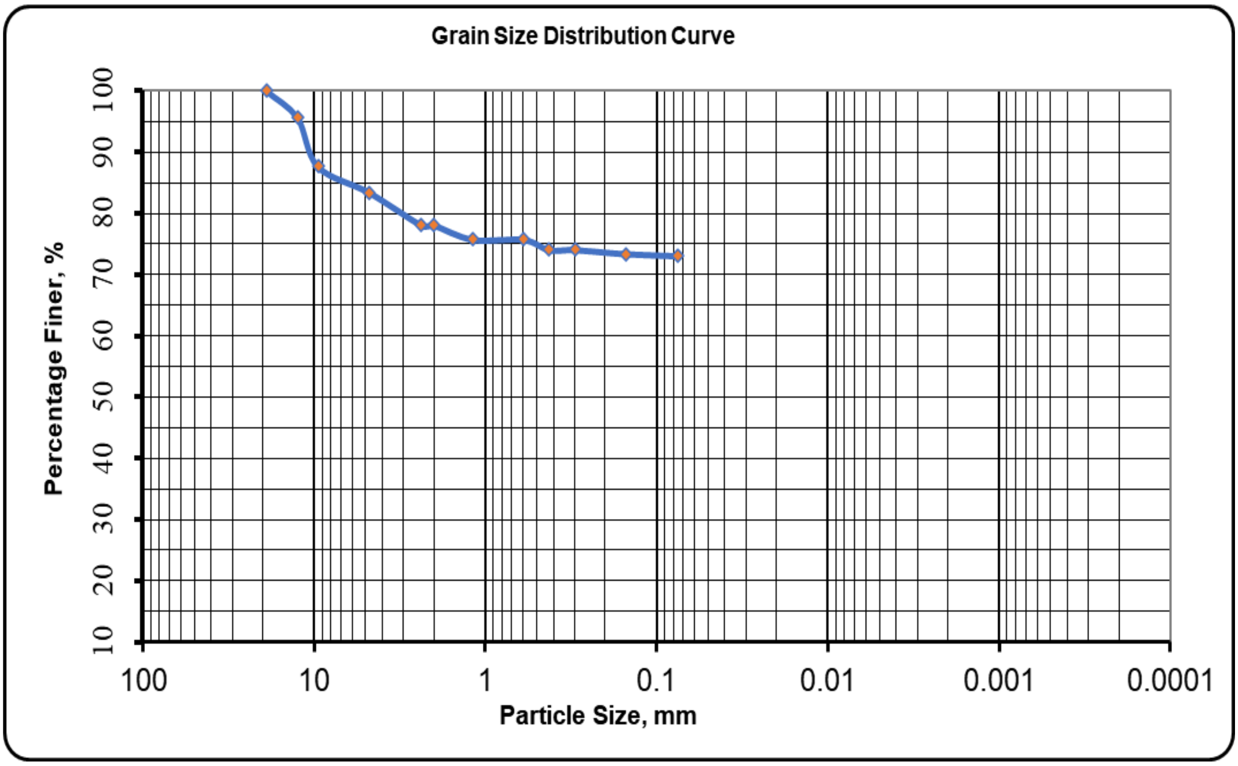

Location: Bethel

Test Method: ASTM D 422

Wet Sieve Analysis					Total mass of sample,		
Sieve No.	Sieve Opening (mm)	Mass of Sieve (g)	Mass of sieve + Retaine	Mass of Retained soil (g)	Percentage Retaine	Cum. Percentage	Percentage Passing
3/4''	19.0	555.4	555.4	0.0	0.0	0.0	100.0
1/2"	12.5	560.7	560.7	0.0	0.0	0.0	100.0
3.8"	9.5	534.8	534.8	0.0	0.0	0.0	100.0
No 4	4.75	571.0	571.0	0.0	0.0	0.0	100.0
No 8	2.36	533.4	536.0	2.6	0.4	0.4	99.6
No 10	2	529.2	530.3	1.1	0.2	0.6	99.4
No 16	1.18	503.5	505.9	2.4	0.4	1.0	99.0
No 30	0.6	452.2	454.4	2.2	0.4	1.4	98.6
No 40	0.425	432.8	434.6	1.8	0.3	1.7	98.3
No 50	0.3	412.5	415.2	2.7	0.5	2.2	97.8
No 100	0.15	403.3	412.7	9.4	1.6	3.8	96.2
No 200	0.075	391.3	398.5	7.2	1.2	5.0	95.0
pan	-------	410.0	969.7	559.7	95.0	100.0	0.0
				589.0	39.26667		

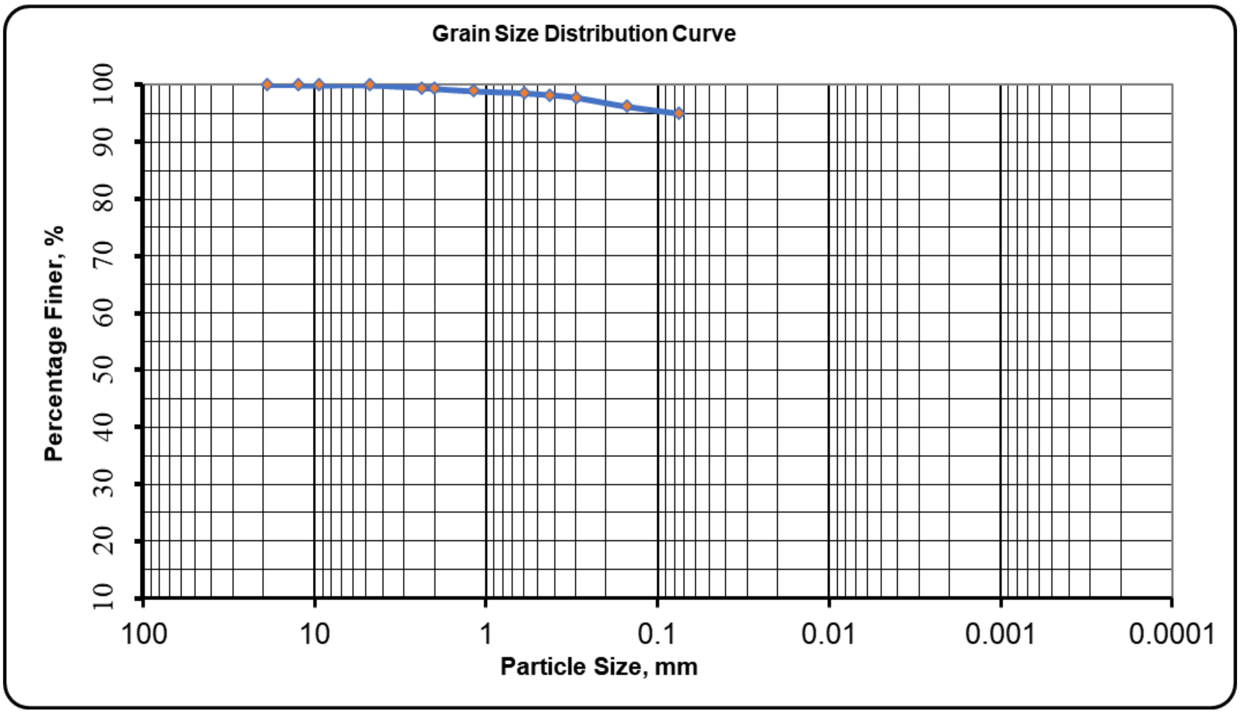

Location: Shegole

Test Method: ASTM D 422

Wet Sieve Analysis					Total mass of sample,		
Sieve No.	Sieve Opening (mm)	Mass of Sieve (g)	Mass of sieve + Retaine	Mass of Retained soil (g)	Percentage Retaine	Cum. Percentage	Percentage Passing
3/4''	19.0	555.4	555.4	0.0	0.0	0.0	100.0
1/2"	12.5	560.7	560.7	0.0	0.0	0.0	100.0
3.8"	9.5	534.8	534.8	0.0	0.0	0.0	100.0
No 4	4.75	571.0	626.0	55.0	2.8	2.8	97.3
No 8	2.36	533.4	658.4	125.0	6.3	9.0	91.0
No 16	1.18	503.5	618.5	115.0	5.8	14.8	85.3
No 40	0.425	432.8	497.8	65.0	3.3	18.0	82.0
No 100	0.15	403.3	453.3	50.0	2.5	20.5	79.5
No 200	0.075	391.3	411.3	20.0	1.0	21.5	78.5
pan	-------	410.0	1980.0	1570.0	78.5	100.0	0.0
				2000.0	133.3333		

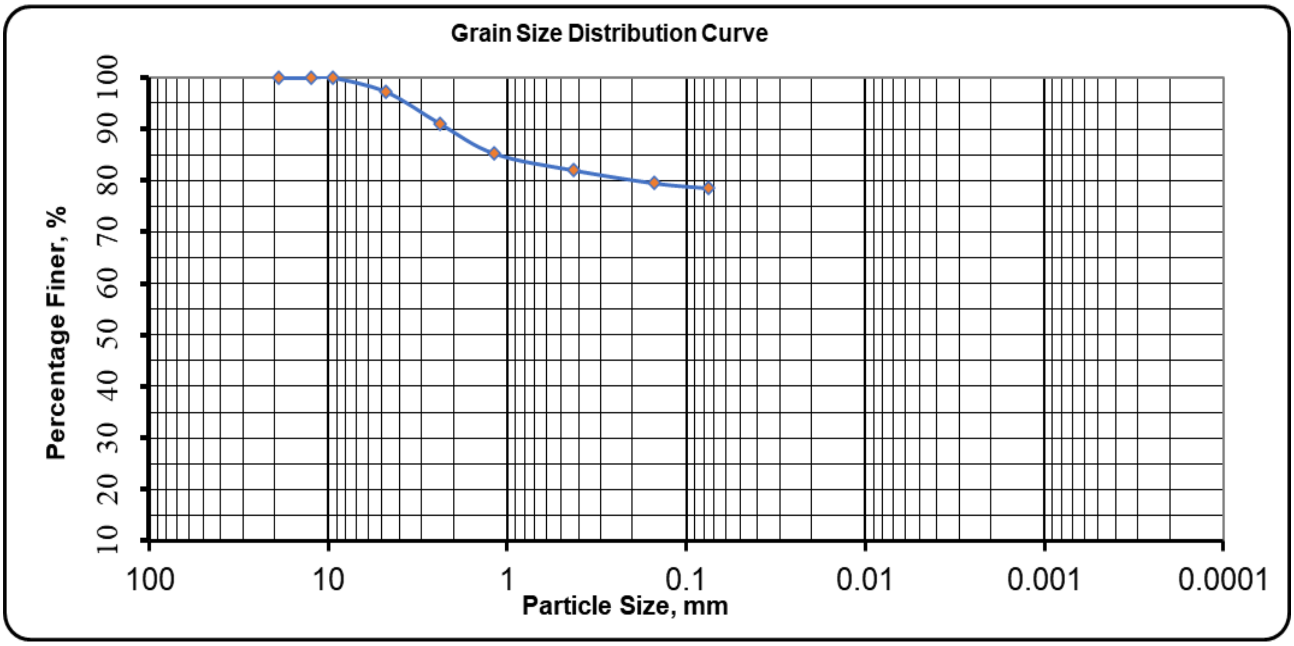

Location: Kore Adebabay

Test Method: ASTM D 422

Wet Sieve Analysis					Total mass of sample,		
Sieve No.	Sieve Opening (mm)	Mass of Sieve (g)	Mass of sieve + Retaine	Mass of Retained soil (g)	Percentage Retaine	Cum. Percentage	Percentage Passing
3/4"	37.5	555.4	555.4	0.0	0.0	0.0	100.0
3/4"	25.0	555.4	581.7	26.3	0.7	0.7	99.3
1/2"	12.5	560.7	601.7	41.0	1.1	1.1	98.9
3.8"	9.5	534.8	548.4	13.6	0.4	0.4	99.6
No 4	4.75	571.0	604.3	33.3	0.9	0.9	99.1
No 10	2	529.2	570.9	41.7	1.1	1.1	98.9
No 16	1.18	503.5	580.4	76.9	2.1	2.1	97.9
No 40	0.425	432.8	507.4	74.6	2.0	2.0	98.0
No 200	0.075	391.3	643.7	252.4	6.8	6.8	93.2
pan	-------	410.0	3573.3	3163.3	85.6	85.6	14.4
				3696.7	246.4487		

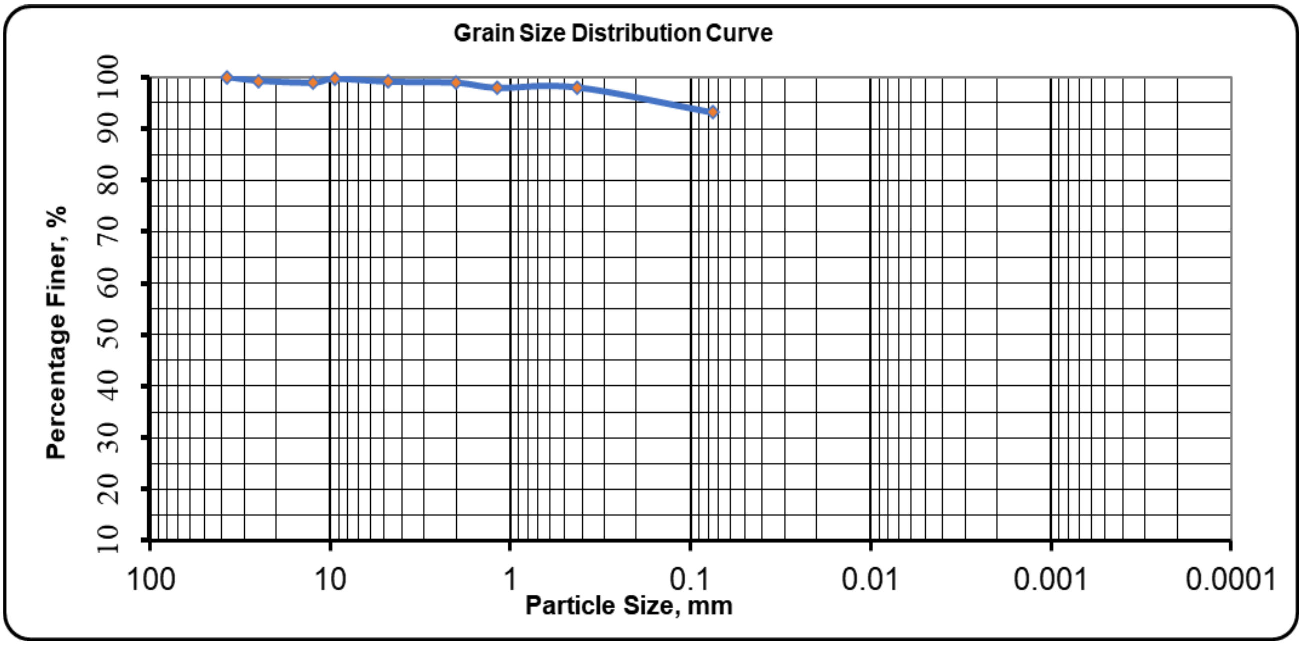

Location: Lideta

Test Method: ASTM D 422

Wet Sieve Analysis					Total mass of sample, 1000g		
Sieve No.	Sieve Opening (mm)	Mass of Sieve (g)	Mass of sieve + Retaine	Mass of Retained soil (g)	Percentage Retained (%)	Cum. Percentage Retained	Percentage Passing (%)
3/4''	19.0	555.4	555.4	0.0	0.0	0.0	100.0
1/2"	12.5	560.7	560.7	0.0	0.0	0.0	100.0
3.8"	9.5	534.8	534.8	0.0	0.0	0.0	100.0
No 4	4.75	571.0	571.0	0.0	0.0	0.0	100.0
No 8	2.36	533.4	533.4	0.0	0.0	0.0	100.0
No 10	2	529.2	544.2	15.0	1.8	1.8	98.2
No 40	0.425	432.8	492.8	60.0	7.4	9.2	90.8
No 200	0.075	391.3	485.3	94.0	11.5	20.8	79.2
pan	-------	410.0	1055.0	645.0	79.2	100.0	0.0
				814.0	54.26666667		

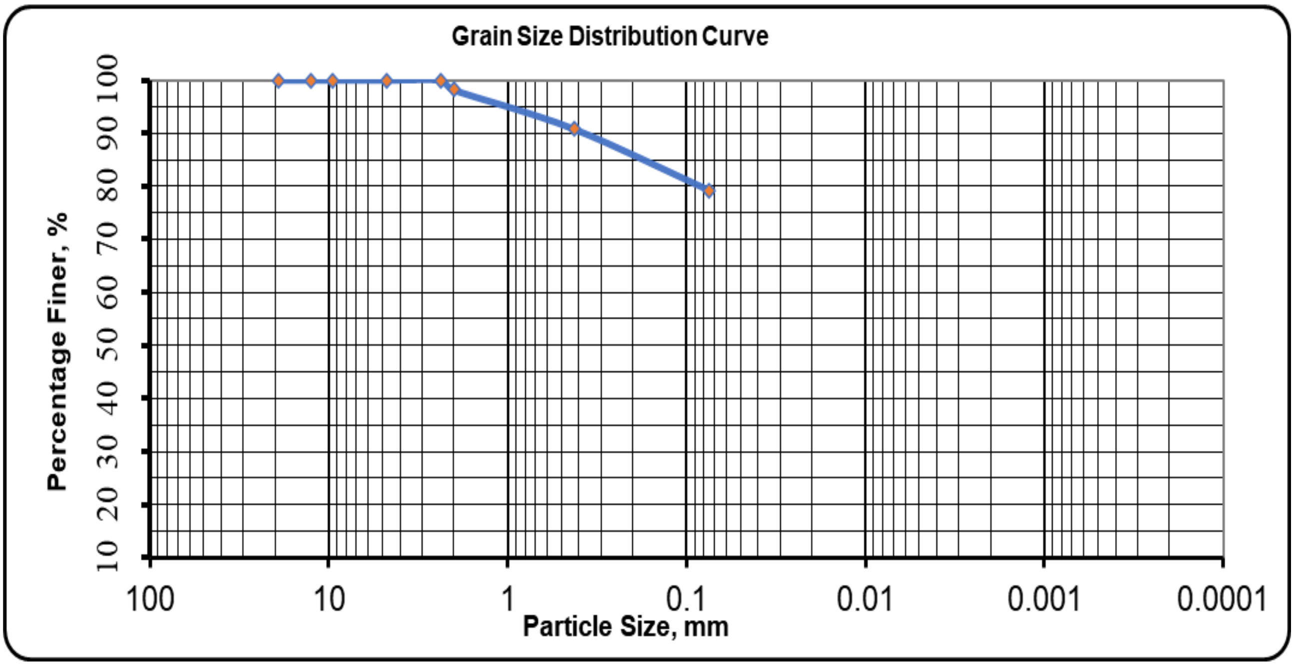

Location: Legehar

Test Method: ASTM D 422

Wet Sieve Analysis					Total mass of sample,		
Sieve No.	Sieve Opening (mm)	Mass of Sieve (g)	Mass of sieve + Retaine	Mass of Retained soil (g)	Percentage Retaine	Cum. Percentage	Percentage Passing
3/4''	50.0	1129.0	1129.0	0.0	0.0	0.0	100.0
3/4''	37.5	1087.0	1087.0	0.0	0.0	0.0	100.0
3/4''	25.0	1212.0	1330.0	118.0	3.0	3.0	97.1
3/4''	19.5	1398.0	1778.0	380.0	9.5	9.5	96.0
1/2"	12.5	560.7	1950.7	1390.0	34.8	34.8	95.0
3.8"	9.5	534.8	1484.8	950.0	23.8	23.8	93.0
No 4	4.75	571.0	821.0	250.0	6.3	6.3	93.8
No 8	2.36	533.4	688.4	155.0	3.9	3.9	96.1
No 16	1.18	503.5	623.5	120.0	3.0	3.0	97.0
No 40	0.425	432.8	522.8	90.0	2.3	2.3	97.8
No 100	0.15	403.3	433.3	30.0	0.8	0.8	99.3
No 200	0.075	391.3	406.3	15.0	0.4	0.4	99.6
pan	-------	410.0	912.0	502.0	12.6		
				3502.0	233.4667		

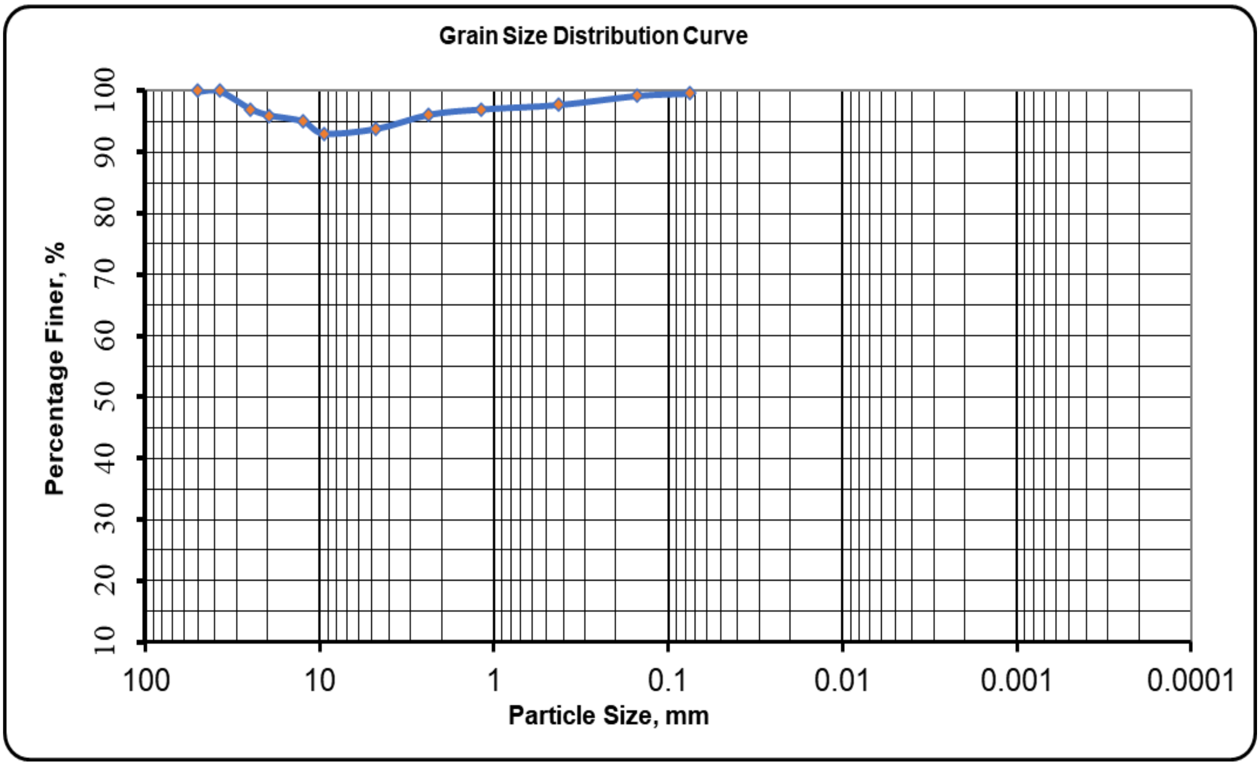

Location: Tikur Anbesa

Test Method: ASTM D 422

Wet Sieve Analysis					Total mass of sample,		
Sieve No.	Sieve Opening (mm)	Mass of Sieve (g)	Mass of sieve + Retaine	Mass of Retained soil (g)	Percentage Retaine	Cum. Percentage	Percentage Passing
3/4''	37.5	1087.0	1087.0	0.0	0.0	0.0	100.0
3/4''	25.0	1212.0	1212.0	0.0	0.0	0.0	100.0
3/4''	19.0	555.4	570.2	14.8	2.5	2.5	97.5
1/2"	12.5	560.7	581.6	20.9	3.5	6.0	94.0
3.8"	9.5	534.8	540.2	5.4	0.9	7.0	93.0
No 4	4.75	571.0	581.5	10.5	1.8	8.7	91.3
No 8	2.36	533.4	564.5	31.1	5.3	14.0	86.0
No 16	1.18	503.5	512.4	8.9	1.5	15.5	84.5
No 30	0.6	452.2	476.6	24.4	4.1	19.7	80.3
No 40	0.425	432.8	446.0	13.2	2.2	21.9	78.1
No 50	0.3	412.5	425.3	12.8	2.2	24.1	75.9
No 100	0.15	403.3	417.6	14.3	2.4	26.5	73.5
No 200	0.075	391.3	407.5	16.2	2.8	29.2	70.8
pan	-------	410.0	827.5	417.5	70.8	100.0	0.0
				590.0	39.33333		

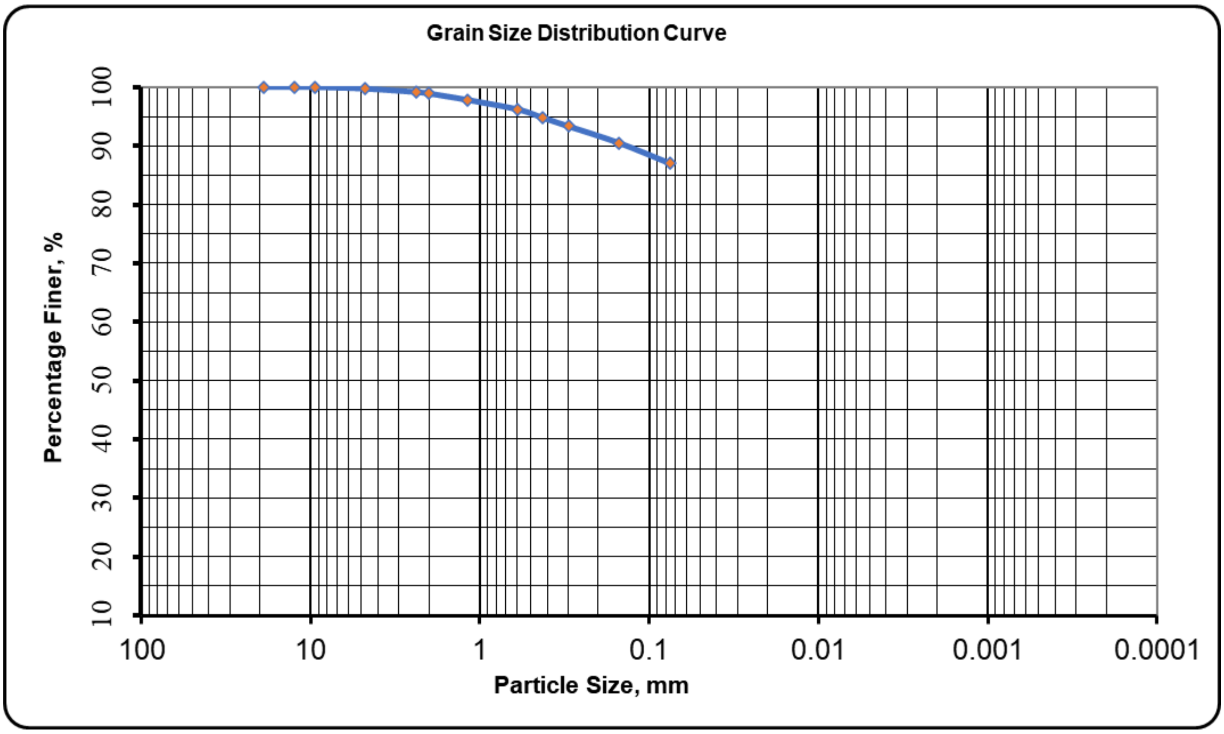

Location: Shiromeda

Test Method: ASTM D 422

Wet Sieve Analysis					Total mass of sample,		
Sieve No.	Sieve Opening (mm)	Mass of Sieve (g)	Mass of sieve + Retaine	Mass of Retained soil (g)	Percentage Retaine	Cum. Percentage	Percentage Passing
3/4''	19.0	555.4	555.4	0.0	0.0	0.0	100.0
1/2"	12.5	560.7	680.7	120.0	2.2	2.2	99.0
3.8"	9.5	534.8	844.8	310.0	5.6	5.6	98.0
No 4	4.75	571.0	811.0	240.0	4.4	4.4	97.0
No 8	2.36	533.4	843.4	310.0	5.6	5.6	95.0
No 16	1.18	503.5	668.5	165.0	3.0	3.0	93.0
130	0.425	432.8	562.8	130.0	2.4	2.4	92.0
No 100	0.15	403.3	503.3	100.0	1.8	1.8	92.0
No 200	0.075	391.3	466.3	75.0	1.4	1.4	91.0
pan	-------	410.0	4460.0	4050.0	73.6	73.6	26.4
				5500.0	366.6667		

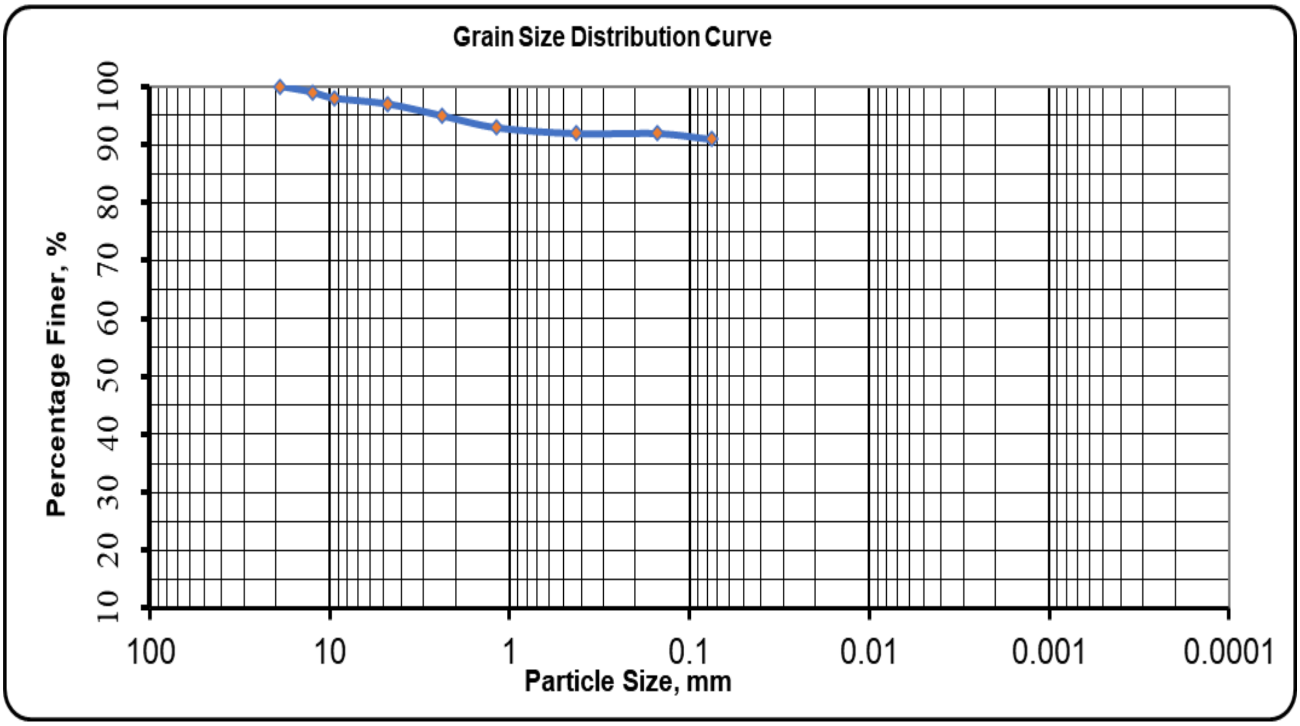

Location: Akaki

Test Method: ASTM D 422

Wet Sieve Analysis					Total mass of sample,		
Sieve No.	Sieve Opening (mm)	Mass of Sieve (g)	Mass of sieve + Retaine	Mass of Retaine d soil (g)	Percent age Retaine	Cum. Percent age	Percent age Passing
3/4"	19.0	555.4	555.4	0.0	0.0	0.0	100.0
1/2"	12.5	560.7	560.7	0.0	0.0	0.0	100.0
3.8"	9.5	534.8	534.8	0.0	0.0	0.0	100.0
No 4	4.75	571.0	571.0	0.0	0.0	0.0	100.0
No 8	2.36	533.4	598.4	65.0	3.3	3.3	96.8
No 10	2	529.2	529.2	0.0	0.0	3.3	96.8
No 16	1.18	503.5	713.5	210.0	10.5	13.8	86.3
No 40	0.425	432.8	552.8	120.0	6.0	19.8	80.3
No 100	0.15	403.3	468.3	65.0	3.3	23.0	77.0
No 200	0.075	391.3	416.3	25.0	1.3	24.3	75.8
pan	-------	410.0	1925.0	1515.0	75.8	100.0	0.0
				2000.0	133.3333		

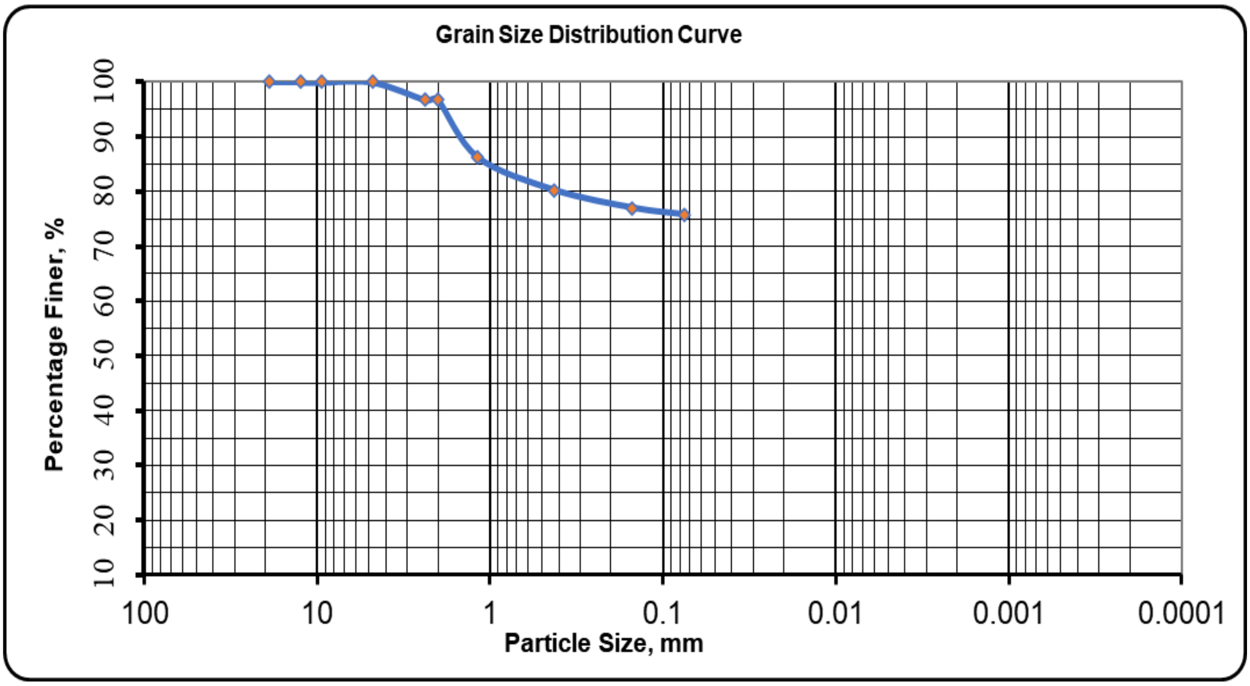

Location: Koye Feche

Test Method: ASTM D 422

Wet Sieve Analysis					Total mass of sample, 1000g		
Sieve No.	Sieve Opening (mm)	Mass of Sieve (g)	Mass of sieve + Retaine	Mass of Retained soil (g)	Percentage Retained (%)	Cum. Percentage Retained (%)	Percentage Passing (%)
3/4''	25.0	1212.0	1212.0	0.0	0.0	0.0	100.0
3/4''	19.0	555.4	556.9	1.5	1.5	1.5	98.5
1/2"	12.5	560.7	565.6	4.9	4.9	6.4	93.6
3.8"	9.5	534.8	537.4	2.6	2.6	9.1	90.9
No 4	4.75	571.0	579.9	8.9	8.9	18.0	82.0
No 10	2	529.2	544.4	15.2	15.2	33.2	66.8
No 16	1.18	503.5	516.7	13.2	13.2	46.4	53.6
No 30	0.6	452.2	459.1	6.9	6.9	53.3	46.7
No 50	0.3	412.5	418.9	6.4	6.4	59.7	40.3
No 100	0.15	403.3	407.3	4.0	4.0	63.8	36.2
No 200	0.075	391.3	394.4	3.1	3.1	66.8	33.2
pan	-------	410.0	443.2	33.2	33.2	100.0	0.0
				100.0	6.666		

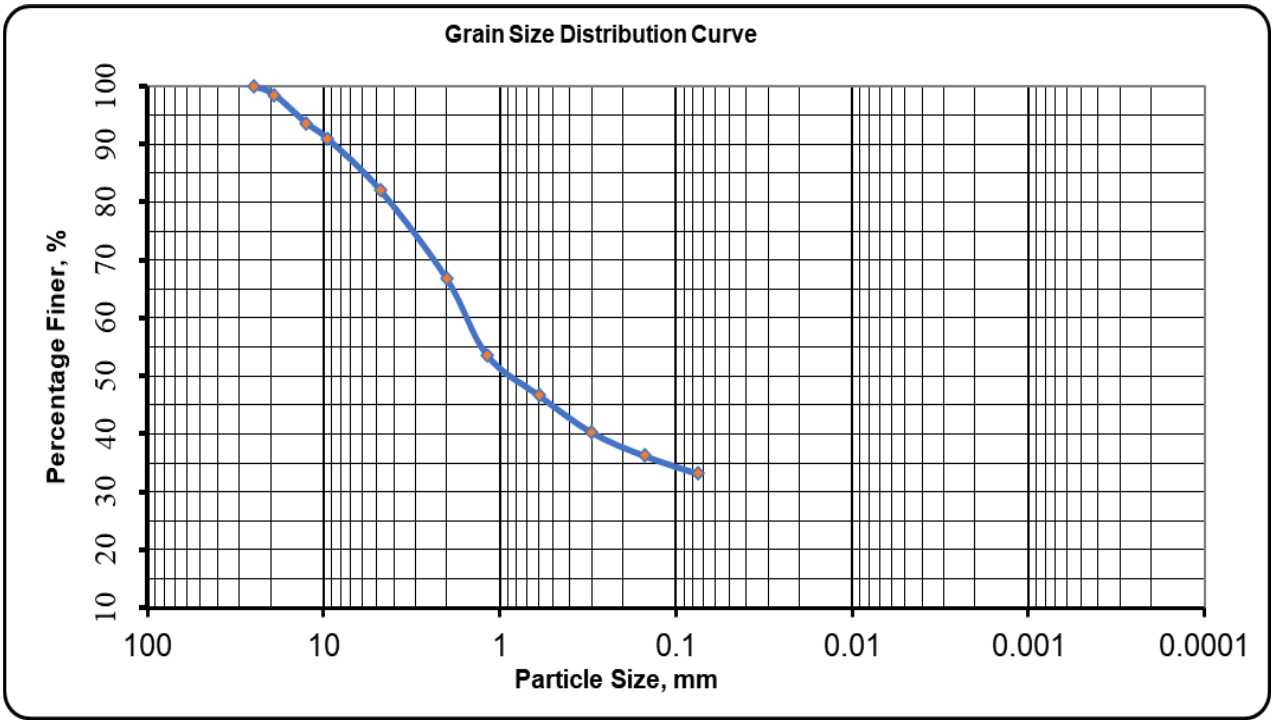

APPENDIX C: DETAILS OF ATTERBERG LIMIT TEST RESULTS

Location: Delber

Test Method: ASTM D 422

Atterberg Limit					
	Liquid Limit			Plastic Limit	
Number of blows	**34**	**27**	**18**		
Weight of can + wet soil (g)	48.5	57.6	56.9	24.1	24.8
Weight of can + dry soil (g)	36.4	41.2	39.9	22	22.6
Weight of can (g)	16.6	16.7	16.5	16.5	16.7
Weight of water (g)	12.1	16.4	17	2.07	2.22
Weight of dry soil (g)	19.8	24.5	23.4	5.52	5.89
w = Water content, w%	61.1	66.7	72.4	37.5	37.69
Average (%)	66.73333333			37.595	
	LL= 66.733			PL=32.18	

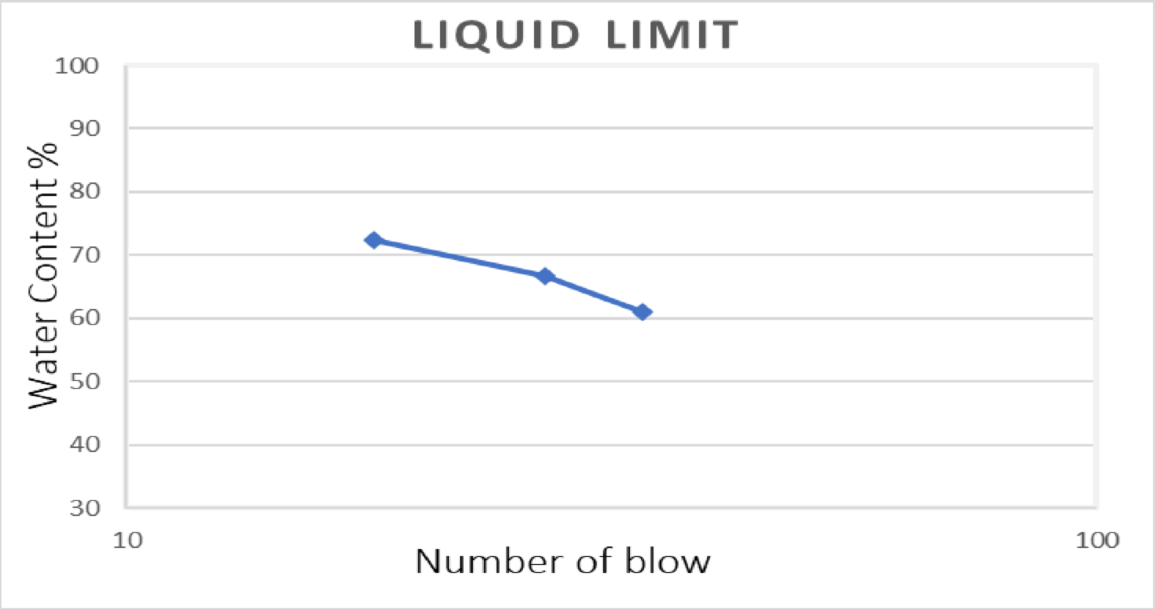

Location: Adisu gebiya

Test Method: ASTM D 422

Atterberg Limit					
	Liquid Limit			Plastic Limit	
Number of blows	**31**	**24**	**17**	-	-
Weight of can + wet soil (g)	77	80.6	82.3	119.1	87.15
Weight of can + dry soil (g)	69.6	73.4	73.7	117.62	85.53
Weight of can (g)	55.5	60.1	58.3	113.05	80.49
Weight of water (g)	7.4	7.2	8.6	1.48	1.62
Weight of dry soil (g)	14.2	13.2	15.4	4.57	5.04
w = Water content, w%	52.2	54.7	56	32.39	32.14
LL at 25 blow & Average PL	54			32	
Plastic Index = LL - PL = 54-32=22					

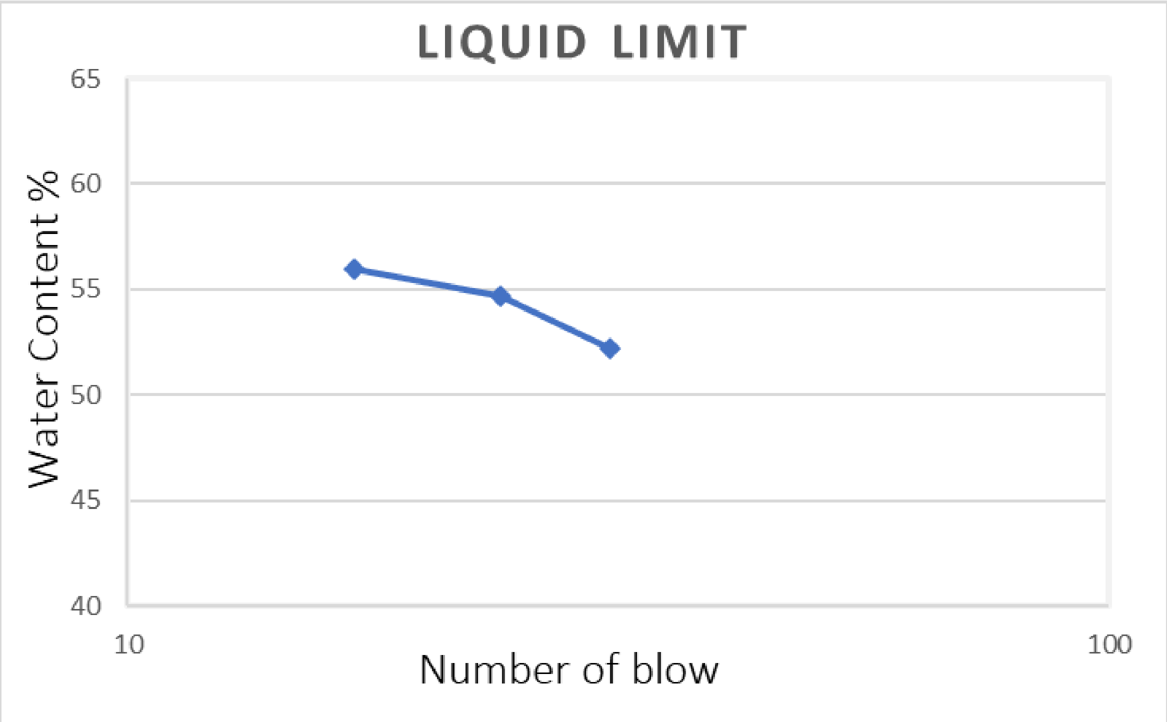

Location: Goro

Test Method: ASTM D 422

Atterberg Limit						
	Liquid Limit				Plastic Limit	
Number of blows	**35**	**26**	**22**	**17**		
Weight of can + wet soil (g)	70.8	76.5	80.7	70	57.8	56.8
Weight of can + dry soil (g)	55.6	58.2	59.6	52.6	50	49.4
Weight of can (g)	29.6	31.4	30.8	30.6	30.6	30.6
Weight of water (g)	15.2	18.3	21.1	17.4	7.8	7.4
Weight of dry soil (g)	26	26.8	28.8	22	19.4	18.8
w = Water content, w%	58.46	68.28	73.26	79.09	40.21	39.36
Average (%)					39.78	
	LL=69.73				PL=39.78	

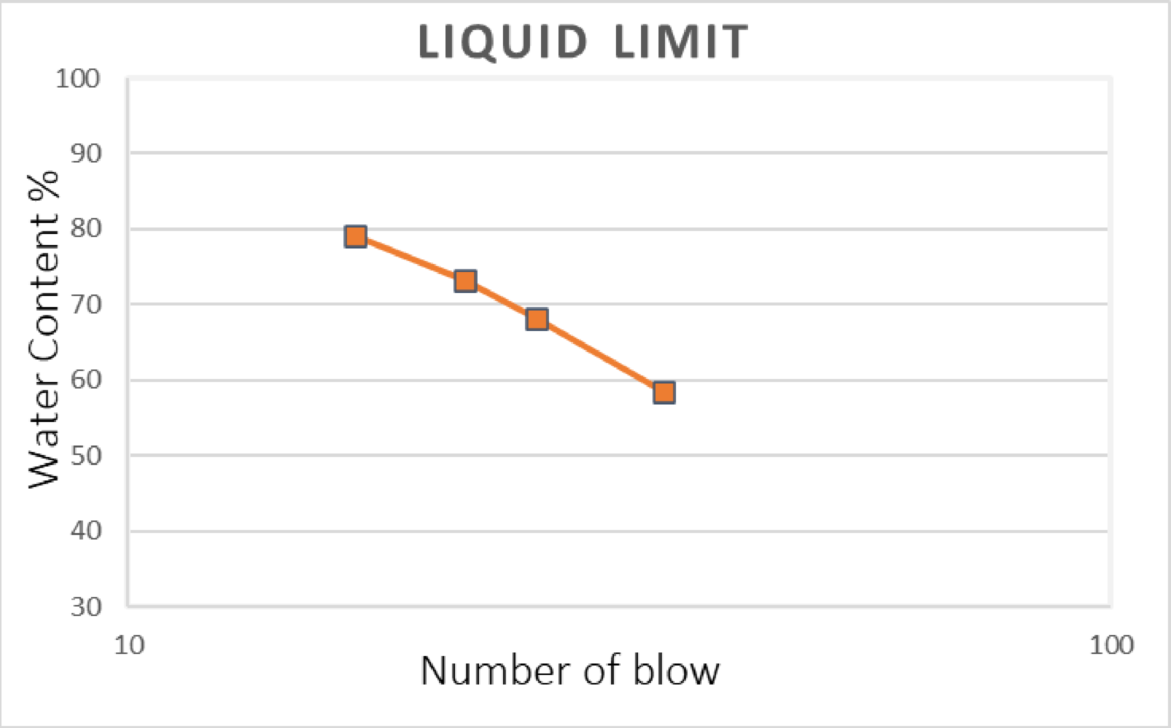

Location: Megenagna

Test Method: ASTM D 422

Atterberg Limit					
	Liquid Limit			Plastic Limit	
Number of blows	**35**	**27**	**18**	-	-
Weight of can + wet soil (g)	40.8	45.2	45.9	13	13
Weight of can + dry soil (g)	32.4	35.2	35.2	12.7	12.7
Weight of can (g)	11.4	11.4	11.5	11.3	11.3
Weight of water (g)	8.4	10	10.7	0.4	0.4
Weight of dry soil (g)	21	23.7	23.7	1.3	1.3
w = Water content, w%	39.9	42.2	44.9	29.8	28
LL at 25 blow & Average PL	43			29	
Plastic Index = LL - PL = 43-29=14					

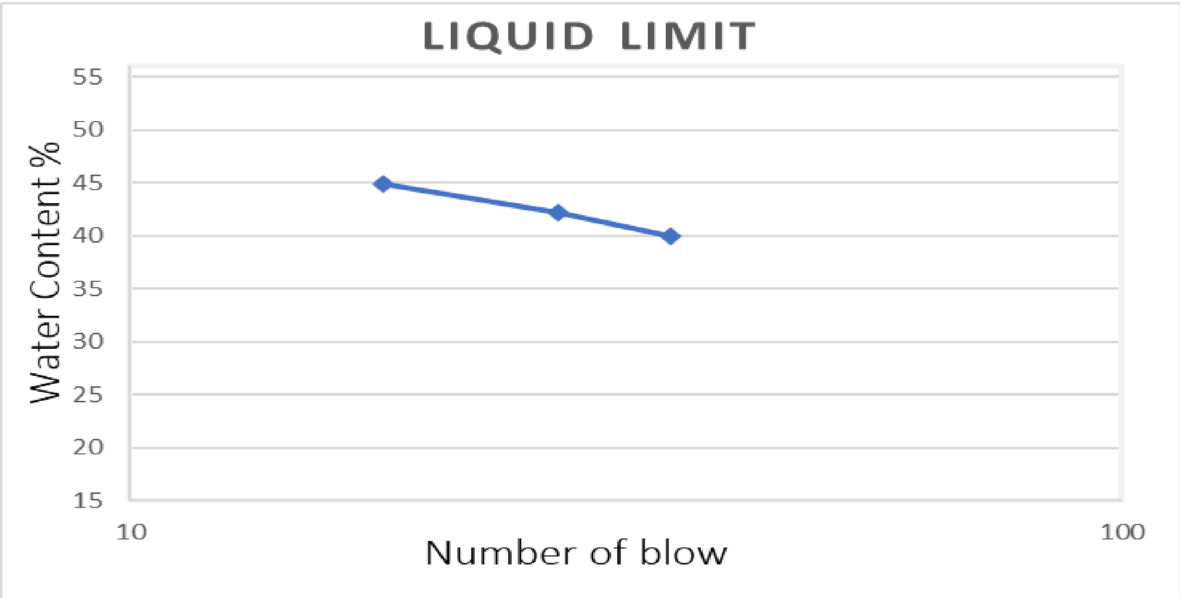

Location: Winget

Test Method: ASTM D 422

Atterberg Limit					
	Liquid Limit			Plastic Limit	
Number of blows	**32**	**23**	**16**	-	-
Weight of can + wet soil (g)	47	50.5	48.5	27.47	27.32
Weight of can + dry soil (g)	36.8	38.7	37.1	25.87	25.69
Weight of can (g)	16.5	16.6	16.6	21.08	20.71
Weight of water (g)	10.2	11.8	11.4	1.6	1.63
Weight of dry soil (g)	20.3	22.1	20.5	4.79	4.98
w = Water content, w%	50.2	53.6	55.9	33.4	32.73
LL at 25 blow & Average PL	52			33	
Plastic Index = LL - PL = 52 -33=29					

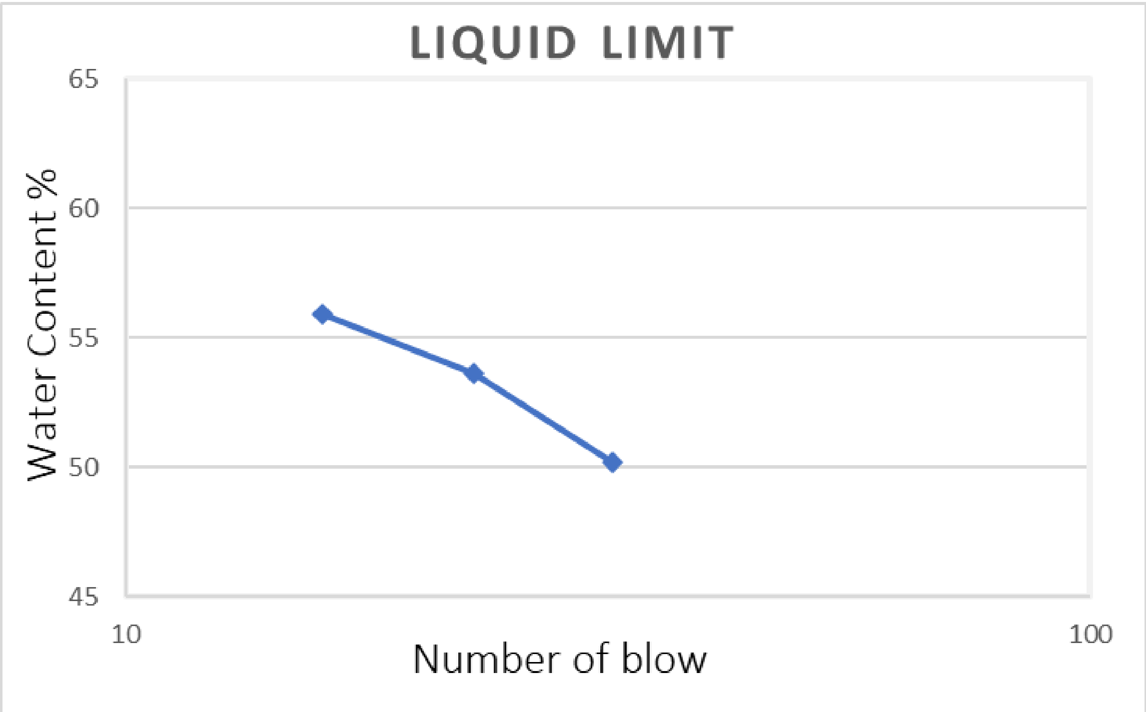

Location: Ayer Tena

Test Method: ASTM D 422

Atterberg Limit						
	Liquid Limit				Plastic Limit	
Number of blows	**37**	**26**	**23**	**16**		
Weight of can + wet soil (g)	76.3	78.5	80.4	81.5	52.8	56.8
Weight of can + dry soil (g)	59.3	59.4	59.7	59.3	47	49.1
Weight of can (g)	31.4	30.2	31	29.8	30.6	30.6
Weight of water (g)	17	19.1	20.7	22.2	5.8	7.7
Weight of dry soil (g)	27.9	29.2	28.7	29.5	16.4	18.5
w = Water content, w%	60.93	65.41	72.13	75.25	35.37	41.62
Average (%)					38.495	
	LL= 68.51				PL=38.49	

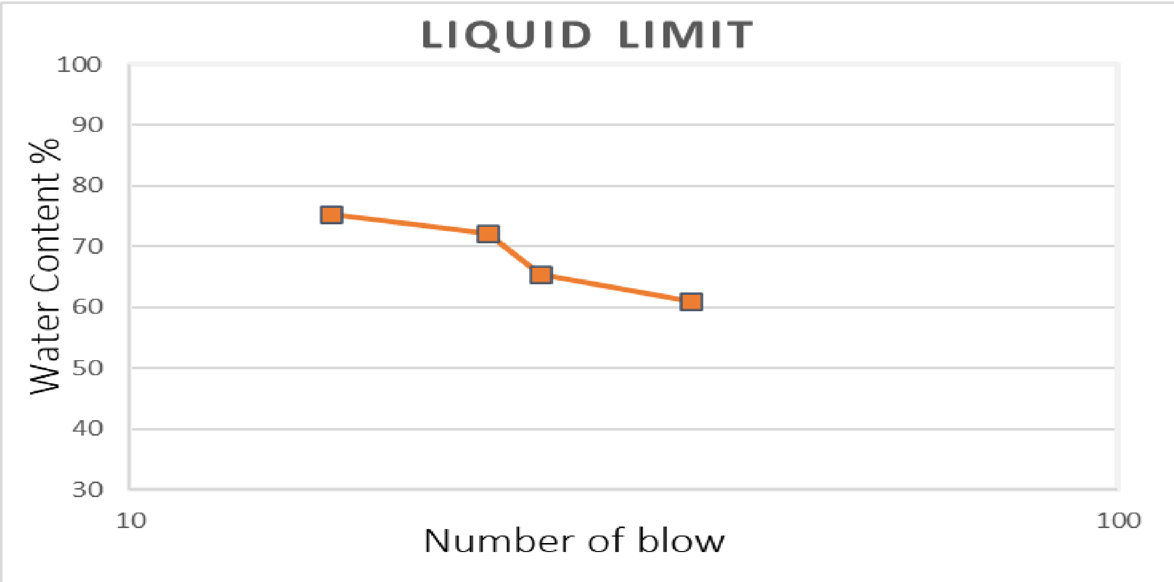

Location: Bethel

Test Method: ASTM D 422

Atterberg Limit						
	Liquid Limit				Plastic Limit	
Number of blows	**17**	**24**	**25**	**35**		
Weight of can + wet soil (g)	45	168	56	48	132	21
Weight of can + dry soil (g)	33	159	41	37	131	19
Weight of can (g)	14	143	16	15	125	14
Weight of water (g)	12	9	15	11	1	2
Weight of dry soil (g)	19	16	25	22	6	5
w = Water content, w%	63.15789	56.25	60	50	16.66667	40
Average (%)					28.33333333	
	LL= 72.23				PL=32.18	

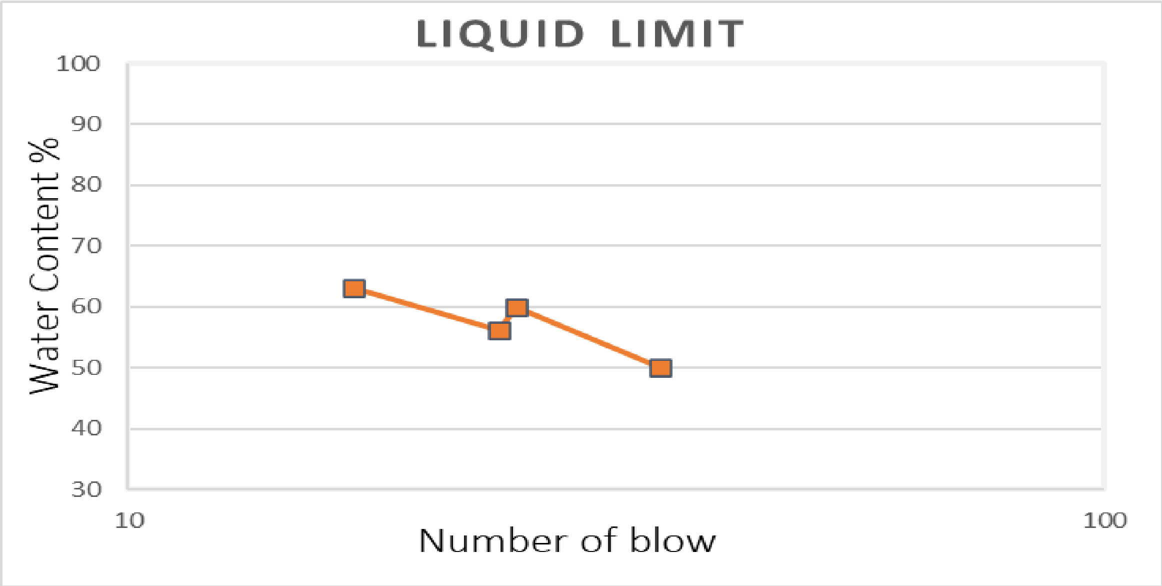

Location: Shgole

Test Method: ASTM D 422

	Liquid Limit				**Plastic Limit**	
Number of blows	**35**	**28**	**25**	**16**		
Weight of can + wet soil (g)	63.25	64.3	65.32	60.21	50.21	48.61
Weight of can + dry soil (g)	51	51.3	51.6	48	44.8	44
Weight of can (g)	29.8	30.2	30.8	31	30.5	30.5
Weight of water (g)	12.25	13	13.72	12.21	5.41	4.61
Weight of dry soil (g)	21.2	21.1	20.8	17	14.3	13.5
w = Water content, w%	57.78302	61.61137	65.96154	71.82353	37.83217	34.14815
Average (%)					35.99015799	
	LL= 65.05				PL=35.99	

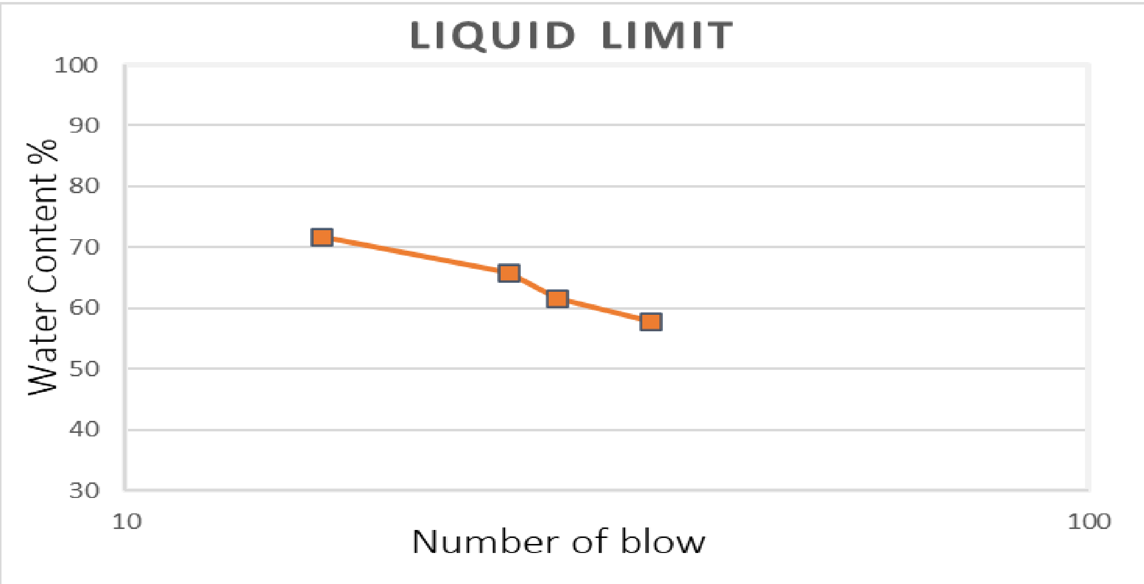

Location: Shegole

Test Method: ASTM D 422

Atterberg Limit						
	Liquid Limit				Plastic Limit	
Number of blows	**35**	**28**	**25**	**16**		
Weight of can + wet soil (g)	63.25	64.3	65.32	60.21	50.21	48.61
Weight of can + dry soil (g)	51	51.3	51.6	48	44.8	44
Weight of can (g)	29.8	30.2	30.8	31	30.5	30.5
Weight of water (g)	12.25	13	13.72	12.21	5.41	4.61
Weight of dry soil (g)	21.2	21.1	20.8	17	14.3	13.5
w = Water content, w%	57.78302	61.61137	65.96154	71.82353	37.83217	34.14815
Average (%)					35.99015799	
	LL= 65.05				PL=35.99	

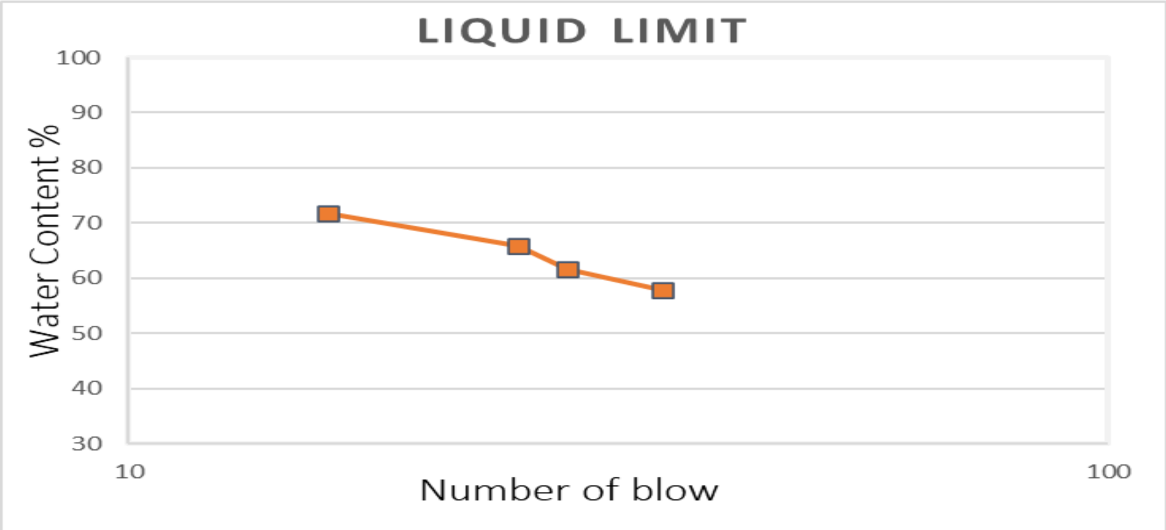

Location: Kore Adebabay

Test Method: ASTM D 422

Atterberg Limit						
	Liquid Limit				Plastic Limit	
Number of blows	**34**	**27**	**24**	**20**		
Weight of can + wet soil (g)	43.44	43.21	43.11	43.06	15.25	14.92
Weight of can + dry soil (g)	36.45	36.15	35.96	35.84	14.83	14.57
Weight of can (g)	23.58	23.39	23.3	23.24	12.79	12.82
Weight of water (g)	6.99	7.06	7.15	7.22	0.42	0.35
Weight of dry soil (g)	12.87	12.76	12.66	12.6	2.04	1.75
w = Water content, w%	54.31235	55.32915	56.47709	57.30159	20.58824	20
Average (%)					20.29411765	
	LL= 55.95				PL=20.29	

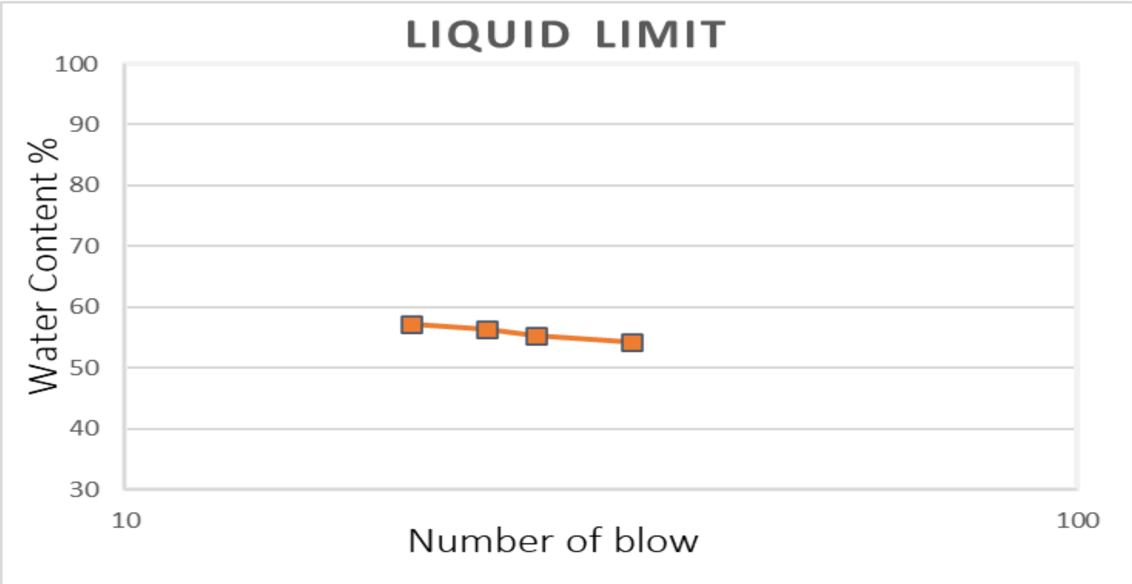

Location: Lideta

Test Method: ASTM D 422

Atterberg Limit					
	Liquid Limit			Plastic Limit	
Number of blows	**31**	**24**	**18**	-	-
Weight of can + wet soil (g)	47.7	50	51.3	13.79	13.78
Weight of can + dry soil (g)	35	36.2	36.9	13.29	13.27
Weight of can (g)	11.4	11.3	11.5	11.59	11.58
Weight of water (g)	12.7	13.8	14.4	0.5	0.51
Weight of dry soil (g)	23.7	24.9	25.4	1.7	1.69
w = Water content, w%	53.5	55.2	56.5	29.41	30.18
LL at 25 blow & Average PL	55			30	
Plastic Index = LL - PL = 55 -30=25					

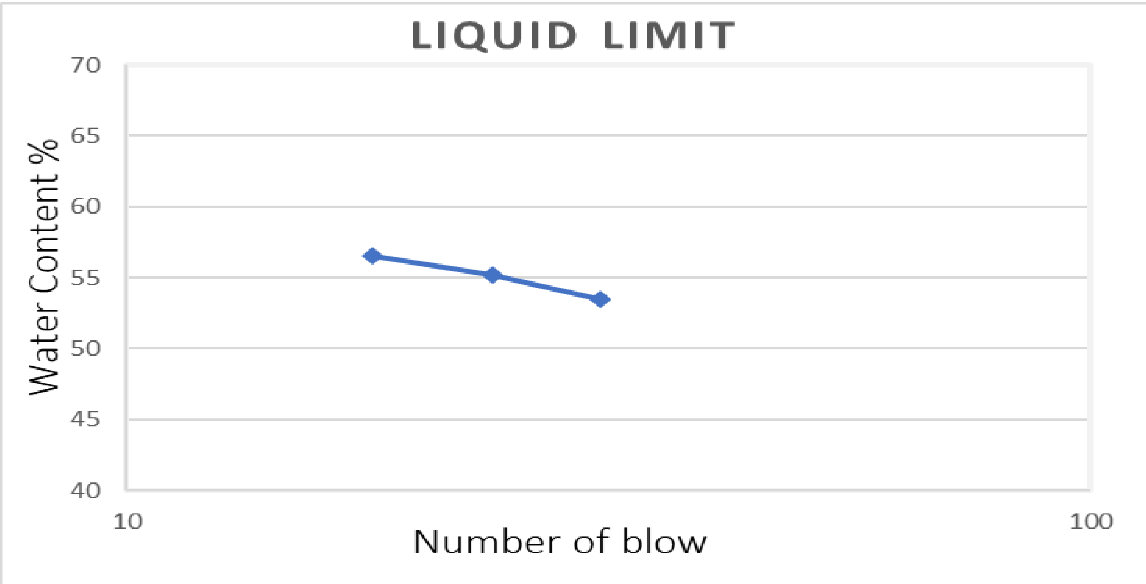

Location: Legehar

Test Method: ASTM D 422

Atterberg Limit						
	Liquid Limit				Plastic Limit	
Number of blows	**35**	**26**	**24**	**17**		
Weight of can + wet soil (g)	68.5	75.6	71.4	69.6	50.8	56.8
Weight of can + dry soil (g)	57.9	61.9	57.9	55.6	45.8	50.8
Weight of can (g)	29.8	30.4	31	31.4	30.6	30.6
Weight of water (g)	10.6	13.7	13.5	14	5	6
Weight of dry soil (g)	28.1	31.5	26.9	24.2	15.2	20.2
w = Water content, w%	37.72242	43.49206	50.18587	57.85124	32.89474	29.70297
Average (%)					31.29885357	
	LL= 47.01				PL=31.29	

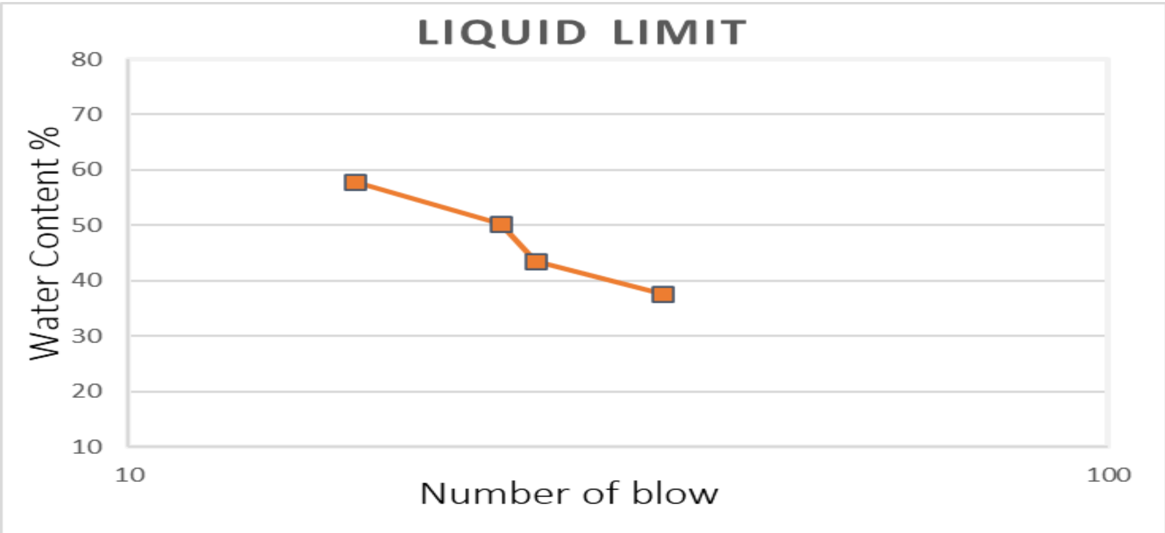

Location: Tikur Anbesa

Test Method: ASTM D 422

Atterberg Limit						
	Liquid Limit				Plastic Limit	
Number of blows	**16**	**25**	**27**	**35**		
Weight of can + wet soil (g)	48.02	42.6	50.1	47.47	21.23	20.26
Weight of can + dry soil (g)	35.426	32.51	37.63	35.81	18.88	19.74
Weight of can (g)	15.6	15.48	15.94	15.76	15.32	15.72
Weight of water (g)	12.594	10.09	12.47	11.66	2.35	0.52
Weight of dry soil (g)	19.826	17.03	21.69	20.05	3.56	4.02
w = Water content, w%	63.52265	59.24839	57.49193	58.15461	66.01124	12.93532
Average (%)					39.47327967	
	LL= 59.25				PL=39.47	

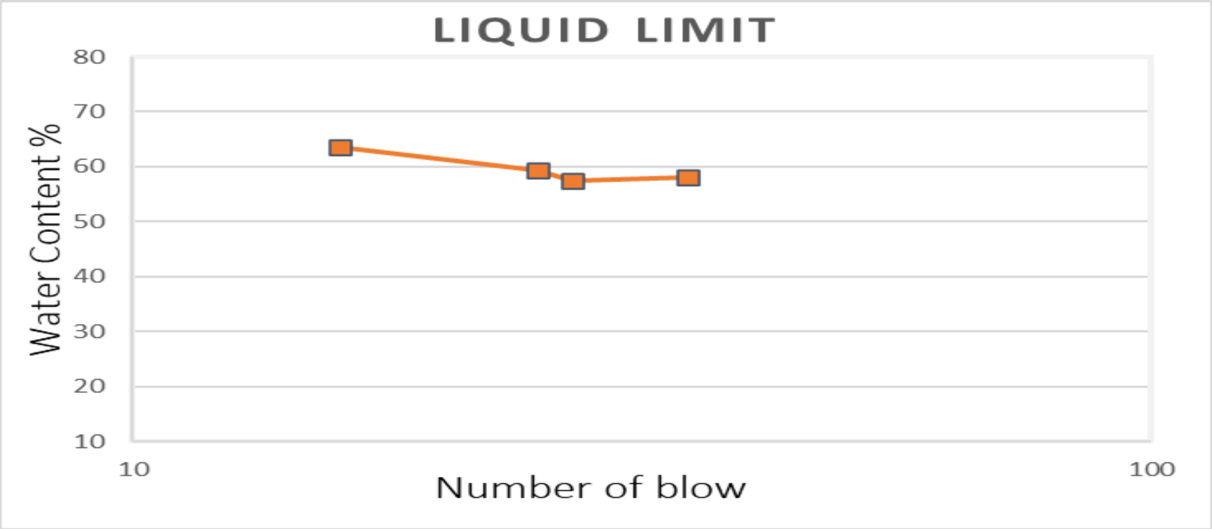

Location: Shiromeda

Test Method: ASTM D 422

Atterberg Limit						
	Liquid Limit				**Plastic Limit**	
Number of blows	**35**	**28**	**24**	**17**		
Weight of can + wet soil (g)	60.32	61.5	59.6	62.3	59.4	48.36
Weight of can + dry soil (g)	49.6	49.8	48.3	49.6	52	43.2
Weight of can (g)	30.2	30.5	29.8	31	30.5	30.5
Weight of water (g)	10.72	11.7	11.3	12.7	7.4	5.16
Weight of dry soil (g)	19.4	19.3	18.5	18.6	21.5	12.7
w = Water content, w%	55.25773	60.62176	61.08108	68.27957	34.4186	40.62992
Average (%)					37.52426296	
	LL= 61.68				PL=37.52	

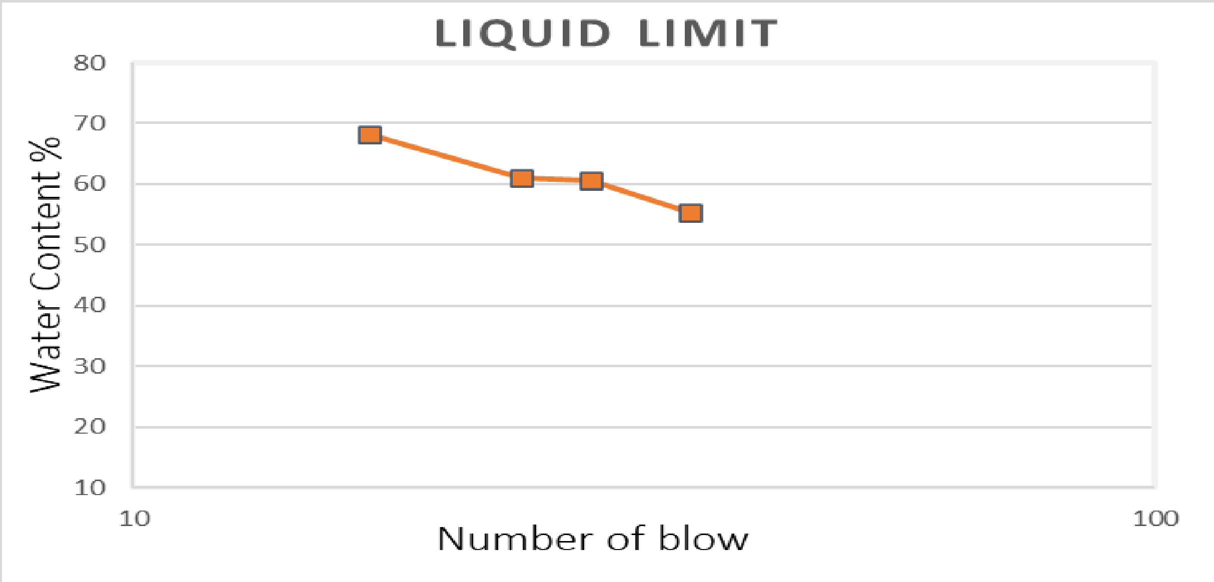

Location: Akaki

Test Method: ASTM D 422

Atterberg Limit						
	Liquid Limit				Plastic Limit	
Number of blows	**37**	**26**	**25**	**18**		
Weight of can + wet soil (g)	78.9	76.8	73.5	70.5	59.6	56.2
Weight of can + dry soil (g)	63.4	61	58	55.2	52	49.6
Weight of can (g)	31.1	32	30.8	29.8	30.6	30.6
Weight of water (g)	15.5	15.8	15.5	15.3	7.6	6.6
Weight of dry soil (g)	32.3	29	27.2	25.4	21.4	19
w = Water content, w%	47.98762	54.48276	56.98529	60.23622	35.51402	34.73684
Average (%)					35.1254304	
	LL= 54.49				PL=35.13	

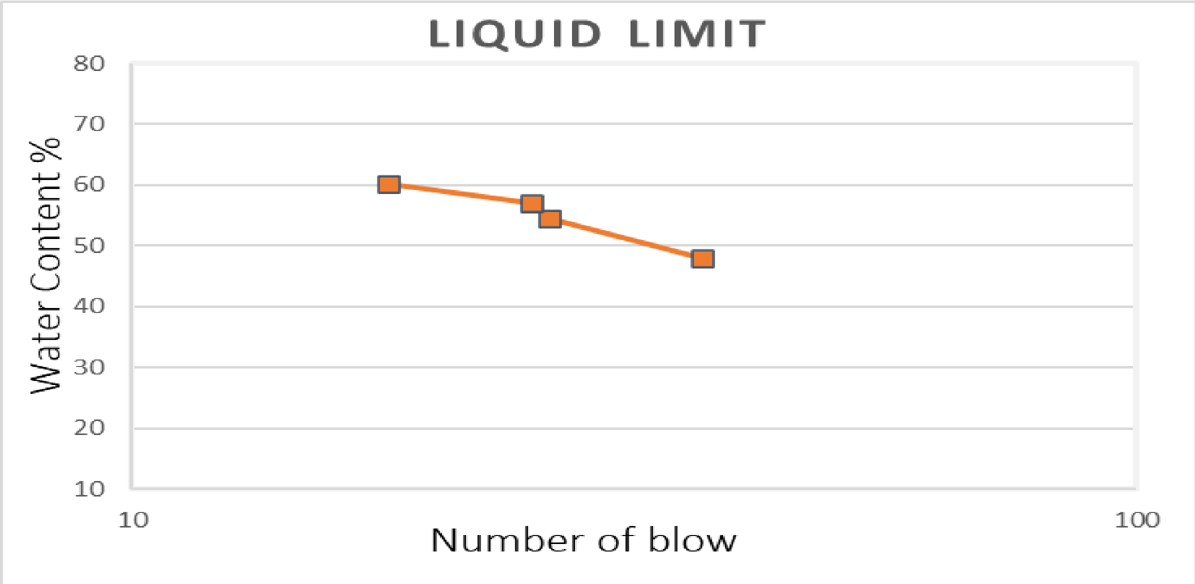

Location: Koyefeche

Test Method: ASTM D 422

Atterberg Limit						
	Liquid Limit				Plastic Limit	
Number of blows	**34**	**27**	**23**	**18**		
Weight of can + wet soil (g)	26.35	29.49	32.46	34.72	27.54	27.54
Weight of can + dry soil (g)	21.65	23.35	24.94	25.64	23.49	23.63
Weight of can (g)	14.85	14.91	15.11	14.77	14.35	14.92
Weight of water (g)	4.7	6.14	7.52	9.08	4.05	3.91
Weight of dry soil (g)	6.8	8.44	9.83	10.87	9.14	8.71
w = Water content, w%	69.11765	72.74882	76.50051	83.53266	44.31072	44.89093
Average (%)					44.60082603	
	LL= 75.4%				PL=44.6%	

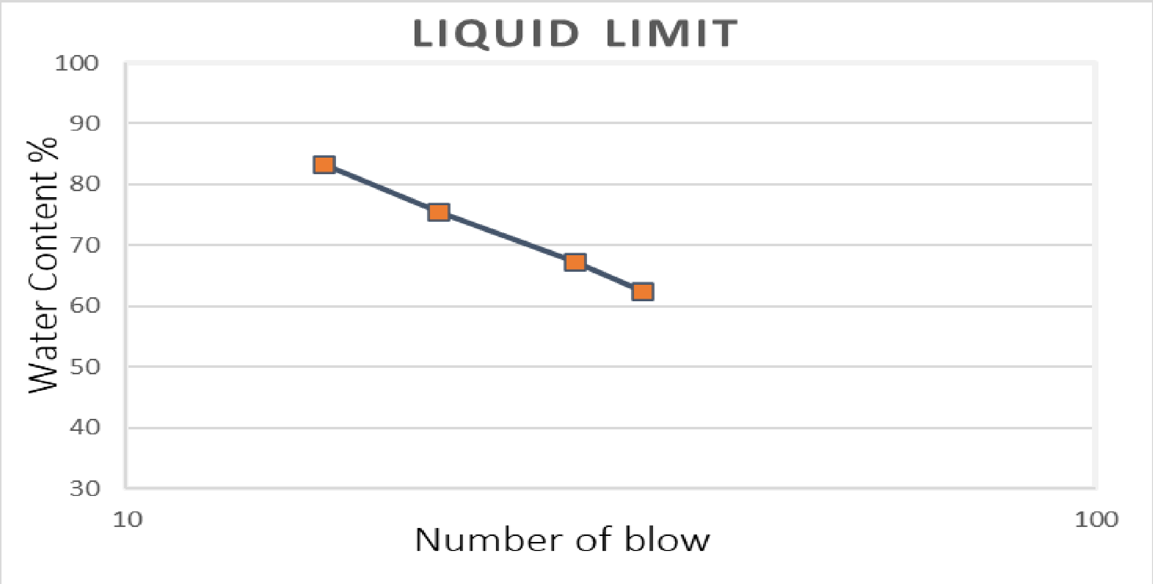

APPENDIX D: DETAILS OF MODIFIED COMPACTION TEST RESULTS

Location: Delber

Test Method: ASTM D 698

Modified Proctor				
	Density			
Determination No.	1	2	3	4
Mass of Mold, g	5433	5433	5433	5433
Mass of mold + Compacted Soil,	9125	9328	9418	9249
Mass of Compacted soil, g	3692	3895	3985	3816
Volume of Mold, cm3	2124	2124	2124	2124
Bulk density, g/cm3	1.74	1.83	1.88	1.80
	Moisture Content			
Conatainer No	B-10	B-5	C-C	A-11
Mass of container, g	61	52	58	54
Mass of container + wet soil, g	296	317	329	327
Mass of ontainer + Dry soil, g	262	273	276	269
Mass of Water, g	34	44	53	58
Mass of Dry soil, g	201	221	218	215
Water Contenet, %	16.92	19.91	24.31	26.98
Dry density, g/cm3	**1.49**	**1.53**	**1.51**	**1.41**
	OMC=22%		MDD=1.54g/cm3	

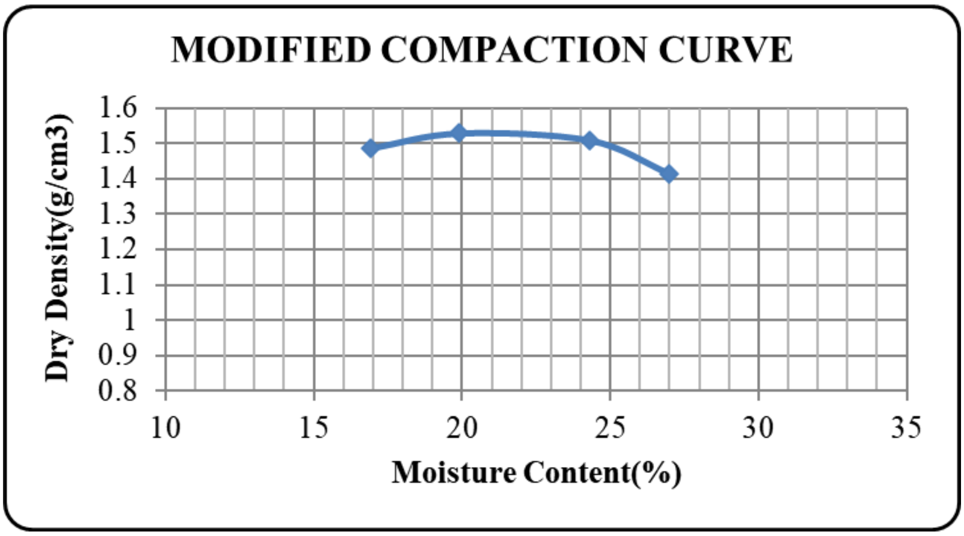

Location: Adisu gebeya

Test Method: ASTM D 698

Modified Proctor				
	Density			
Determination No.	1	2	3	4
Mass of Mold, g	5433	5433	5433	5433
Mass of mold + Compacted Soil,	9178	9548	9684	9528
Mass of Compacted soil, g	3745	4115	4251	4095
Volume of Mold, cm3	2124	2124	2124	2124
Bulk density, g/cm3	1.76	1.94	2.00	1.93
	Moisture Content			
Conatainer No	B-10	B-5	C-C	A-11
Mass of container, g	108.3	112.35	107.7	113.05
Mass of container + wet soil, g	309	295.59	324.62	309.44
Mass of ontainer + Dry soil, g	278.5	263.27	281.51	265
Mass of Water, g	30.5	32.32	43.11	44.44
Mass of Dry soil, g	170.2	150.92	173.81	151.95
Water Contenet, %	17.92	21.42	24.80	29.25
Dry density, g/cm3	**1.50**	**1.60**	**1.60**	**1.49**
	OMC=23.4%		MDD=1.61g/cm3	

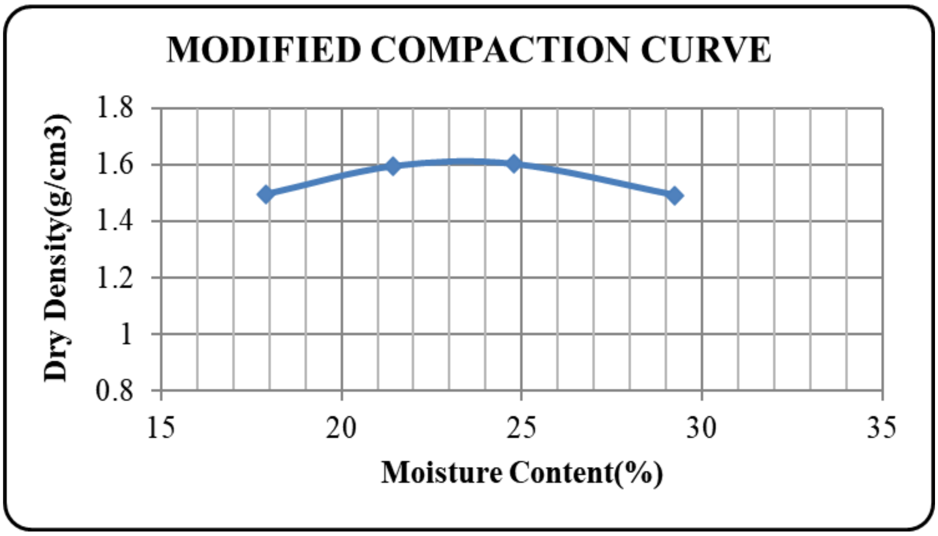

Location: Goro

Test Method: ASTM D 698

Modified Proctor				
	Density			
Determination No.	1	2	3	4
Mass of Mold, g	5561	5561	5561	5561
Mass of mold + Compacted Soil,	7112	7194	7237	7232
Mass of Compacted soil, g	1551	1633	1676	1671
Volume of Mold, cm3	944	944	944	944
Bulk density, g/cm3	1.64	1.73	1.78	1.77
	Moisture Content			
Conatainer No	B-10	B-5	C-C	A-11
Mass of container, g	30.5	29.8	30.9	31.5
Mass of container + wet soil, g	176.3	160	185.2	170.8
Mass of ontainer + Dry soil, g	157	140.9	160.2	146.2
Mass of Water, g	19.3	19.1	25	24.6
Mass of Dry soil, g	126.5	111.1	129.3	114.7
Water Contenet, %	15.26	17.19	19.33	21.45
Dry density, g/cm3	**1.43**	**1.48**	**1.49**	**1.46**
	OMC=19.3%		MDD=1.49g/cm3	

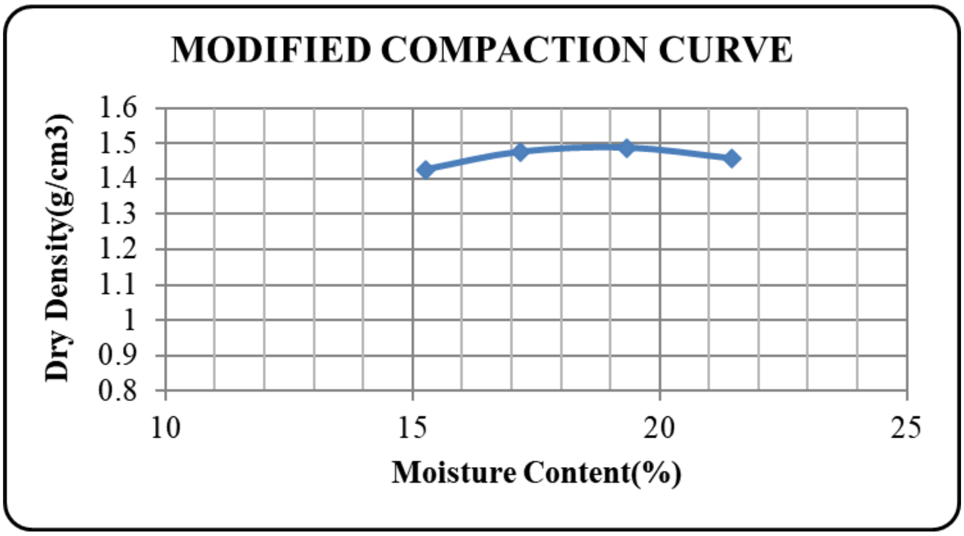

Location: Megenagna

Test Method: ASTM D 698

Modified Proctor				
	Density			
Determination No.	1	2	3	4
Mass of Mold, g	5433	5433	5433	5433
Mass of mold + Compacted Soil,	9144	9387	9571	9508
Mass of Compacted soil, g	3711	3954	4138	4075
Volume of Mold, cm3	2124	2124	2124	2124
Bulk density, g/cm3	1.75	1.86	1.95	1.92
	Moisture Content			
Conatainer No	B-10	B-5	C-C	A-11
Mass of container, g	45.96	42.19	41.35	41.64
Mass of container + wet soil, g	218.65	219.14	219.2	219.65
Mass of ontainer + Dry soil, g	193.74	191.06	187.46	182.97
Mass of Water, g	24.91	28.08	31.74	36.68
Mass of Dry soil, g	147.78	148.87	146.11	141.33
Water Contenet, %	16.86	18.86	21.72	25.95
Dry density, g/cm3	**1.50**	**1.57**	**1.60**	**1.52**
	OMC=21.9%		MDD=1.60g/cm3	

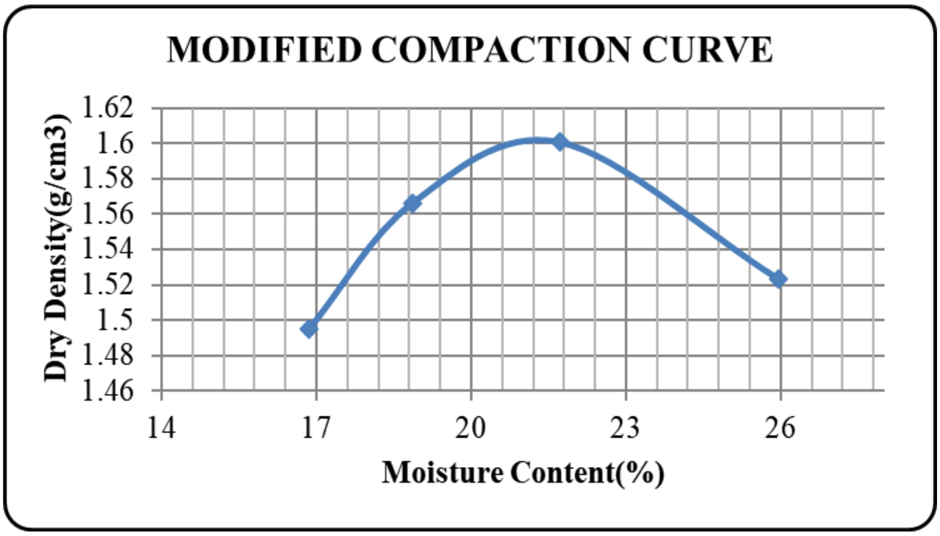

Location: Winget

Test Method: ASTM D 698

Modified Proctor				
	Density			
Determination No.	1	2	3	4
Mass of Mold, g	4982	4982	4982	4982
Mass of mold + Compacted Soil,	8240	8758	9130	9060
Mass of Compacted soil, g	3258	3776	4148	4078
Volume of Mold, cm3	2124	2124	2124	2124
Bulk density, g/cm3	1.53	1.78	1.95	1.92
	Moisture Content			
Conatainer No	B-10	B-5	C-C	A-11
Mass of container, g	30.85	30.51	31.31	30.17
Mass of container + wet soil, g	126.03	159.35	133.07	126.86
Mass of ontainer + Dry soil, g	110.26	135.07	111.03	103.58
Mass of Water, g	15.77	24.28	22.04	23.28
Mass of Dry soil, g	79.41	104.56	79.72	73.41
Water Contenet, %	19.86	23.22	27.65	31.71
Dry density, g/cm3	**1.28**	**1.44**	**1.53**	**1.46**
	OMC=27.6%		MDD=1.53g/cm3	

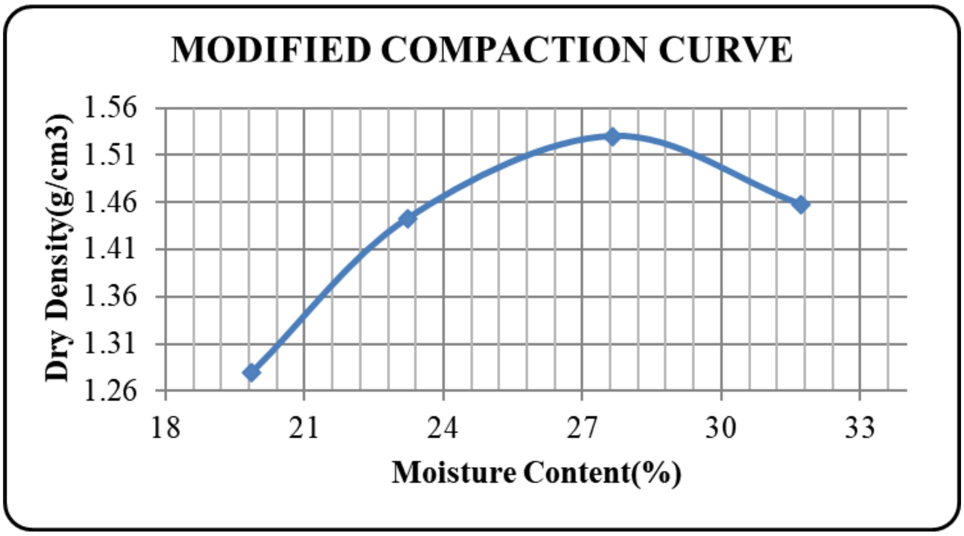

Location: Ayer Tena

Test Method: ASTM D 698

Modified Proctor				
	Density			
Determination No.	1	2	3	4
Mass of Mold, g	5561	5561	5561	5561
Mass of mold + Compacted Soil,	7121	7228	7290	7285
Mass of Compacted soil, g	1560	1667	1729	1724
Volume of Mold, cm3	944	944	944	944
Bulk density, g/cm3	1.65	1.77	1.83	1.83
	Moisture Content			
Conatainer No	B-10	B-5	C-C	A-11
Mass of container, g	29.4	31.5	31	32.5
Mass of container + wet soil, g	170.4	160.5	190.5	176.9
Mass of ontainer + Dry soil, g	153	142.3	165.5	152
Mass of Water, g	17.4	18.2	25	24.9
Mass of Dry soil, g	123.6	110.8	134.5	119.5
Water Contenet, %	14.08	16.43	18.59	20.84
Dry density, g/cm3	**1.45**	**1.52**	**1.54**	**1.51**
	OMC=18.6%		MDD=1.54g/cm3	

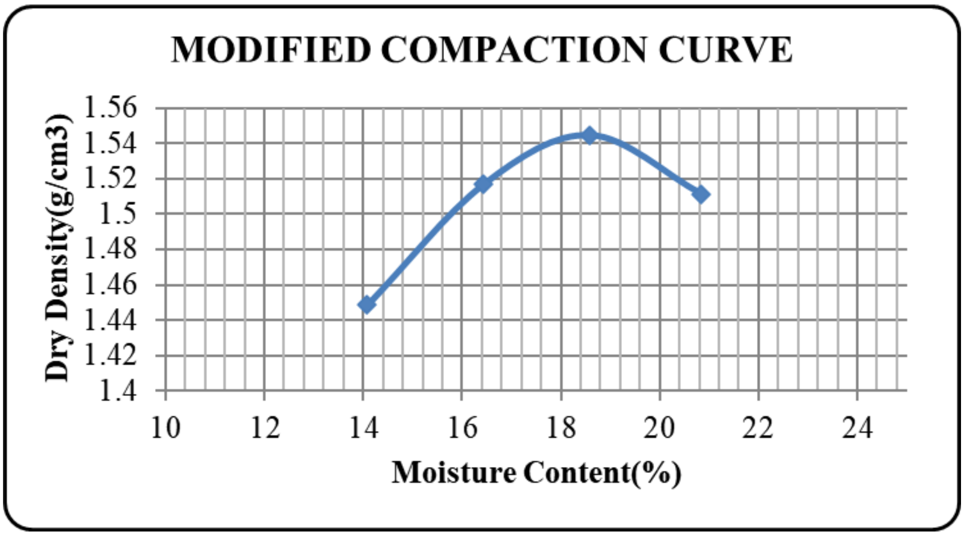

Location: Bethel

Test Method: ASTM D 698

Modified Proctor				
	Density			
Determination No.	1	2	3	4
Mass of Mold, g	4710	4710	4710	4710
Mass of mold + Compacted Soil,	6380	6515	6633	6610
Mass of Compacted soil, g	1670	1805	1923	1900
Volume of Mold, cm3	944	944	944	944
Bulk density, g/cm3	1.77	1.91	2.04	2.01
	Moisture Content			
Conatainer No	B-10	B-5	C-C	A-11
Mass of container, g	15.45	15.78	15.71	15.14
Mass of container + wet soil, g	99	71.3	79.4	99.64
Mass of ontainer + Dry soil, g	87.44	62.34	67.91	82.96
Mass of Water, g	11.56	8.96	11.49	16.68
Mass of Dry soil, g	71.99	46.56	52.2	67.82
Water Contenet, %	16.06	19.24	22.01	24.59
Dry density, g/cm3	**1.52**	**1.60**	**1.67**	**1.62**
	OMC=22.01%		MDD=1.67g/cm3	

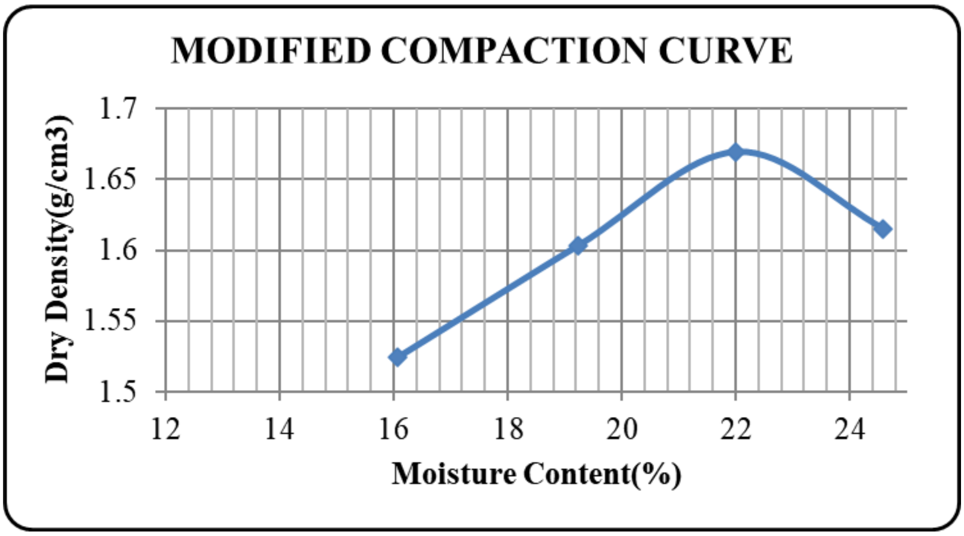

Location: Shegole

Test Method: ASTM D 698

Modified Proctor				
	Density			
Determination No.	1	2	3	4
Mass of Mold, g	5561	5561	5561	5561
Mass of mold + Compacted Soil,	7068	7134	7185	7183
Mass of Compacted soil, g	1507	1573	1624	1622
Volume of Mold, cm3	944	944	944	944
Bulk density, g/cm3	1.60	1.67	1.72	1.72
	Moisture Content			
Conatainer No	B-10	B-5	C-C	A-11
Mass of container, g	30.5	29.8	30.9	31.5
Mass of container + wet soil, g	174.4	167.2	176.6	172
Mass of ontainer + Dry soil, g	153	145	150.5	145
Mass of Water, g	21.4	22.2	26.1	27
Mass of Dry soil, g	122.5	115.2	119.6	113.5
Water Contenet, %	17.47	19.27	21.82	23.79
Dry density, g/cm3	**1.36**	**1.40**	**1.41**	**1.39**
	OMC=21.82%		MDD=1.41g/cm3	

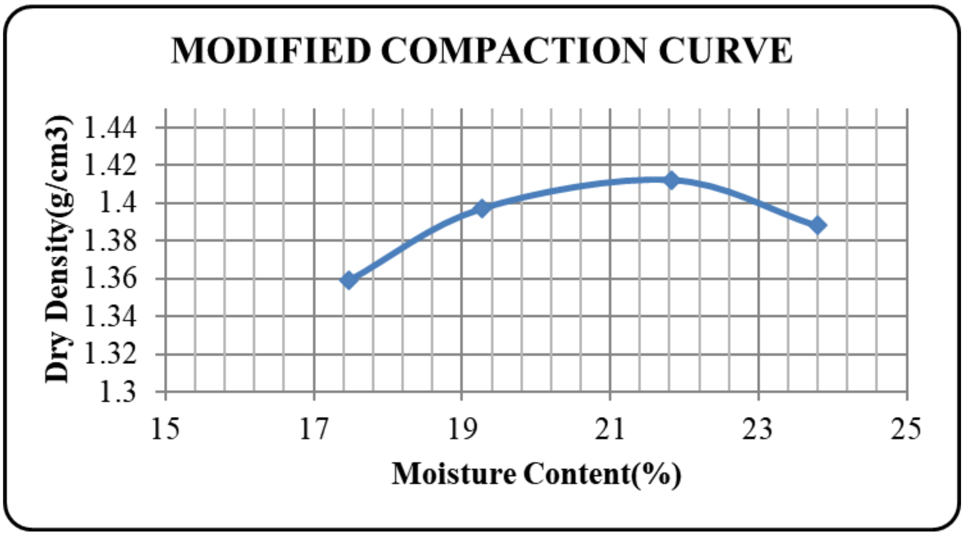

Location: Kore adebabay

Test Method: ASTM D 698

Modified Proctor				
	Density			
Determination No.	1	2	3	4
Mass of Mold, g	5350	5350	5350	5350
Mass of mold + Compacted Soil,	6904	7131	7252	7250
Mass of Compacted soil, g	1554	1781	1902	1900
Volume of Mold, cm3	944	944	944	944
Bulk density, g/cm3	1.65	1.89	2.01	2.01
	Moisture Content			
Conatainer No	B-10	B-5	C-C	A-11
Mass of container, g	69.6	67.1	68.5	67.1
Mass of container + wet soil, g	234.5	228.2	225.8	223
Mass of ontainer + Dry soil, g	220.8	204.7	195.7	184.4
Mass of Water, g	13.7	23.5	30.1	38.6
Mass of Dry soil, g	151.2	137.6	127.2	117.3
Water Contenet, %	9.06	17.08	23.66	32.91
Dry density, g/cm3	**1.51**	**1.61**	**1.63**	**1.51**
	OMC=23.66%		MDD=1.55g/cm3	

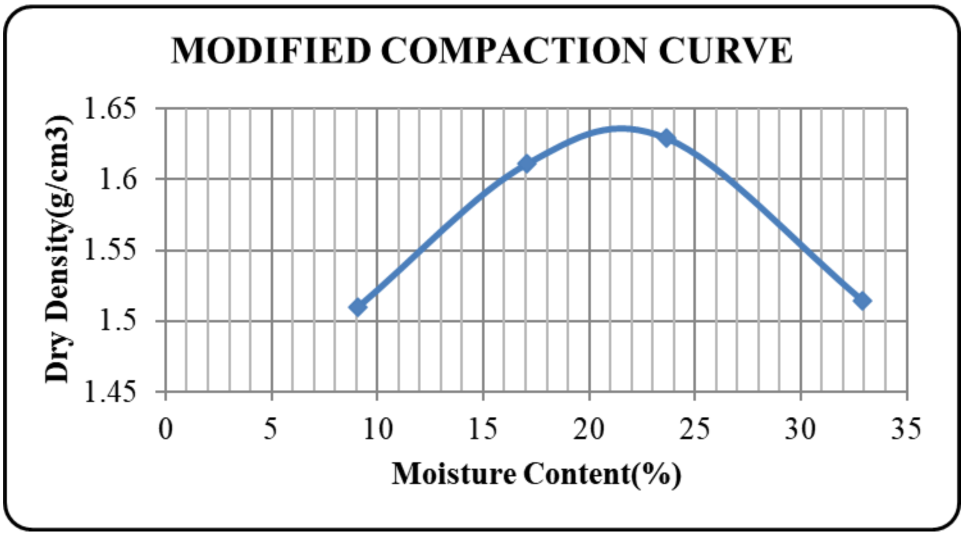

Location: Lideta

Test Method: ASTM D 698

Modified Proctor				
	Density			
Determination No.	1	2	3	4
Mass of Mold, g	5442	5442	5442	5442
Mass of mold + Compacted Soi	8850	9261	9412	9271
Mass of Compacted soil, g	3408	3819	3970	3829
Volume of Mold, cm3	2124	2124	2124	2124
Bulk density, g/cm3	1.60	1.80	1.87	1.80
	Moisture Content			
Conatainer No	B-10	B-5	C-C	A-11
Mass of container, g	41.28	41.59	44.41	40.65
Mass of container + wet soil, g	212.29	241.21	186.18	172.47
Mass of ontainer + Dry soil, g	187	207.08	156.21	139.68
Mass of Water, g	25.29	34.13	29.97	32.79
Mass of Dry soil, g	145.72	165.49	111.8	99.03
Water Contenet, %	25.29	34.13	29.97	32.79
Dry density, g/cm3	**1.28**	**1.34**	**1.44**	**1.36**
	OMC=23.3%		MDD=1.52g/cm3	

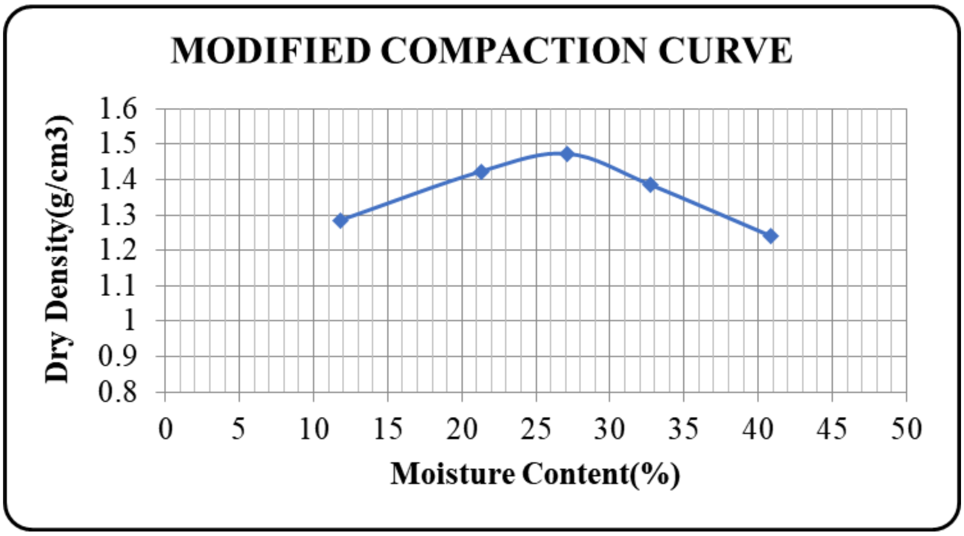

Location: Legehar

Test Method: ASTM D 698

Modified Proctor				
	Density			
Determination No.	1	2	3	4
Mass of Mold, g	5561	5561	5561	5561
Mass of mold + Compacted Soil,	7441	7519	7565	7561
Mass of Compacted soil, g	1880	1958	2004	2000
Volume of Mold, cm3	944	944	944	944
Bulk density, g/cm3	1.99	2.07	2.12	2.12
	Moisture Content			
Conatainer No	B-10	B-5	C-C	A-11
Mass of container, g	30.8	31.4	31.2	30.2
Mass of container + wet soil, g	163	174.4	175.6	175.5
Mass of ontainer + Dry soil, g	153.6	161.6	160.4	158
Mass of Water, g	9.4	12.8	15.2	17.5
Mass of Dry soil, g	122.8	130.2	129.2	127.8
Water Contenet, %	7.65	9.83	11.76	13.69
Dry density, g/cm3	**1.85**	**1.89**	**1.90**	**1.86**
	OMC=11.7%		MDD=1.9g/cm3	

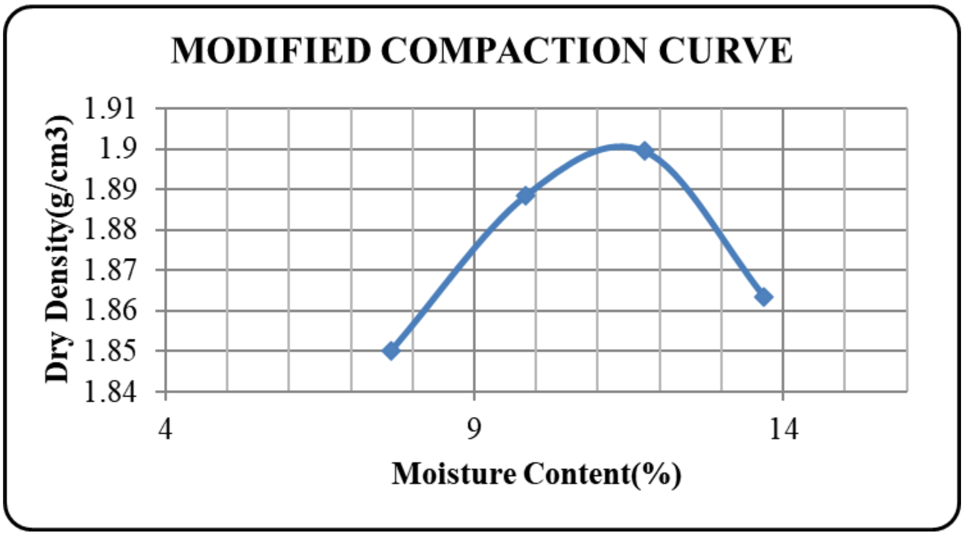

Location: Tikur Anbesa

Test Method: ASTM D 698

Modified Proctor					
	Density				
Determination No.	1	2	3	4	5
Mass of Mold, g	5561	5561	5561	5561	5561
Mass of mold + Cor	7057	7141	7213	7330	7310
Mass of Compacted	1496	1580	1652	1769	1749
Volume of Mold, cm	944	944	944	944	944
Bulk density, g/cm3	1.58	1.67	1.75	1.87	1.85
	Moisture Content				
Conatainer No	B-10	B-5	C-C	A-11	B-9
Mass of container, g	16.14	15.77	11.17	15.43	15.84
Mass of container +	101.6	101.1	94.6	103.61	95.7
Mass of ontainer + D	90.18	88.56	81.24	86.97	77.35
Mass of Water, g	11.42	12.54	13.36	16.64	18.35
Mass of Dry soil, g	74.04	72.79	70.07	71.54	61.51
Water Contenet, %	15.42	17.23	19.07	23.26	29.83
Dry density, g/cm3	**1.37**	**1.43**	**1.47**	**1.52**	**1.43**
	OMC=23.23%		MDD=1.52g/cm3		

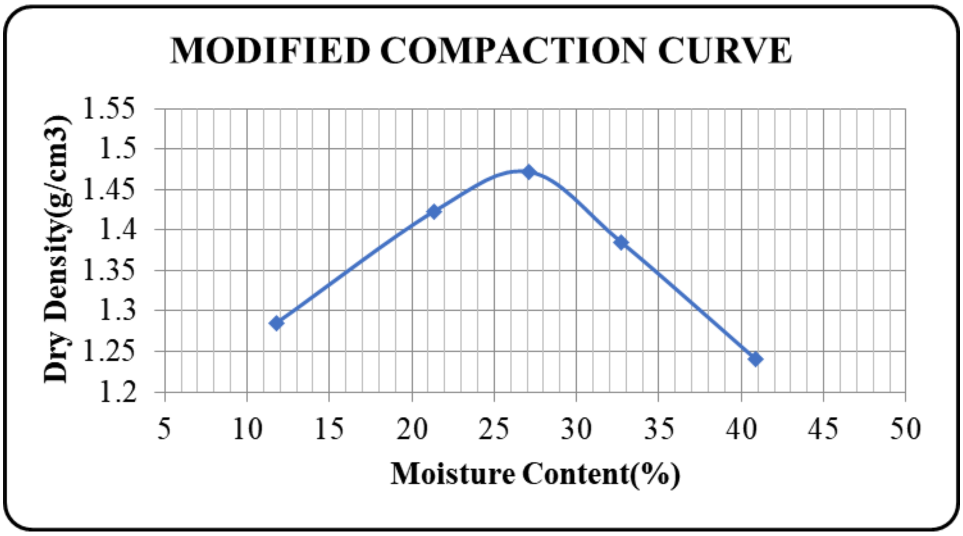

Location: Shiro meda

Test Method: ASTM D 698

Modified Proctor				
	Density			
Determination No.	1	2	3	4
Mass of Mold, g	5561	5561	5561	5561
Mass of mold + Compacted Soil,	7147.7	7223.2	7267.7	7263.2
Mass of Compacted soil, g	1586.7	1662.2	1706.7	1702.2
Volume of Mold, cm3	944	944	944	944
Bulk density, g/cm3	1.68	1.76	1.81	1.80
	Moisture Content			
Conatainer No	B-10	B-5	C-C	A-11
Mass of container, g	30.6	31.6	31	32.4
Mass of container + wet soil, g	165.5	175	163.6	163.3
Mass of ontainer + Dry soil, g	146	152	140.6	138.5
Mass of Water, g	19.5	23	23	24.8
Mass of Dry soil, g	115.4	120.4	109.6	106.1
Water Contenet, %	16.90	19.10	20.99	23.37
Dry density, g/cm3	**1.44**	**1.48**	**1.49**	**1.46**
	OMC=21%		MDD=1.49g/cm3	

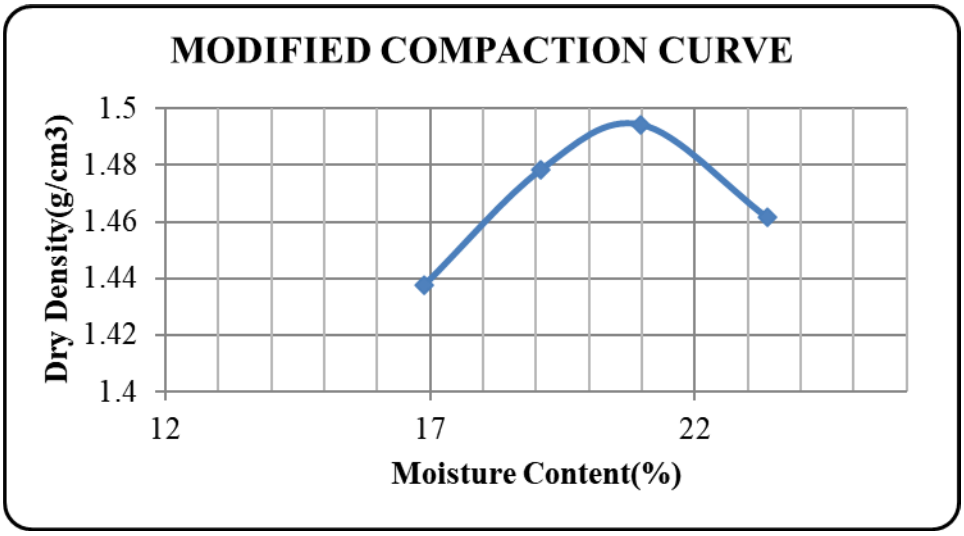

Location: Akaki kality

Test Method: ASTM D 698

Modified Proctor				
	Density			
Determination No.	1	2	3	4
Mass of Mold, g	5561	5561	5561	5561
Mass of mold + Compacted Soil,	7139	7201	7245	7241
Mass of Compacted soil, g	1578	1640	1684	1680
Volume of Mold, cm3	944	944	944	944
Bulk density, g/cm3	1.67	1.74	1.78	1.78
	Moisture Content			
Conatainer No	B-10	B-5	C-C	A-11
Mass of container, g	30.6	31.2	30.9	31.5
Mass of container + wet soil, g	170	170.9	185.3	176.8
Mass of ontainer + Dry soil, g	150.2	149	158.9	150
Mass of Water, g	19.8	21.9	26.4	26.8
Mass of Dry soil, g	119.6	117.8	128	118.5
Water Contenet, %	16.56	18.59	20.63	22.62
Dry density, g/cm3	**1.43**	**1.46**	**1.48**	**1.45**
	OMC=20.63%		MDD=1.48g/cm3	

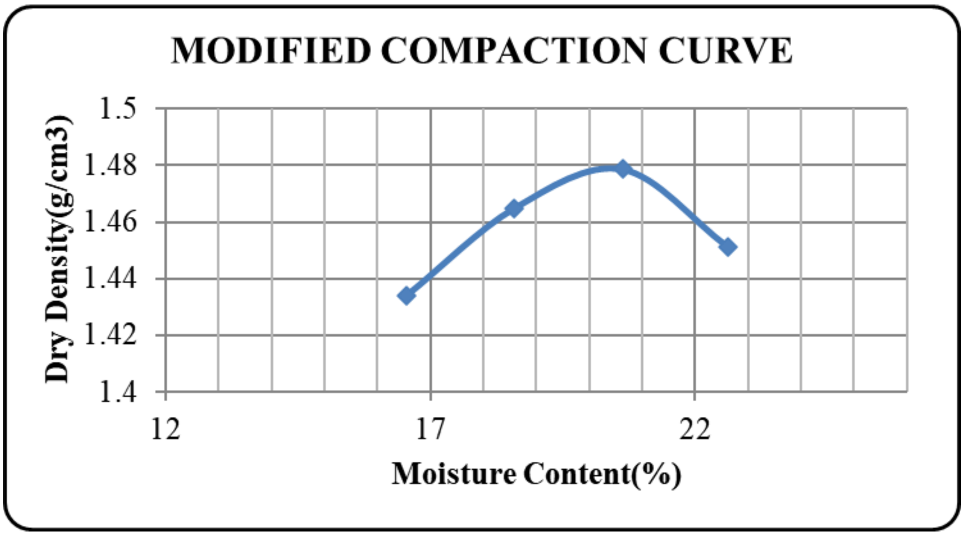

Location: Koye Feche

Test Method: ASTM D 698

Modified Proctor				
	Density			
Determination No.	1	2	3	4
Mass of Mold, g	3921	3921	3921	3921
Mass of mold + Compacted Soil,	5455	5580	5642.8	5600
Mass of Compacted soil, g	1534	1659	1721.8	1679
Volume of Mold, cm3	944	944	944	944
Bulk density, g/cm3	1.63	1.76	1.82	1.78
	Moisture Content			
Conatainer No	B-10	B-5	C-C	A-11
Mass of container, g	16	16.3	16.5	10
Mass of container + wet soil, g	129.6	86	94.6	90.7
Mass of ontainer + Dry soil, g	107	70.7	76.3	70.3
Mass of Water, g	22.6	15.3	18.3	20.4
Mass of Dry soil, g	91	54.4	59.8	60.3
Water Contenet, %	24.84	28.13	30.60	33.83
Dry density, g/cm3	**1.30**	**1.37**	**1.40**	**1.33**
	OMC=20.63%		MDD=1.48g/cm3	

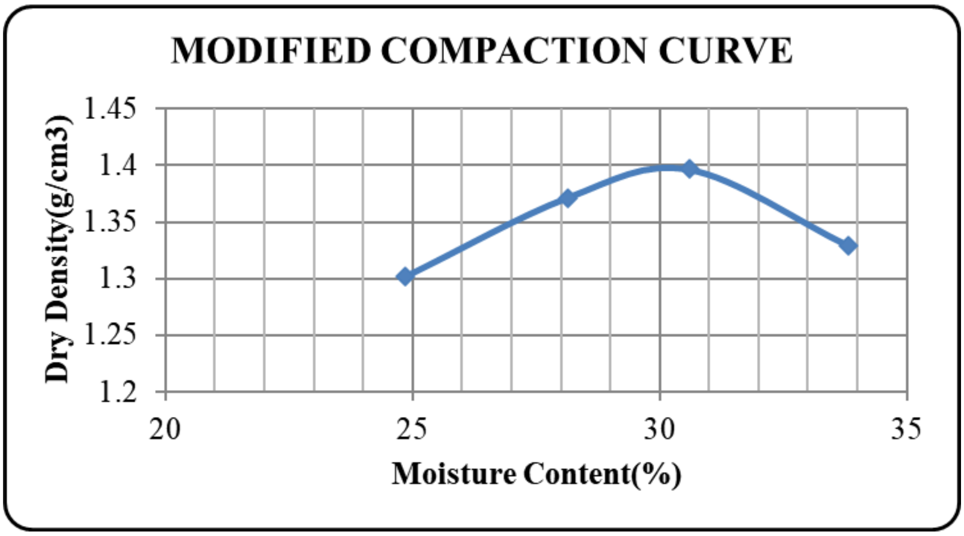

APPENDIX E: DETAILS OF CALIFORNIA BEARING RATIO TEST RESULTS

Location: Delber

Test Method: AASHTO T-193

N0	Penetration (mm)	10 Blow		25 Blow		56 Blow	
		Load (KN)	Stress (Mpa)	Load (KN)	Stress (Mpa)	Load (KN)	Stress (Mpa)
1	0.00	0.00	0.000	0.00	0.000	0	0.000
	0.64	0.25	5.000	0.36	7.000	0.48	9.000
	1.27	0.40	8.000	0.55	11.000	0.7	14.000
2	1.96	0.51	10.000	0.68	13.000	0.86	17.000
3	2.54	0.59	11.000	0.76	15.000	0.96	19.000
4	3.18	0.64	12.000	0.81	16.000	1	19.000
5	3.81	0.69	13.000	0.86	17.000	1.06	20.000
6	4.45	0.73	14.000	0.91	17.000	1.11	21.000
	5.08	0.77	15.000	0.95	18.000	1.15	22.000
7	7.62	0.4	19.000	1.17	23.000	1.37	26.000
Penetration (mm)	**Standard Load (Mpa)**	CBR (%)		CBR (%)		CBR (%)	
2.54	6.90	**4.43**		**5.75**		**7.26**	
5.08	10.30	3.87		4.75		5.75	

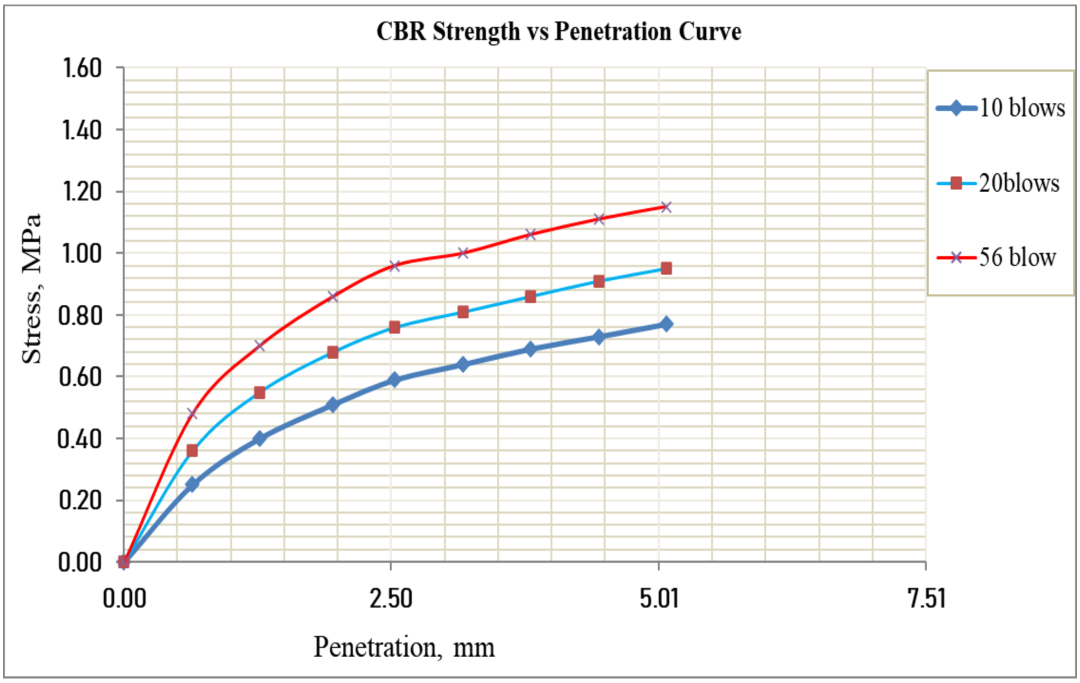

Location: Adisu gebiya

Test Method: AASHTO T-193

N0	Penetration (mm)	10 Blow		25 Blow		56 Blow	
		Load (KN)	Stress (Mpa)	Load (KN)	Stress (Mpa)	Load (KN)	Stress (Mpa)
1	0.00	0.00	0.000	0.00	0.000	0	0.000
2	0.64	0.17	3.000	0.31	6.000	0.53	10.000
3	1.27	0.31	6.000	0.49	9.000	0.84	16.000
4	1.96	0.44	9.000	0.64	12.000	1.12	22.000
5	2.54	0.5	10.000	0.73	14.000	1.25	24.000
6	3.18	0.55	11.000	0.8	15.000	1.31	25.000
7	3.81	0.57	11.000	0.85	16.000	1.37	26.000
8	4.45	0.59	11.000	0.9	17.000	1.41	27.000
9	5.08	0.62	12.000	0.96	18.000	1.47	28.000
10	7.62	0.73	14.000	1.09	21.000	1.59	31.000
Penetration (mm)	**Standard Load (Mpa)**	CBR (%)		CBR (%)		CBR (%)	
2.54	6.90	**3.77**		**5.49**		**9.45**	
5.08	10.30	3.13		4.79		7.36	

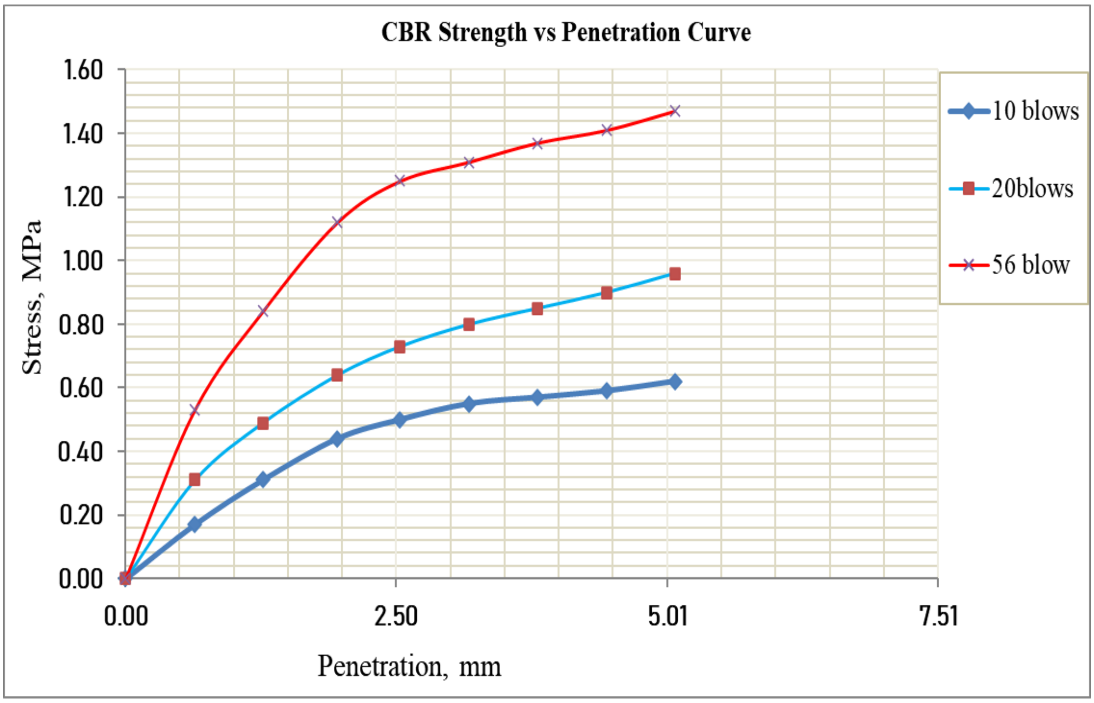

Location: Megenagna

Test Method: AASHTO T-193

N0	Penetration (mm)	10 Blow		25 Blow		56 Blow	
		Load (KN)	Stress (Mpa)	Load (KN)	Stress (Mpa)	Load (KN)	Stress (Mpa)
1	0.00	0.00	0.000	0.00	0.000	0	0.000
2	0.64	0.42	8.000	0.67	13.000	0.88	17.000
3	1.27	0.67	13.000	0.93	18.000	1.14	22.000
4	1.96	0.93	18.000	1.19	23.000	1.4	27.000
5	2.54	1.14	22.000	1.42	27.000	1.66	32.000
6	3.18	1.3	25.000	1.61	31.000	1.87	36.000
7	3.81	1.45	28.000	1.76	34.000	2.02	38.000
8	4.45	1.61	31.000	1.92	37.000	2.18	42.000
9	5.08	1.65	32.000	2.08	40.000	2.28	44.000
10	7.62	1.76	34.000	2.23	43.000	2.44	47.000

Penetration (mm)	**Standard Load (Mpa)**	CBR (%)	CBR (%)	CBR (%)
2.54	6.90	**8.60**	**10.70**	**12.40**
5.08	10.30	10.30	10.38	11.41

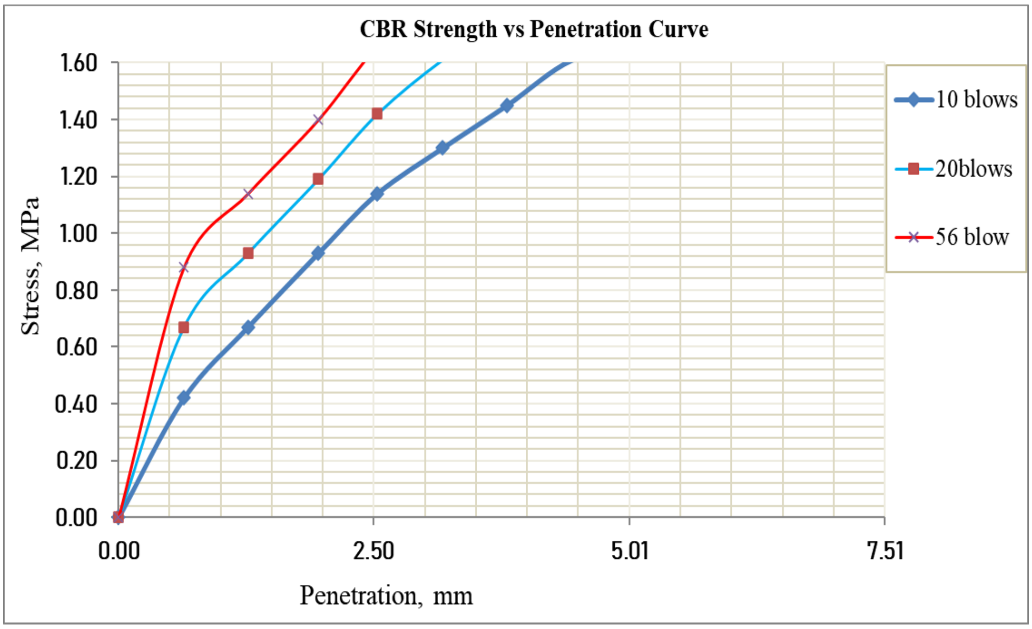

Location: Winget

Test Method: AASHTO T-193

N0	Penetration (mm)	10 Blow		25 Blow		56 Blow	
		Load (KN)	Stress (Mpa)	Load (KN)	Stress (Mpa)	Load (KN)	Stress (Mpa)
1	0.00	0.00	0.000	0.00	0.000	0	0.000
2	0.64	0.55	32.000	0.68	13.000	0.79	37.000
3	1.27	0.81	47.000	1.00	18.000	1.13	53.000
4	1.96	0.98	56.000	1.19	23.000	1.28	60.000
5	2.54	1.11	61.000	1.3	27.000	1.41	66.000
6	3.18	1.15	64.000	1.36	31.000	1.49	70.000
7	3.81	1.19	68.000	1.45	34.000	1.55	73.000
8	4.45	1.23	70.000	1.49	37.000	1.6	75.000
9	5.08	1.28	73.000	1.55	40.000	1.64	77.000
10	7.62	1.58	84.000	1.79	43.000	1.96	92.000

Penetration (mm)	**Standard Load (Mpa)**	CBR (%)	CBR (%)	CBR (%)
2.54	6.90	**8.30**	**9.70**	**10.50**
5.08	10.30	6.40	7.80	8.20

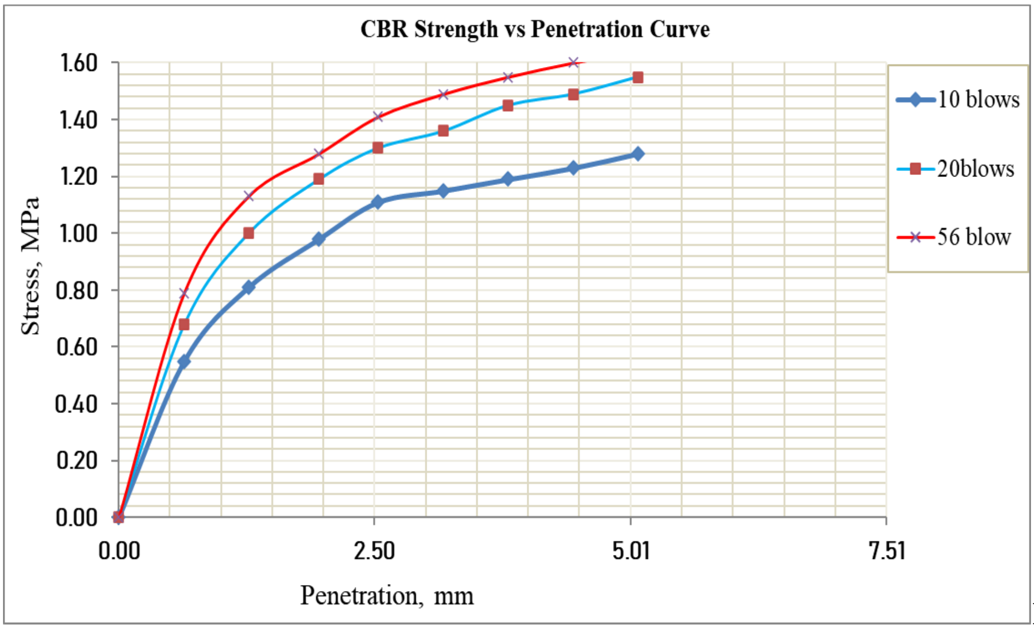

Location:

Lideta

Test Method: AASHTO T-193

N0	Penetration (mm)	10 Blow		25 Blow		56 Blow	
		Load (KN)	Stress (Mpa)	Load (KN)	Stress (Mpa)	Load (KN)	Stress (Mpa)
1	0.00	0.00	0.000	0.00	0.000	0	0.000
2	0.64	0.16	3.000	0.21	4.000	0.28	5.000
3	1.27	0.27	5.000	0.38	7.000	0.46	9.000
4	1.96	0.4	8.000	0.52	10.000	0.61	12.000
5	2.54	0.47	9.000	0.62	12.000	0.72	14.000
6	3.18	0.52	10.000	0.69	13.000	0.82	16.000
7	3.81	0.57	11.000	0.74	14.000	0.9	17.000
8	4.45	0.62	12.000	0.8	15.000	0.96	18.000
9	5.08	0.67	13.000	0.85	16.000	1.01	19.000
10	7.62	0.83	16.000	1.04	20.000	1.2	23.000
Penetration (mm)	**Standard Load (Mpa)**	CBR (%)		CBR (%)		CBR (%)	
2.54	6.90	**3.54**		**4.68**		**5.43**	
5.08	10.30	3.35		4.27		5.03